

Review on sediment scour,
transport, and deposit in
coastal environments,
including under tsunami
forcing

Jørgen Fredsøe, Techn.
Univ. Denmark

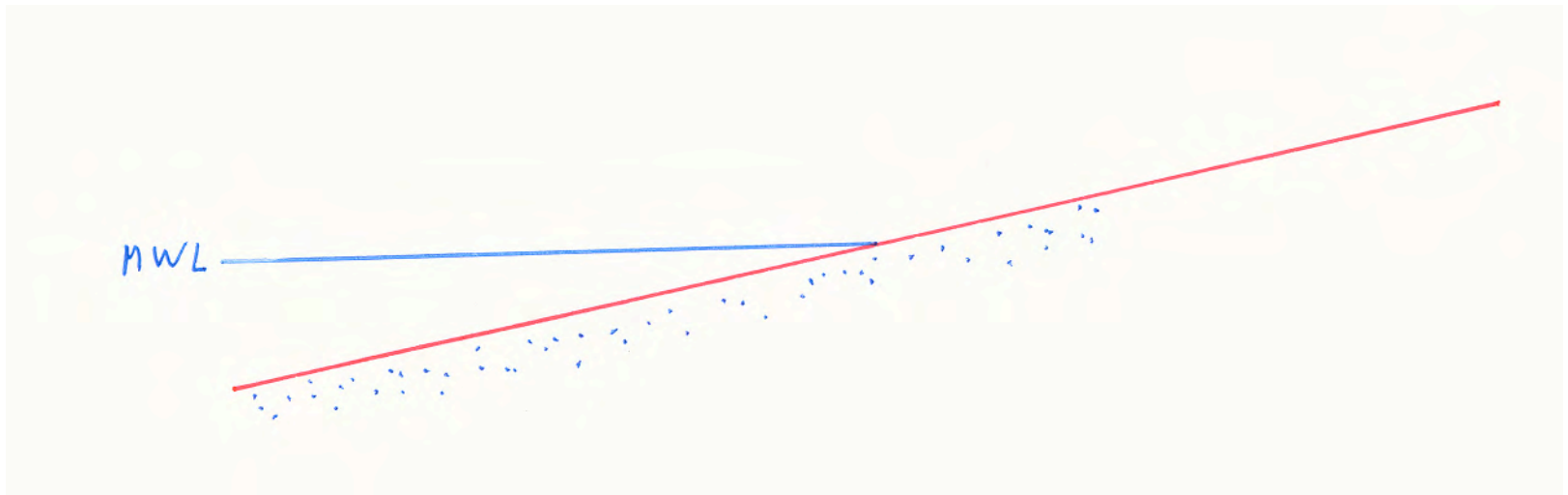
At which location are the flow velocity largest?

Carrier et al 2003: at the moving shoreline.

Max inshore direction: initial waveform depression.
Offshore directed if initial wave have a dominant elevation characteristic.



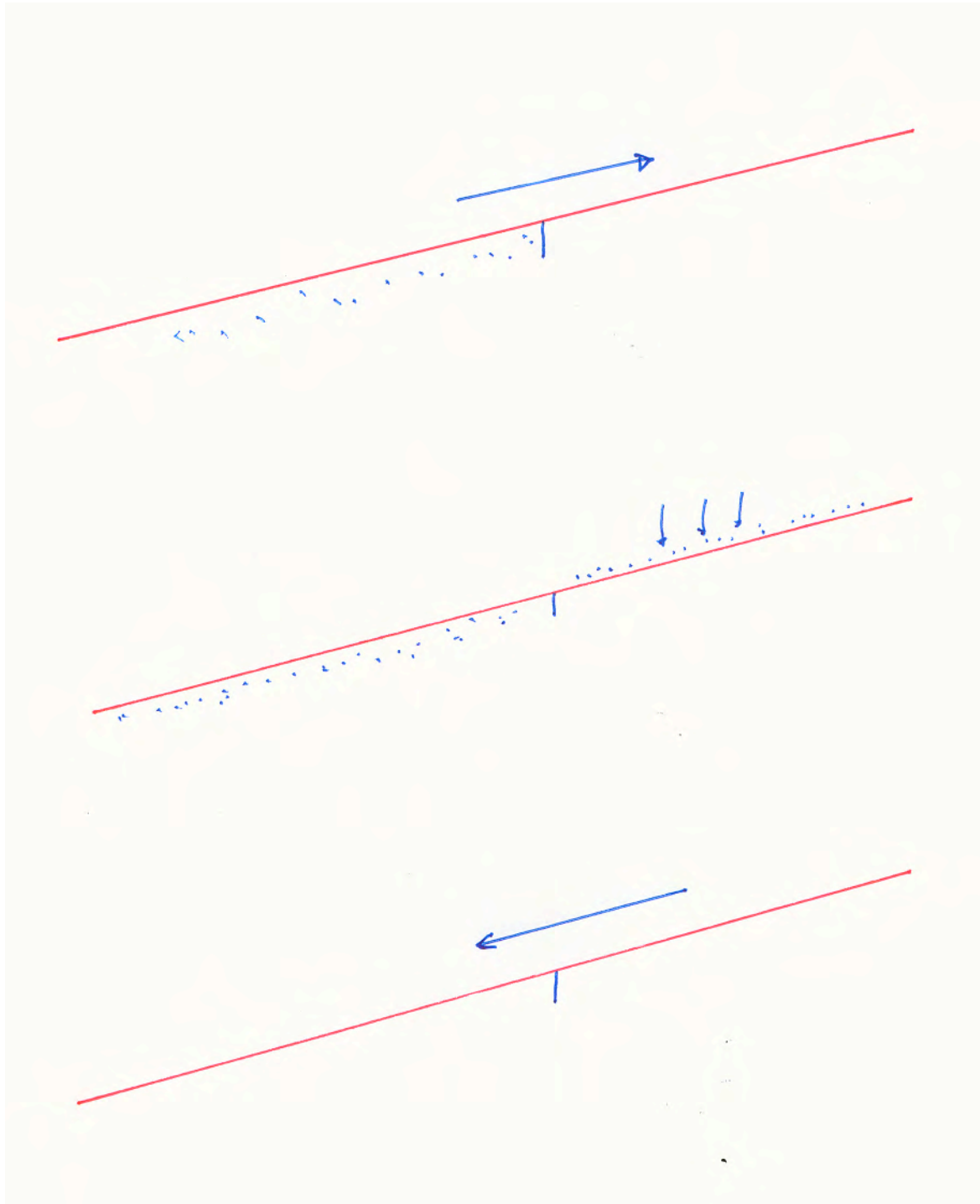
Soil properties?? Sand in the sea – and in the beach. Brought further onshore: ???



I: Run up: on-shore sediment transport

II:
Sedimentation

III: Draw down :offshore sediment transport

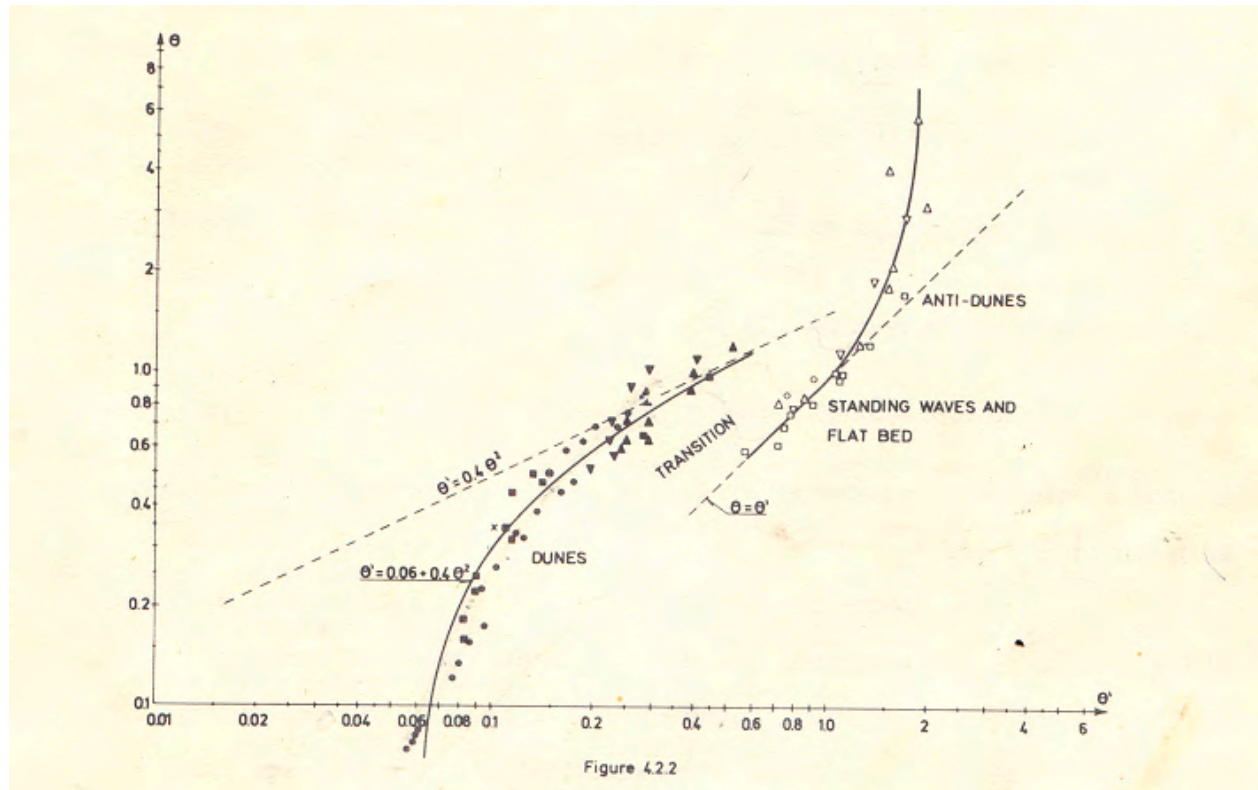


Flow velocities

River flow:

- lower reaches: flood: 2.5-4 m/s, Sand
- Upper reaches, Mountain streams: 4-6 m/s, stones





Rivers: Engelund-Hansen: θ smaller than 2-3

But coarser fractions can be
mobilized





Waves

$D=40$ m $T=15$ sec $H=20$ m (e.g. theNorth
Sea) :

$U(\text{max})=3.7$ m/s θ about 5. (thin boundary
layer).

Tsunami: T=13 min, Amplitude=0.75 m in
2000 m waterdepth

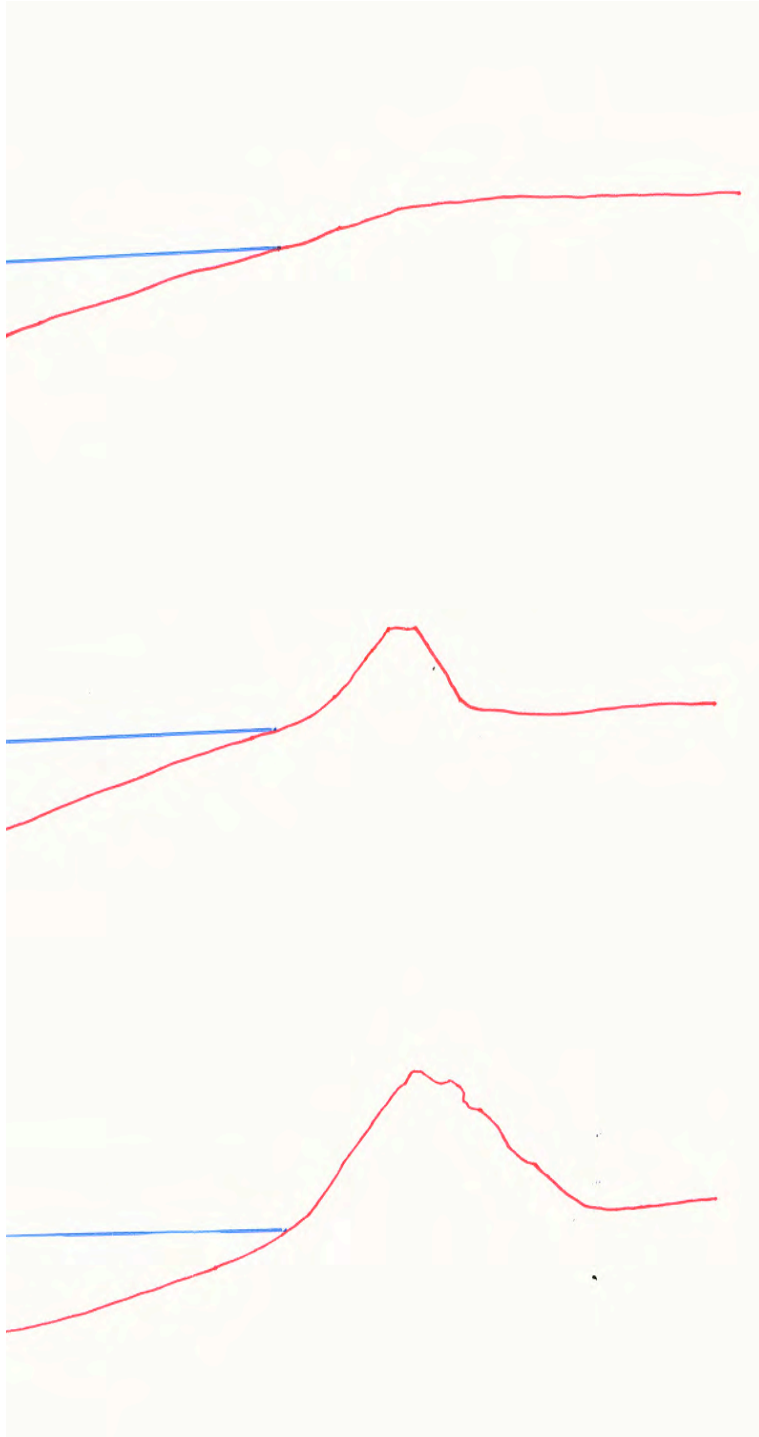
$$\xi = \frac{S}{\sqrt{H_0 / L_\infty}}$$

- Slope: 1/15: $\xi = 53$, Vertical run-up=3.5 m, U(max)= 0.42 m/sec
- S=1/120: $\xi = 6.6$, run-up=9.9 m, U=9.5 m/sec

Observed or estimated flow velocities

- Hokkaido 1993: 10-18 m/s (Tsutsumi et al, ASCE, 2000) (evaluated by considering deformation of railway tracks)





Morphology
on land:

Flat

Dikes

Dunes

Planform view

longshore variations in
dune crest level etc





Picture by Barbara Keating

2004 Indian Ocean Tsunami

- Incised Erosional Channels
(30 m long & 1 m deep)



What special is there about a Tsunami from a hydrodynamic/sediment-transport point of view, compared to coastal or river environment.

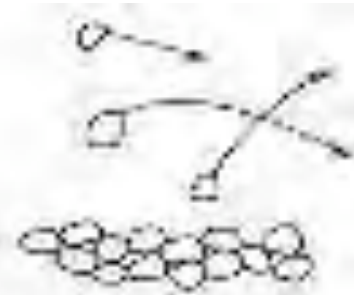
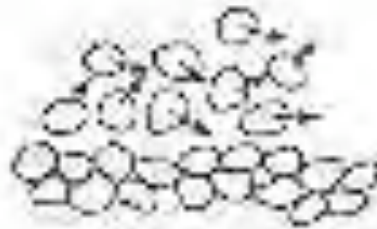
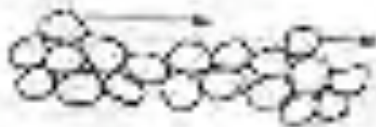
- Magnitude of flow velocity
- Duration (transient problem)
- The magnitude of run-up
- Flow reversal
- Groundwater flow
- Sediment properties.(fine sediment+large V)

What to focus on?

1. Basic concepts of sand transport mechanisms
2. Boundary layers (bed friction) and turbulence in waves.
3. Net transport in a Tsunami
4. Scour in waves

PART 1: Non-cohesive sediment transport modeling

Some simple physical considerations on transport of bed load, suspended load and sheet flow

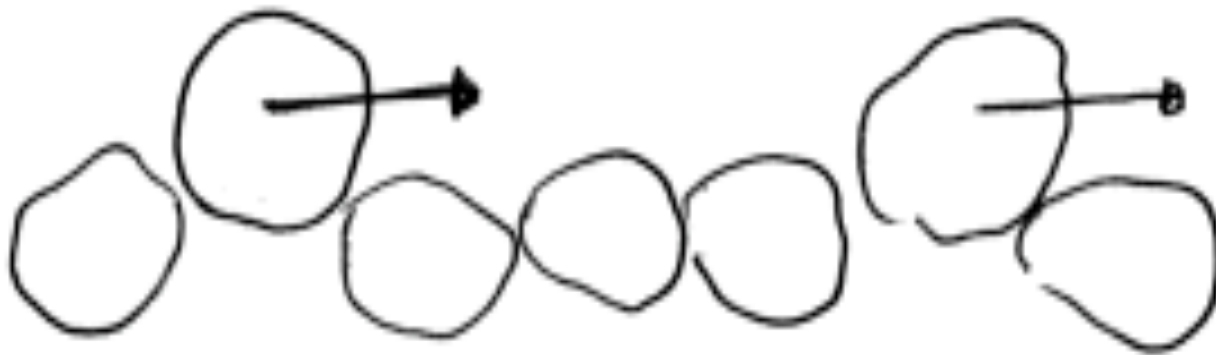


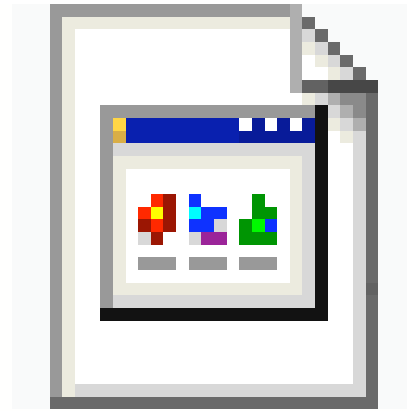
$$\tau, U, \sqrt{u'^2}$$



$$F_d = \frac{1}{2} \rho c_D \left[\alpha U_f - U_B \right]^2 \frac{\pi}{4} d^2$$

$$F_s = W \mu_d = \frac{\pi}{6} \rho g (s - 1) d^3 \mu_d$$



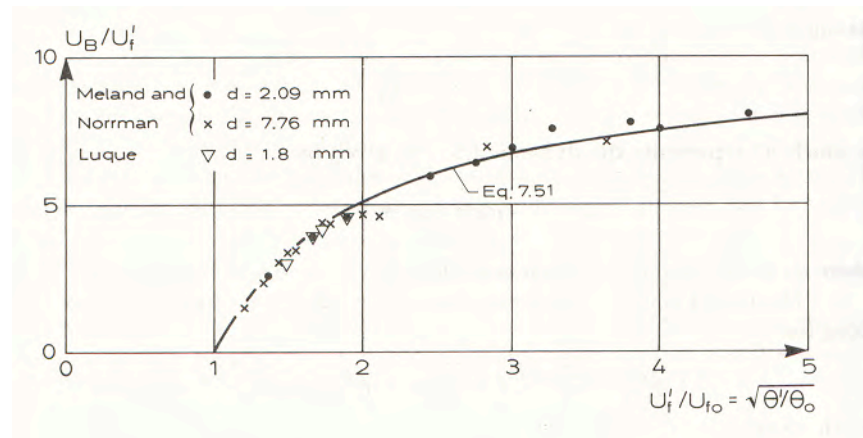


bedload transport.mov

$$F_d = \frac{1}{2} \rho c_D \left[\alpha U_f - U_B \right]^2 \frac{\pi}{4} d^2$$

$$F_s = W \mu_d = \frac{\pi}{6} \rho g (s - 1) d^3 \mu_d$$

$$\frac{U_b}{U_f} = \alpha U_f \left[1 - 0.7 \sqrt{\frac{\theta_c}{\theta}} \right]$$

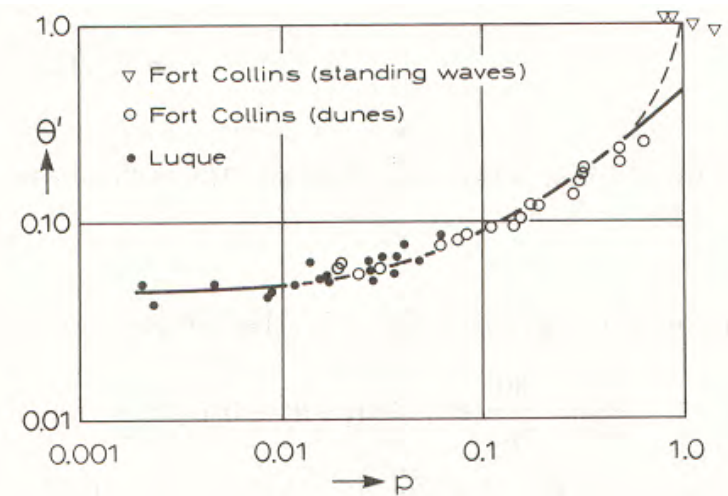


Tau is transferred to the grains as drag, so τ decreases to the critical

$$\tau_b = \tau_c + nF_D$$

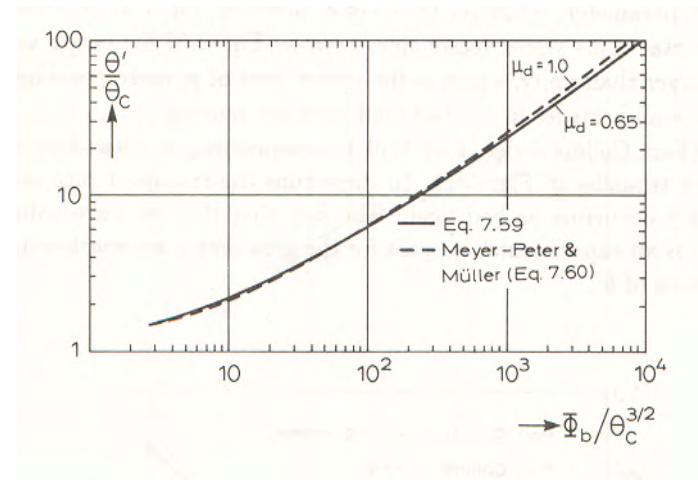
$$\theta = \frac{\tau_b}{\rho g (s-1) d}$$

$$\theta = \theta_c + \frac{\pi}{6} \mu_d p$$



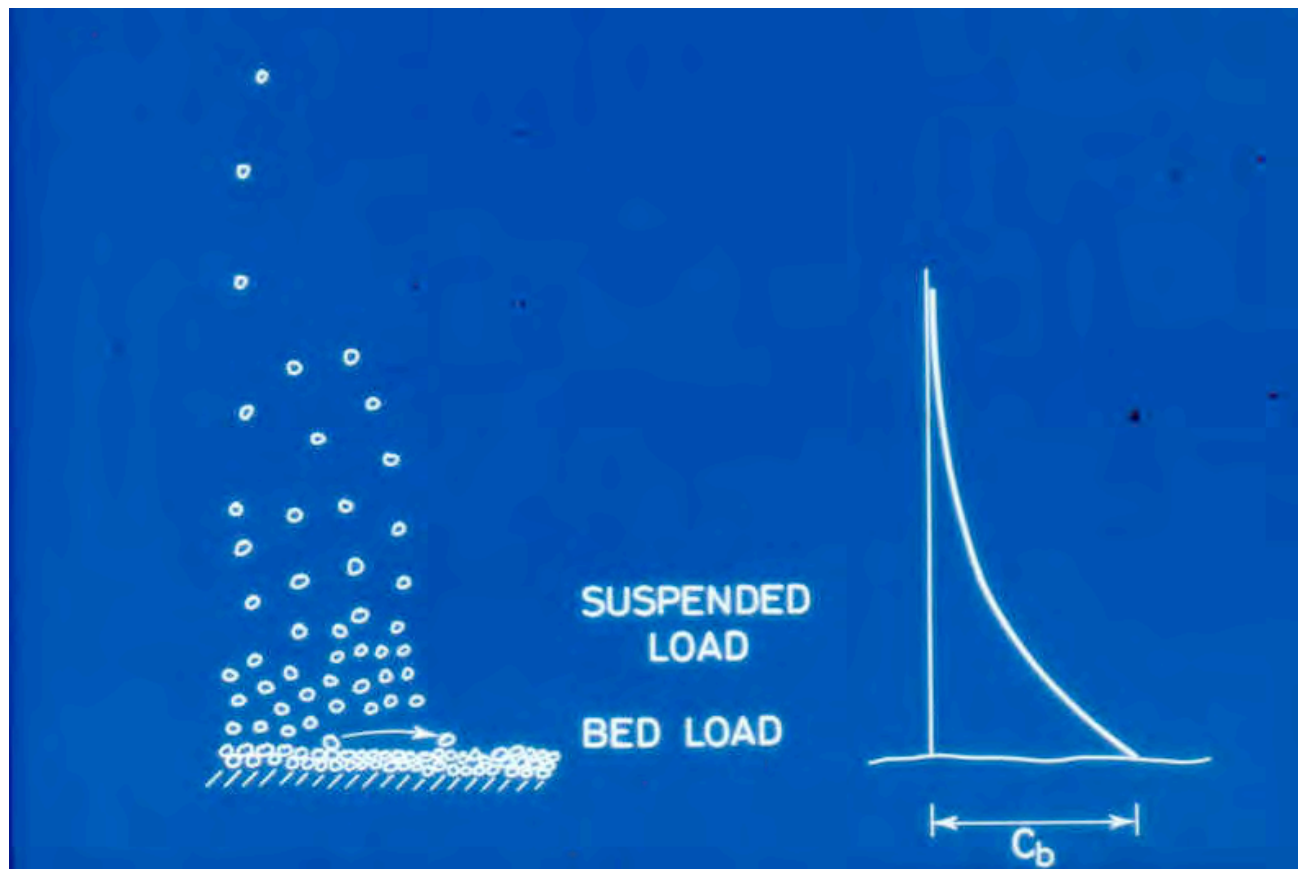
$$q_b = \frac{\pi}{6} d^3 \frac{p}{d^2} U_b$$

$$\Phi_b = \frac{q_b}{\sqrt{(s-1)gd^3}} = 8(\theta - \theta_c)^{3/2}$$



$$C = C_b \left(\frac{D-z}{z} \frac{b}{D-b} \right)^Z$$

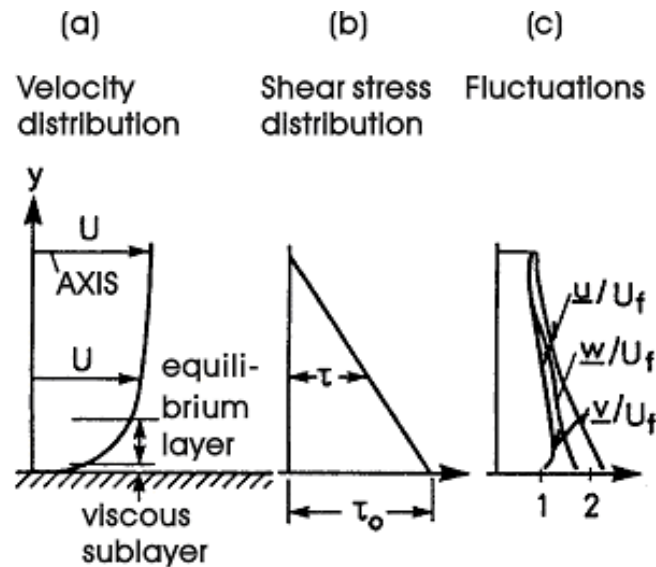
$$Z = \frac{w}{\kappa U_f}$$



Suspended sediment

- Requirement for a bed particle to go into suspension

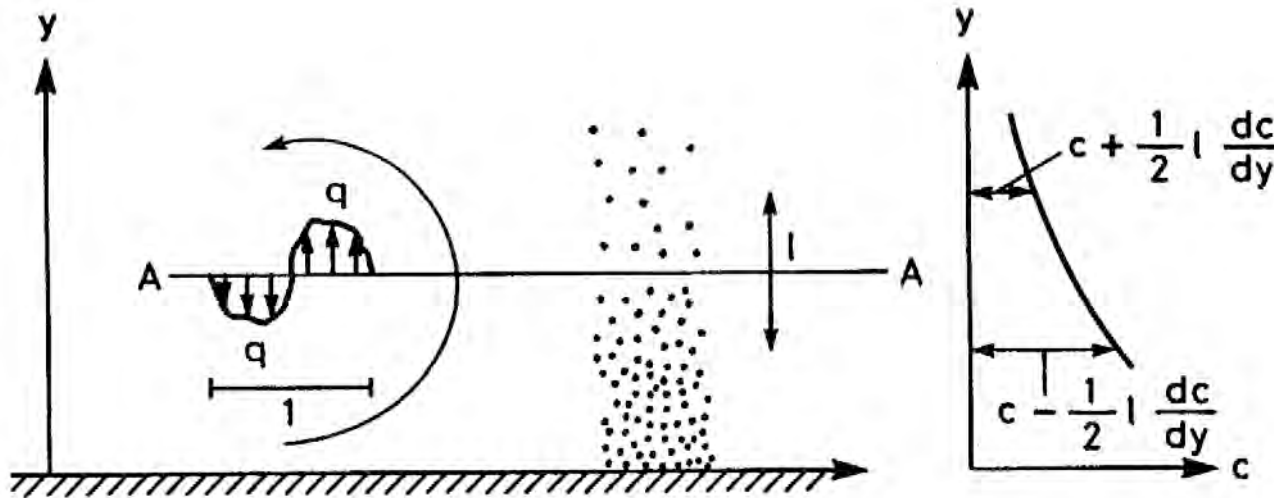
$$\frac{w_s}{U_f} \leq 0.8 - 1.0$$



Settling=diffusion

mixing length= l , vertical velocity fluctuation= Λ

$$cw + \frac{1}{2} v l \frac{dc}{dy} = 0$$



Problems

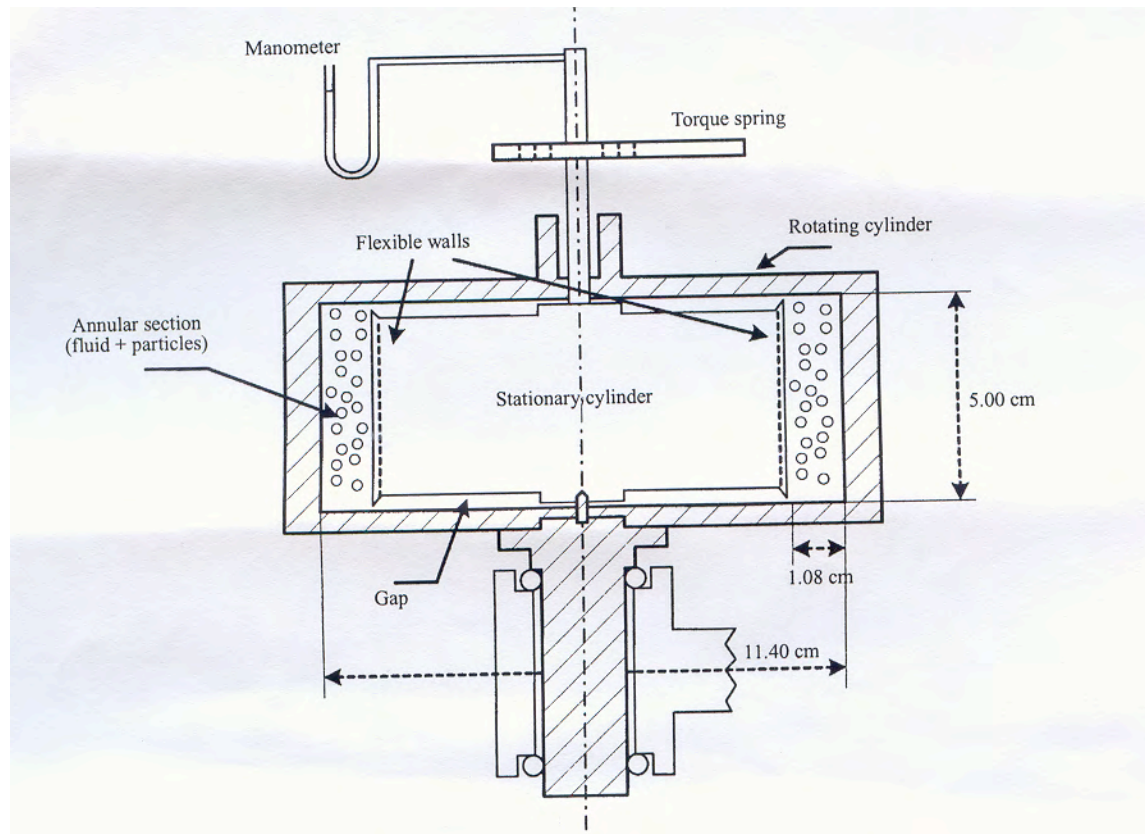
Bed concentration

Influence of coherent structures in the
turbulence

Bagnold 1954

Experiments on a gravity-free dispersion of large solid spheres in a Newtonian fluid under shear

By R. A. BAGNOLD, F.R.S.



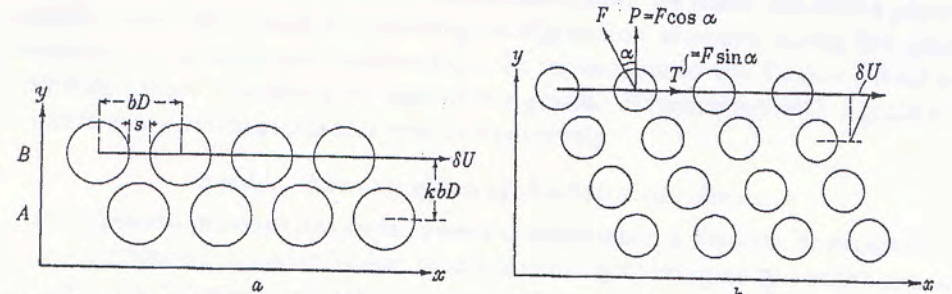
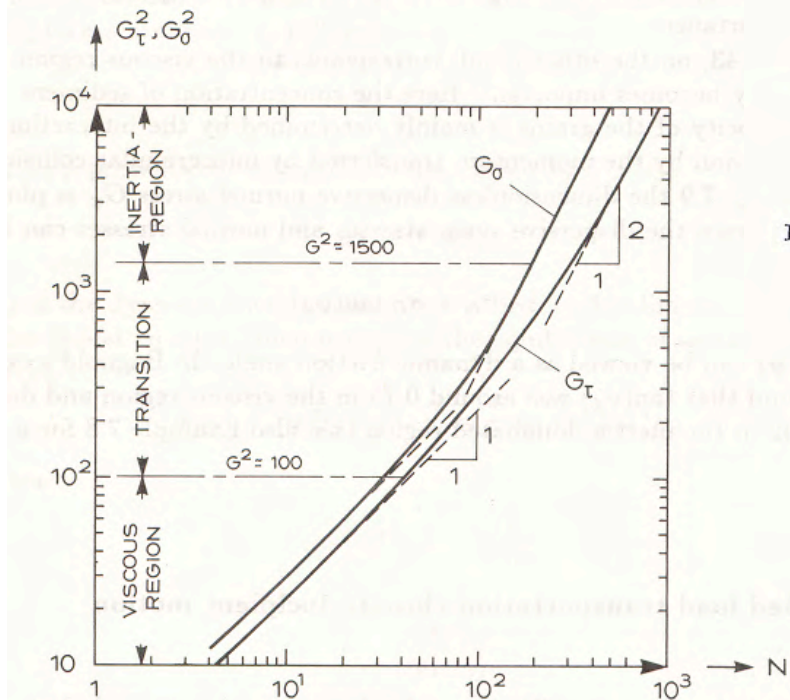


FIGURE 1. *a*, Cross-section of equidistant grain arrangement (three-dimensional). (Grains of alternate layers displaced in z -direction.) *b*, Two-dimensional sketch of possible statistically preferred grain arrangement (non-equidistant) which might allow of dispersive pressure proportional to shear stress, in a viscous fluid.

J. Fluid Mech. (2002), vol. 452, pp. 1–24. © 2002 Cambridge University Press
DOI: 10.1017/S0022112001006577 Printed in the United Kingdom

Revisiting the 1954 suspension experiments of R. A. Bagnold

By M. L. HUNT¹, R. ZENIT², C. S. CAMPBELL³
AND C. E. BRENNEN¹

$$\mu' = \mu(1 - \phi / \phi_m)^{2.5\phi_m}$$

ϕ =solid fraction, =0.64

Bagnold-1954

$$\frac{\sigma}{\rho} = 0.013s \left(\lambda d \frac{dU}{dz} \right)^2$$

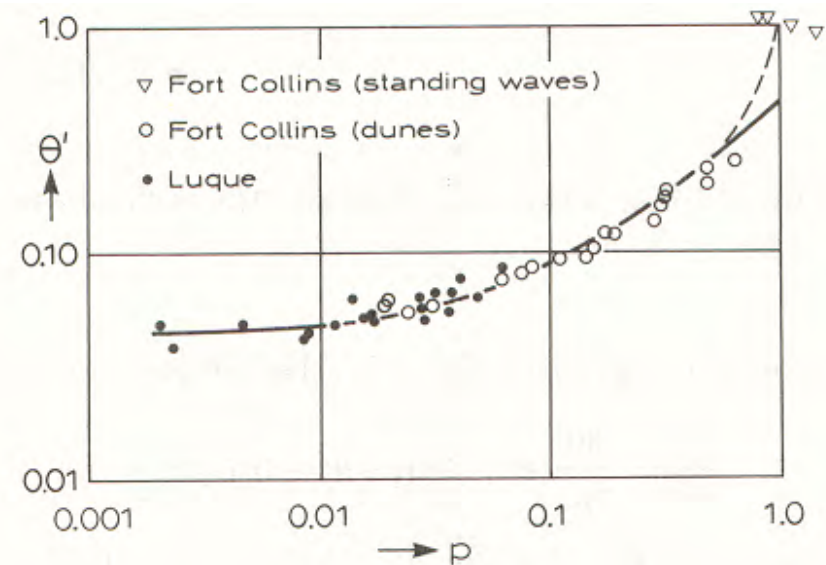
$$c = \frac{0.65}{(1 + 1/\lambda)^3}$$

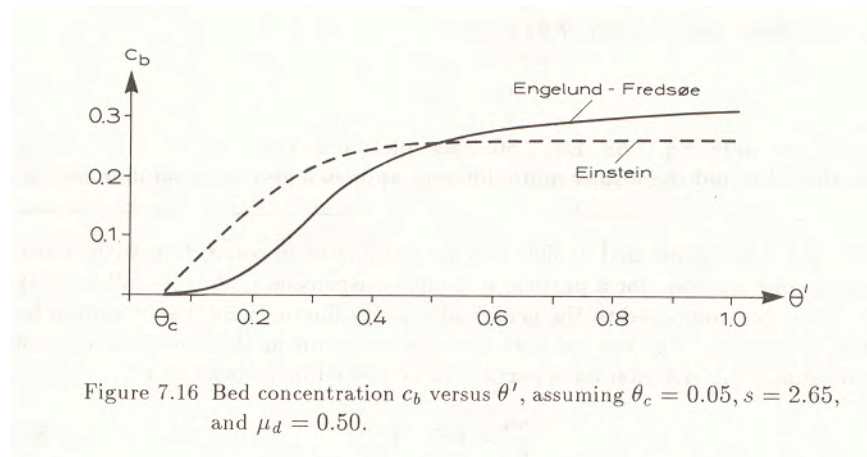
Bed concentration of suspended sediment

$$\frac{\tau_s}{\rho} = 0.013s \left(\lambda d \frac{dU}{dz} \right)^2$$

$$\tau_b = \tau_c + nF_D + \tau_s$$

$$\tau_s = \frac{0.013}{K^2} s \theta \lambda_b^2$$





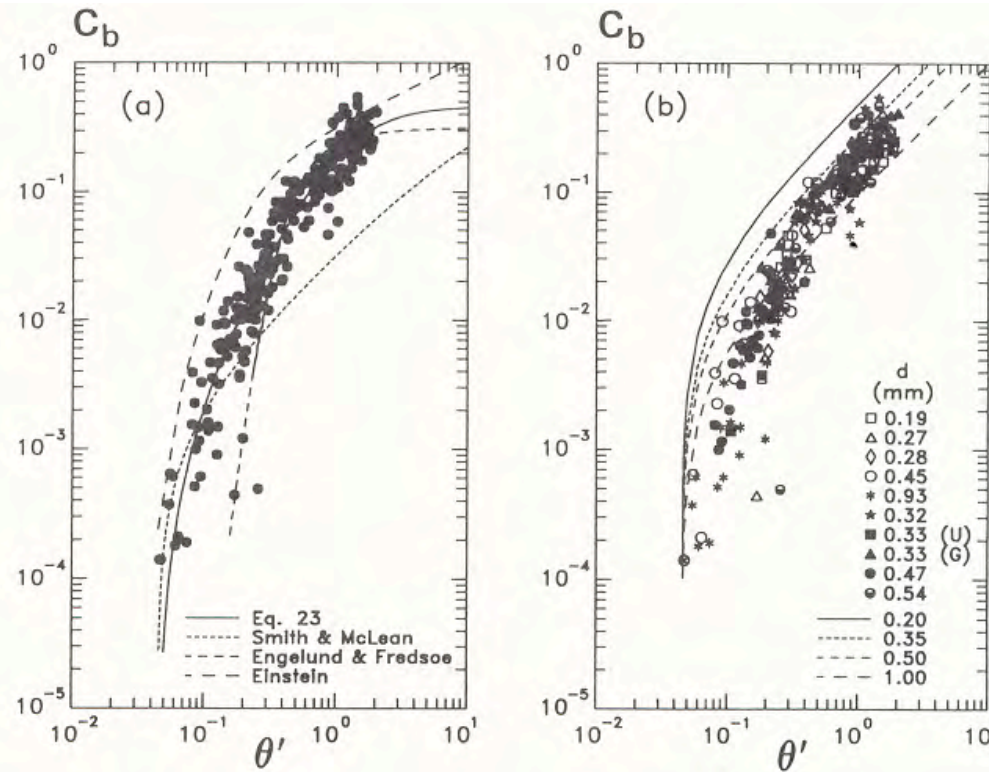


FIG. 7(a). Comparison of Einstein's, Smith and McLean's, and Engelund and Fredsøe's Formulations to Values of c_b Determined; and (b) Comparison of van Rijn's Relation for c_b to Experimental Values

Sheet flow

- Wilson 1966:”The moving solid particles appeared generally to be travelling in a dense layer immediately above the bed supported by intergranular collisions rather than by fluid turbulence”

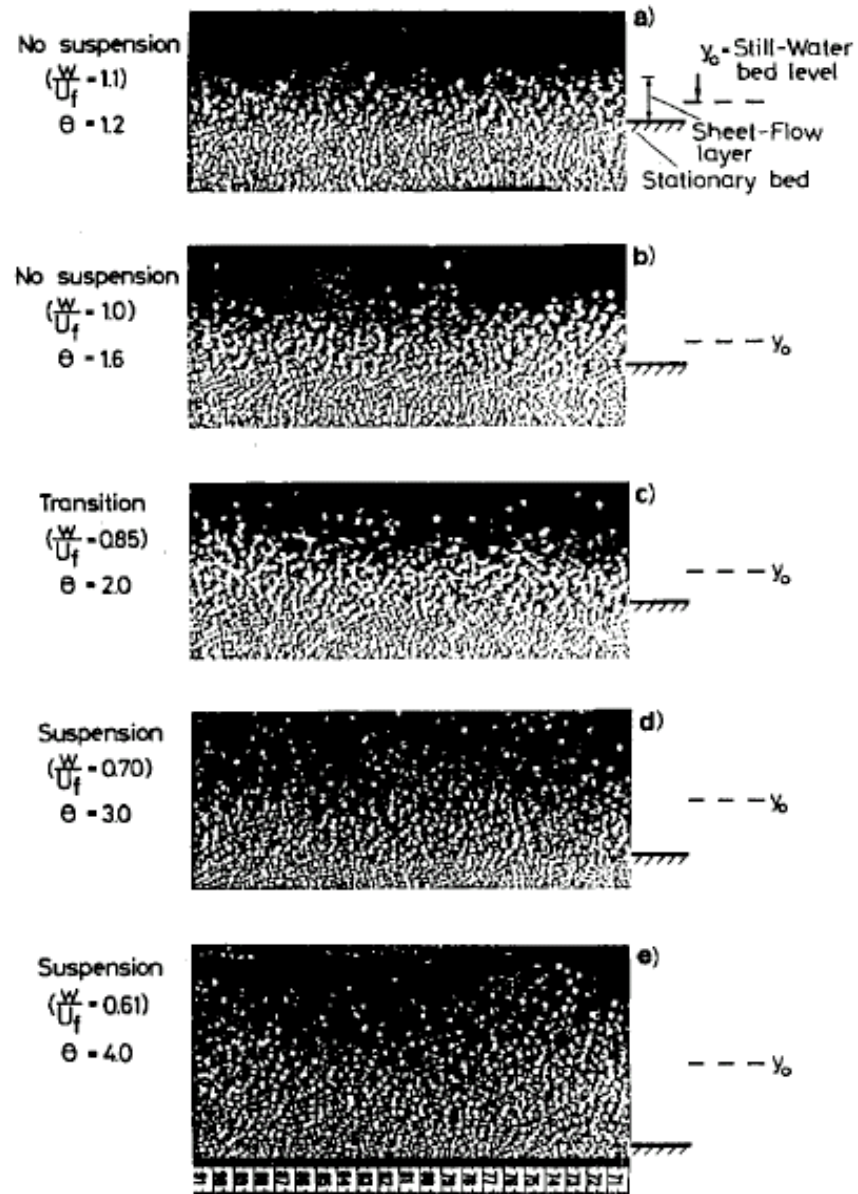


FIG. 4. Sequence illustrating Transition from "No Suspension" Sheet-Flow Regime to "Suspension" Sheet-Flow Regime for Tests Referred to in Fig. 3(b): (a) $\theta = 1.2$; (b) $\theta = 1.6$; (c) $\theta = 2.0$; (d) $\theta = 3.0$; (e) $\theta = 4.0$

Break: Sheet flow movie

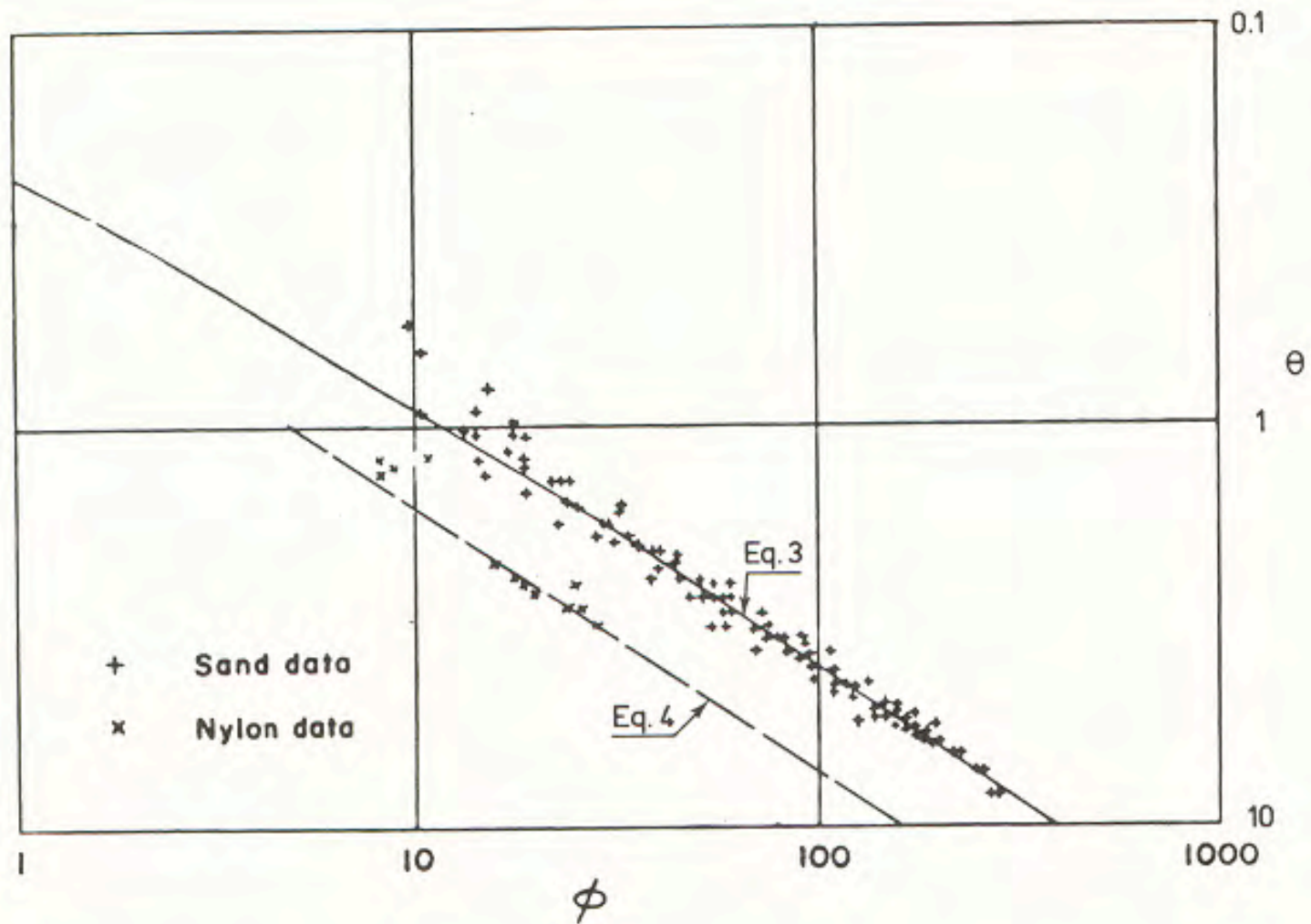
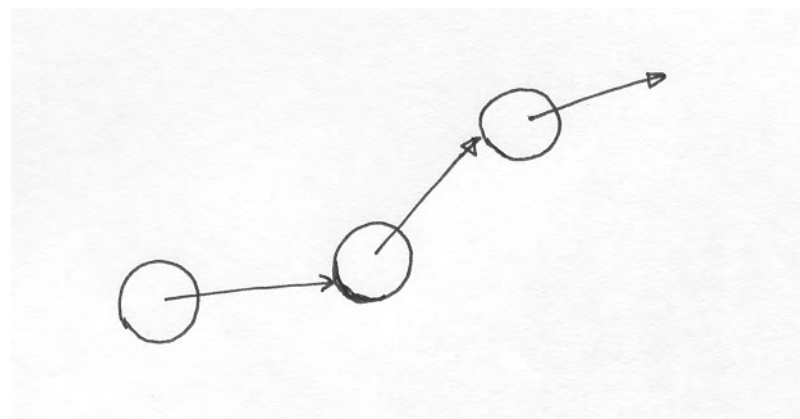


Fig. 1. Wilson's experimental data, Ref. [2].

Collisions between particles create a stress field (a particle pressure P or σ)

- Jenkins(1987) kinetic theory for rapid grain flow
- Jenkins and Hanes (JFM 1998): turbulent velocity fluctuations neglected
- Hsu, Jenkins and Liu (Proc Royal Soc 2004): incl description of turbulence



A simple sheet flow model(Engelund 1981)

- Based on Bagnolds expression
- Assumes the particles to move with max concentration in a layer of considerable thickness - compared to the grain diameter

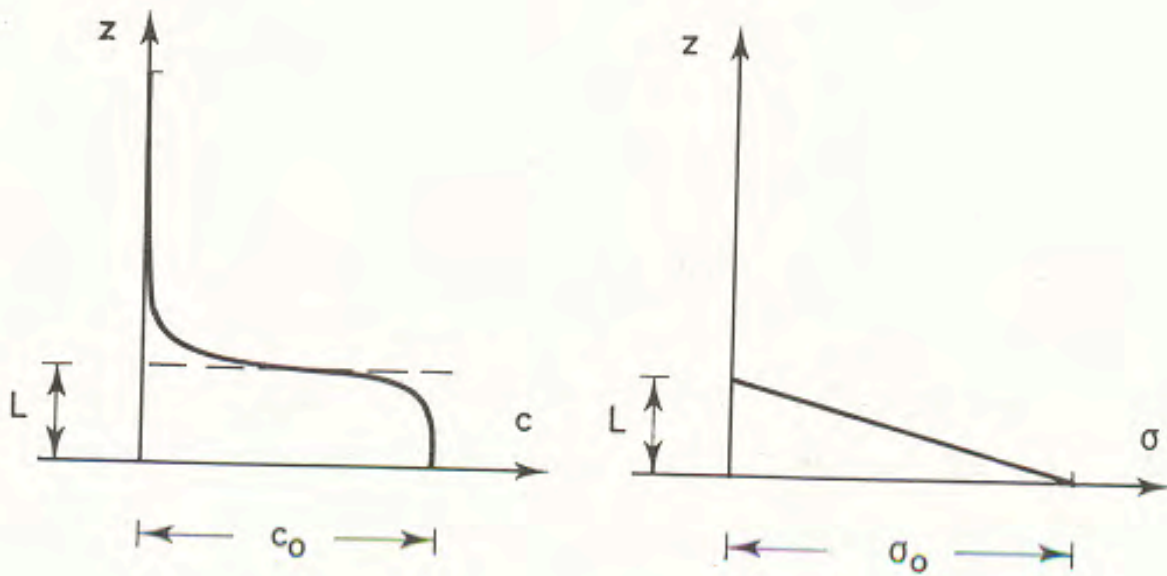


Fig. 2. Distribution of sediment concentration c and dispersive stress σ .

$$(\rho_s - \rho_f)cg + \frac{d\sigma}{dz} = 0$$

or

$$\frac{d\left(\frac{\sigma}{\rho}\right)}{dz} = -c(s-1)g$$

$$\frac{\sigma_0}{\rho} = c_0(s-1)gL$$

$$\frac{dU}{dz} = \frac{U_f}{\kappa z},$$

$$z = d$$

$$\frac{\sigma_0}{\rho} = 0.013s \left(\lambda_0 d \frac{dU}{dz} \right)^2$$

$$= 0.013s \left(\lambda_0 d \frac{U_f}{\kappa d} \right)^2 \approx 1.3s U_f^2$$

$$d^p = c^0 \Gamma \Omega^B$$

$$U_B = K U_f$$

$$K = 10.5$$

$$c_0 = .33$$

$$\frac{L}{d} = 1.3s\theta$$

$$\Phi_b = 4.5s\theta^{3/2}$$

$s=2.670$: eq3

$s=1.138$: eq4

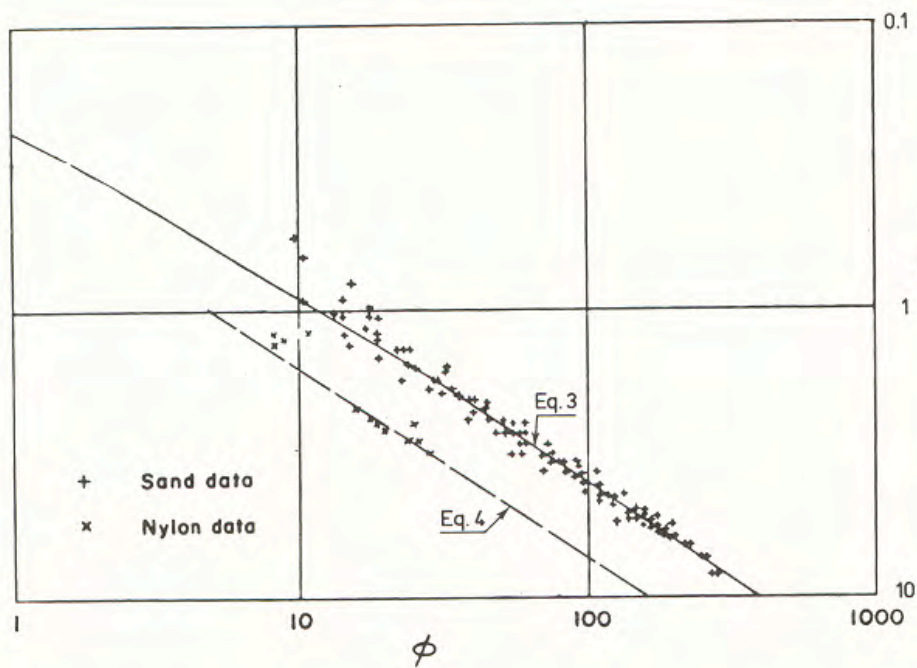


Fig. 1. Wilson's experimental data, Ref. [2].

$$\Phi = 12(\theta - \theta_c)^{3/2}$$

$$\Phi = 5(\theta - \theta_c)^{3/2}$$

Hsu et al, 2004

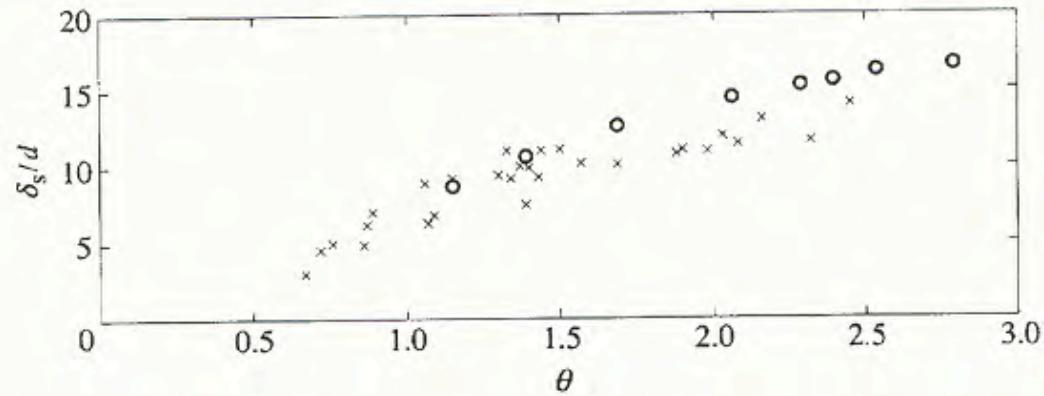


Figure 5. Comparison of sheet layer thickness δ_s . \circ , results from the present model; \times , visual observations by Sumer *et al.*

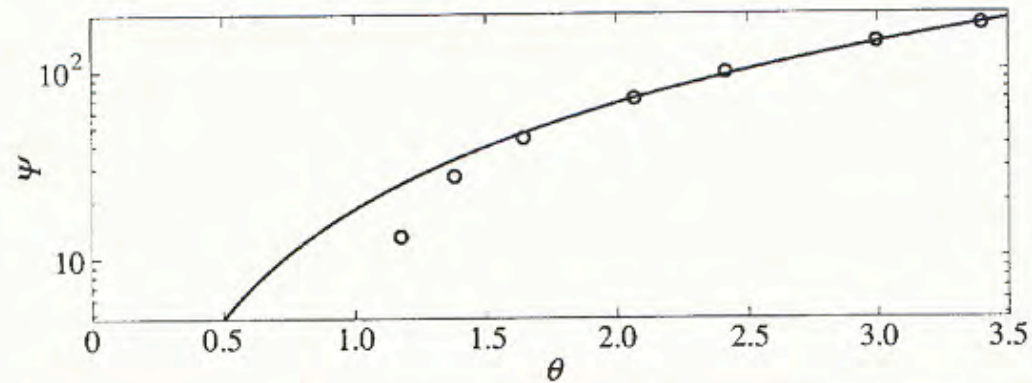


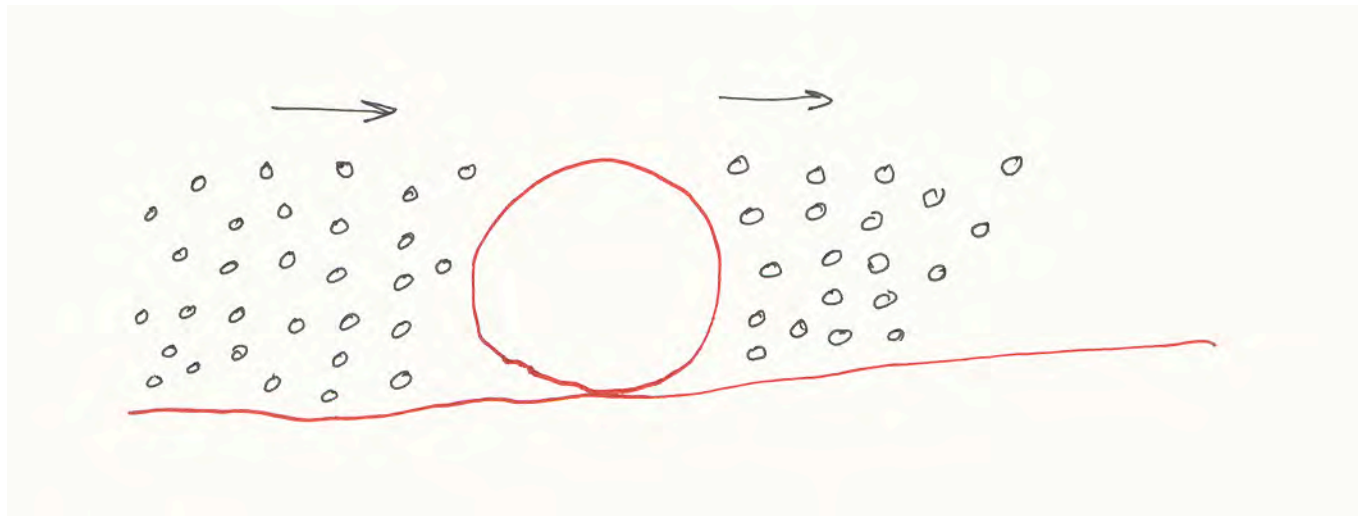
Figure 6. Non-dimensional total sediment transport rate $\Psi = q_s / (d\sqrt{(s-1)gd})$ with respect to the Shields parameter. \circ , Results from the present model; —, $\Psi = 20.0(\theta - 0.05)^{1.8}$.

Sediment mixtures



$$F_d = \frac{1}{2} \rho c_D [\alpha U_f - U_B]^2 \frac{\pi}{4} d^2$$

$$F_s = W \mu_d = \frac{\pi}{6} \rho g (s - 1) d^3 \mu_d$$



Bed forms: not in sheet flow

Flow direction :
bottom right to
top left corner



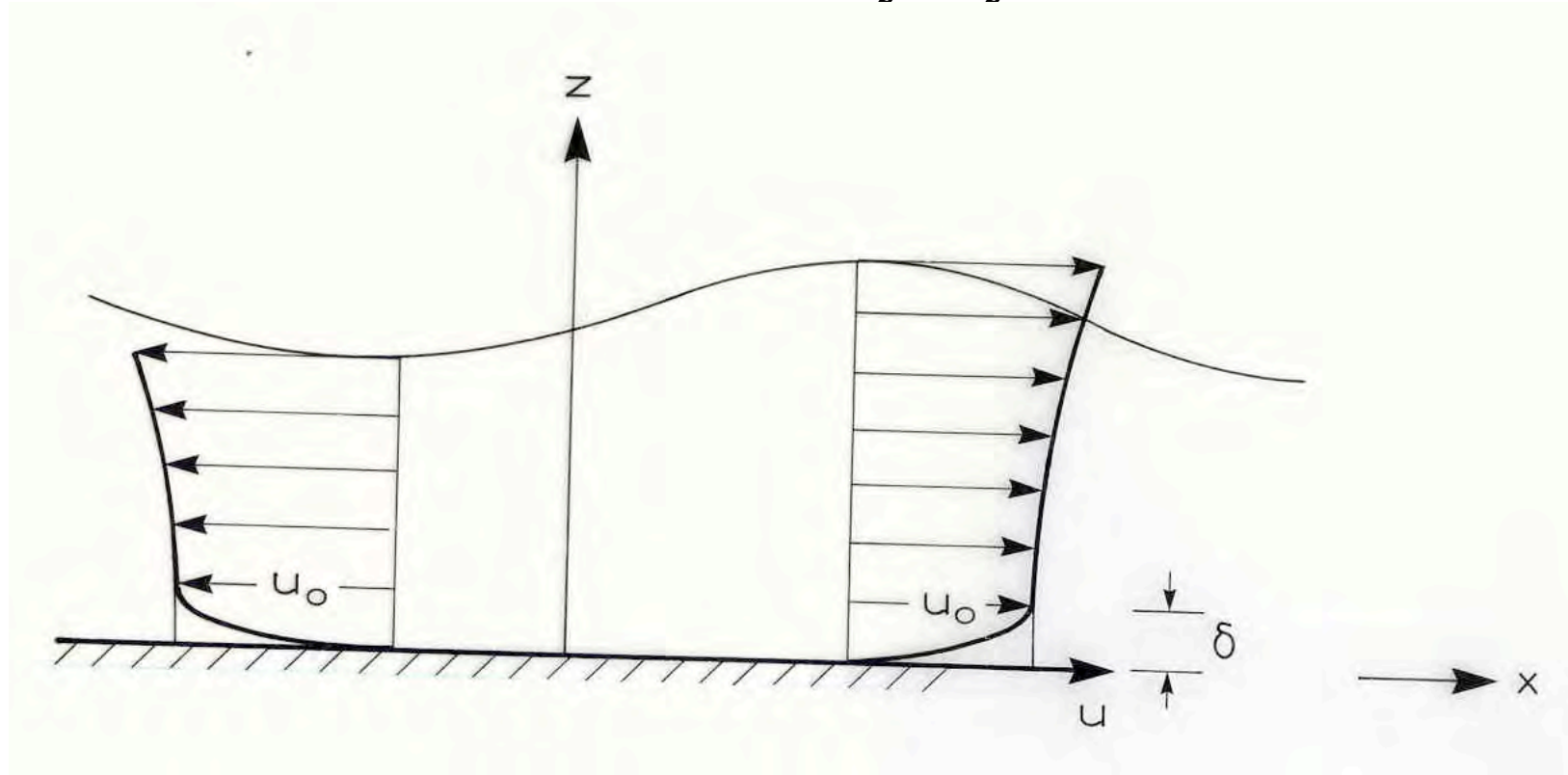
Conclusions:

- Sediment transport in a tsunami will usually be as sheet flow and in suspension.
- Models are available for the sheet flow in current
- Coarse sediment will be transported as bedload, but might be easier mobilized due to presence of fine sediment
 - The transition from the sheet flow layer to the suspended sediment is not fully described, and the bottom boundary condition for the suspended sediment needs clarification
 - Transport of mixtures needs to be studied

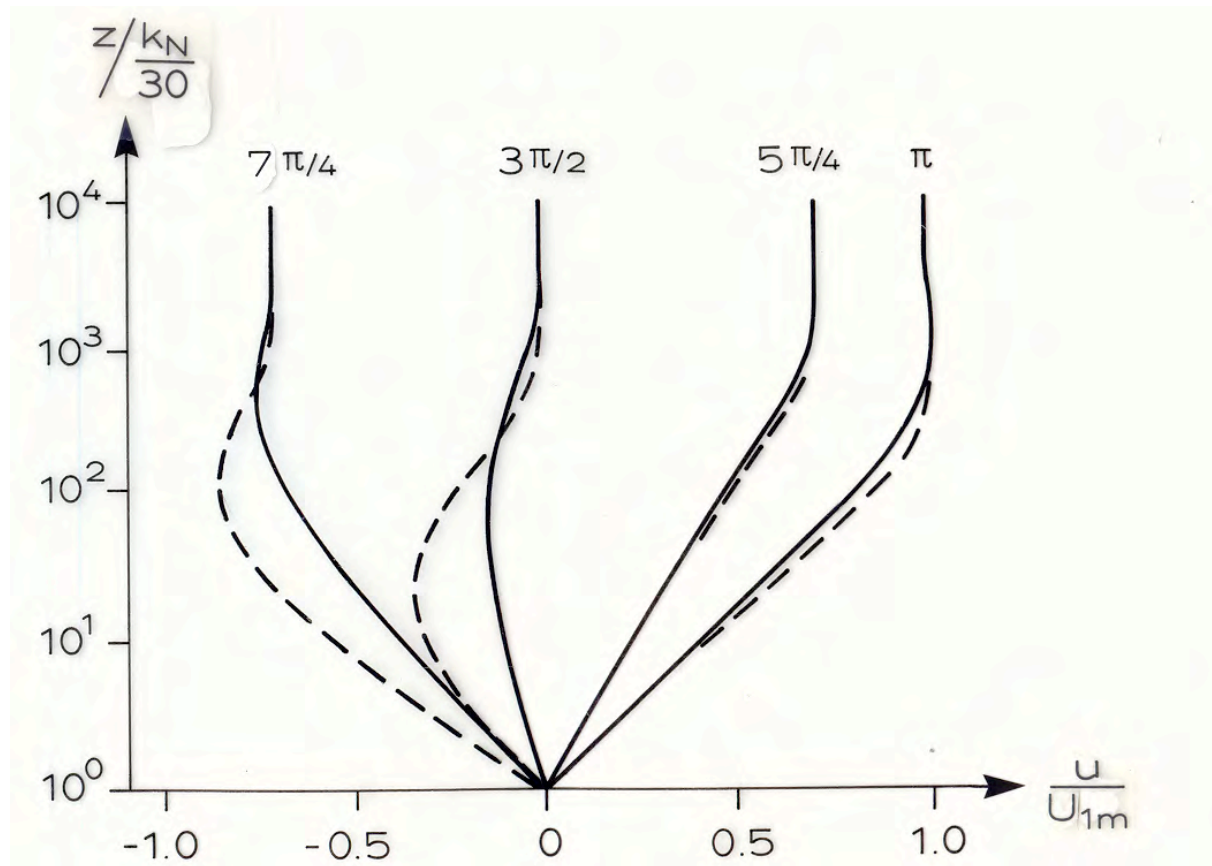
PART 2: SEDIMENTTRANSPORT IN WAVES

- Needed for sediment transport : friction, level of turbulence

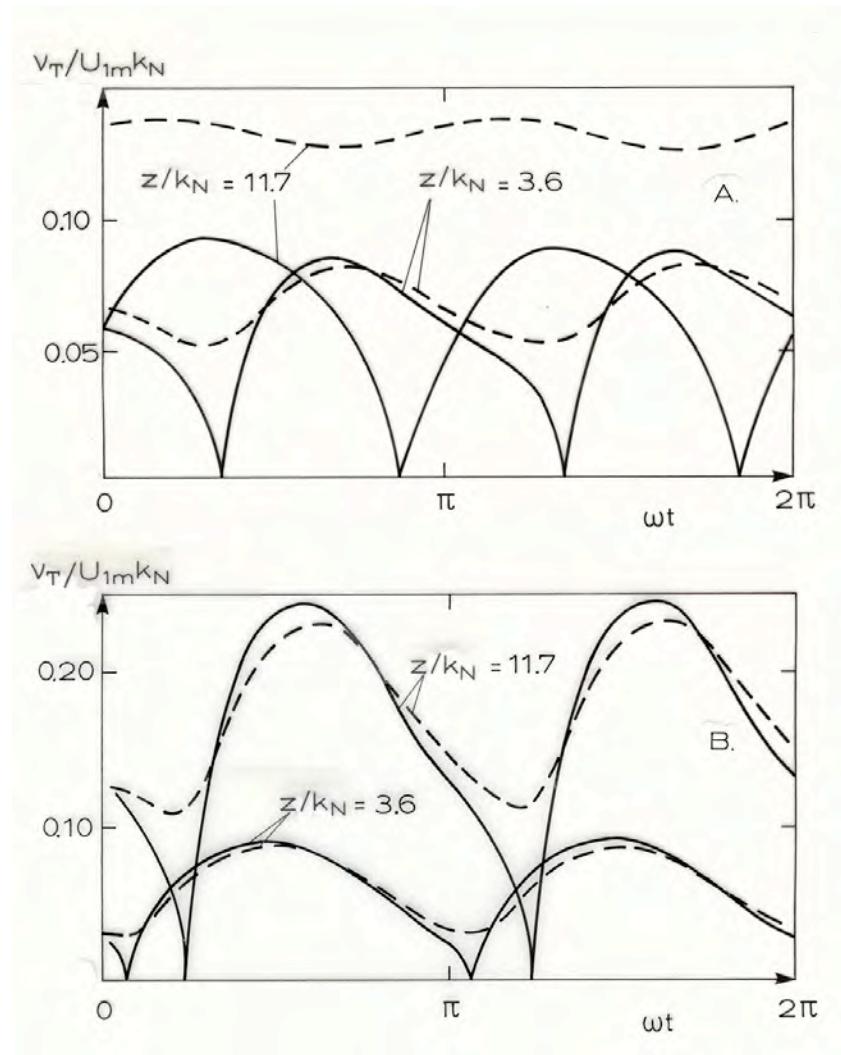
Potential flow and Wave boundary layer



Flow velocities in the wbl



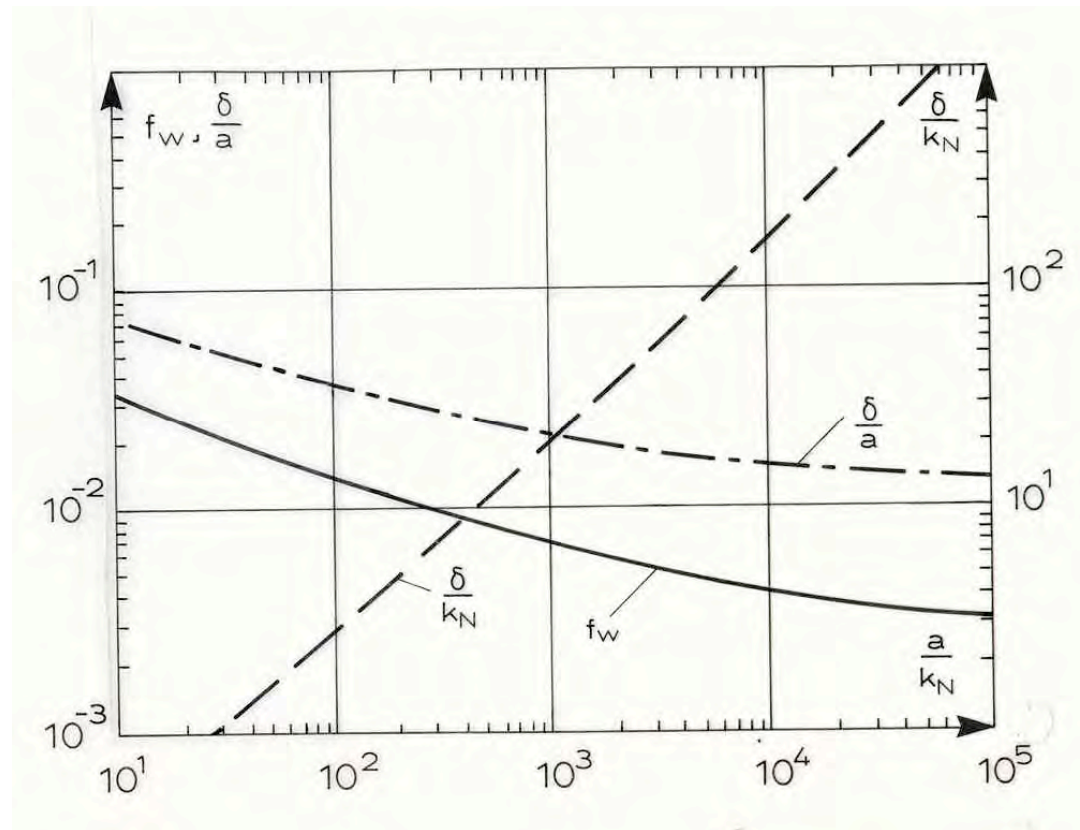
Turbulence level in wbl



Friction factor

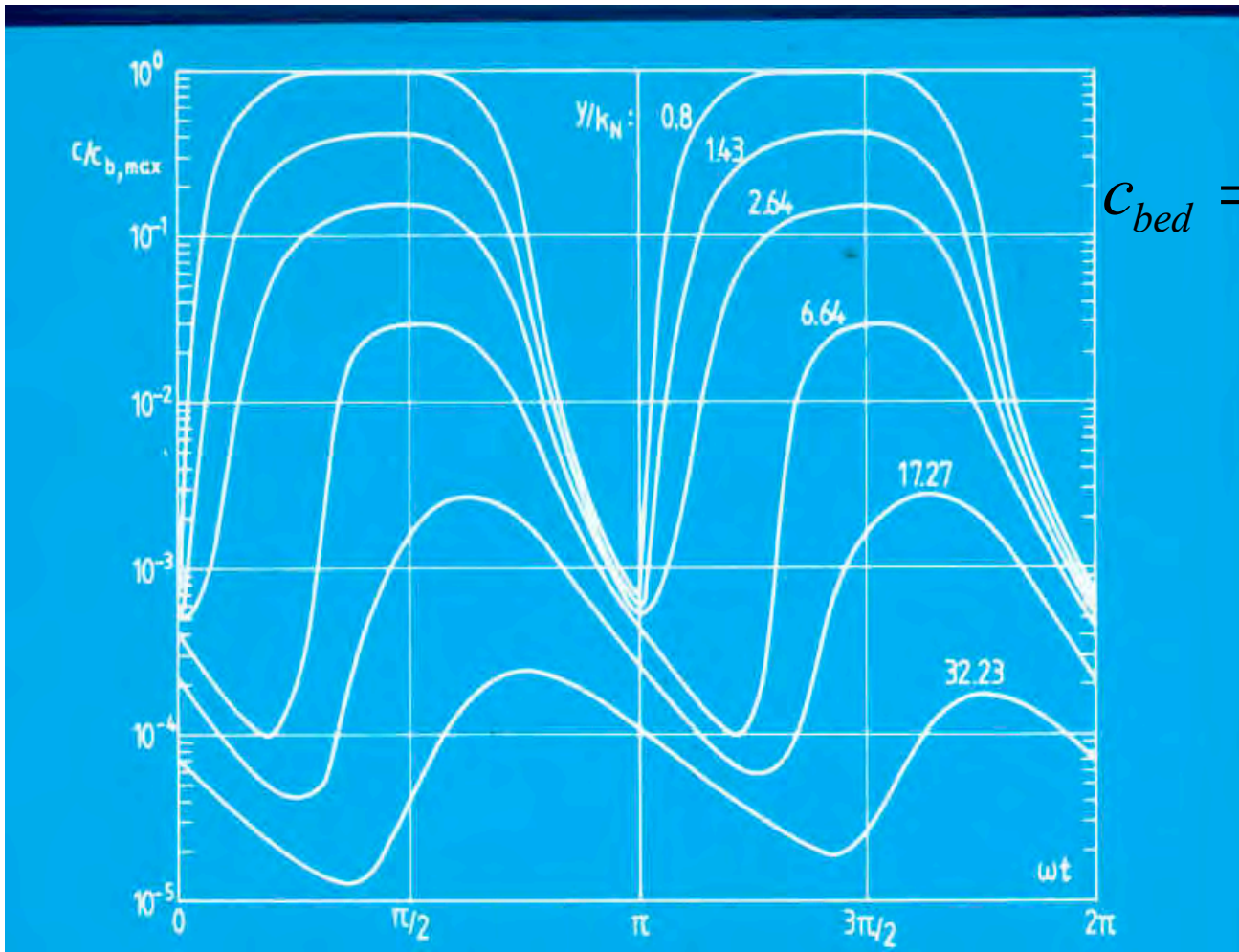
Boundary layer thickness

$$f_w = \frac{1}{2} \rho U_{10}^2$$



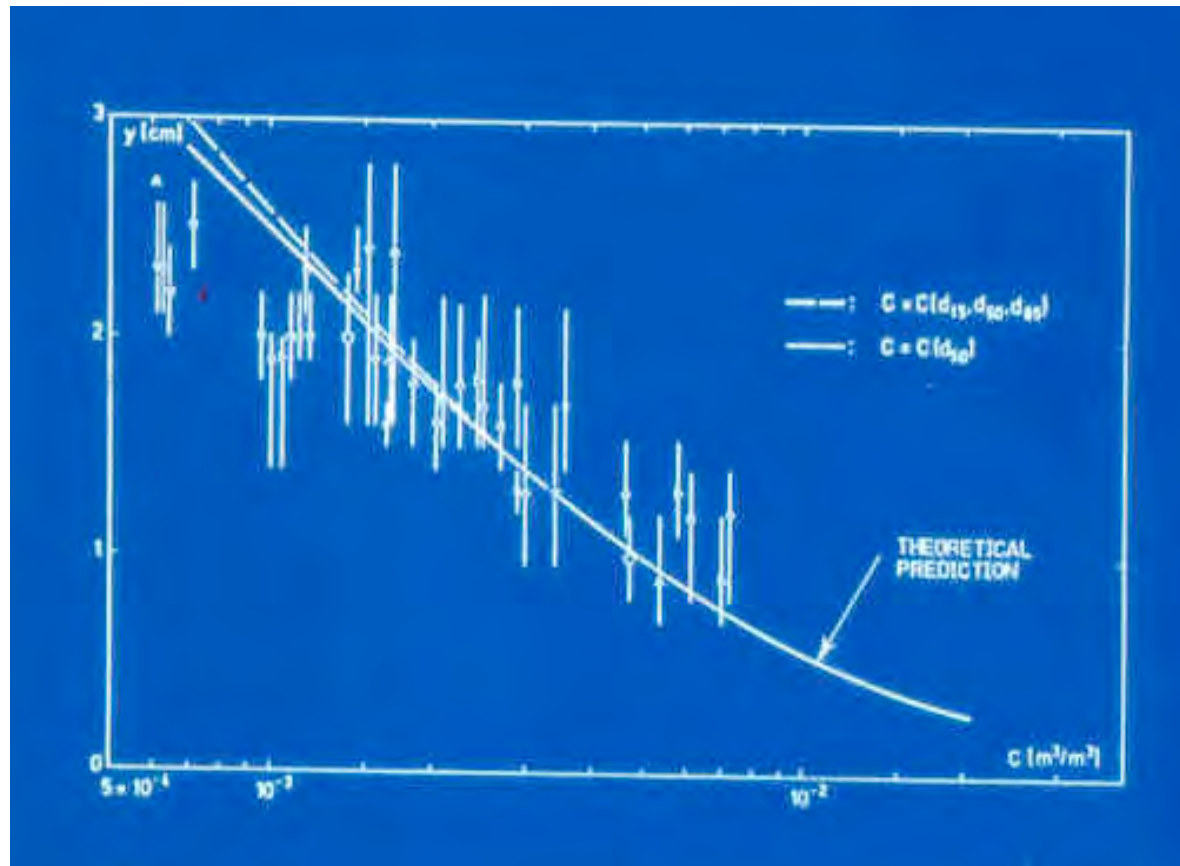
Vertical distribution of sediment

$$\frac{\partial c}{\partial t} = \frac{\partial}{\partial y} \left(wc + \varepsilon \frac{\partial c}{\partial y} \right)$$

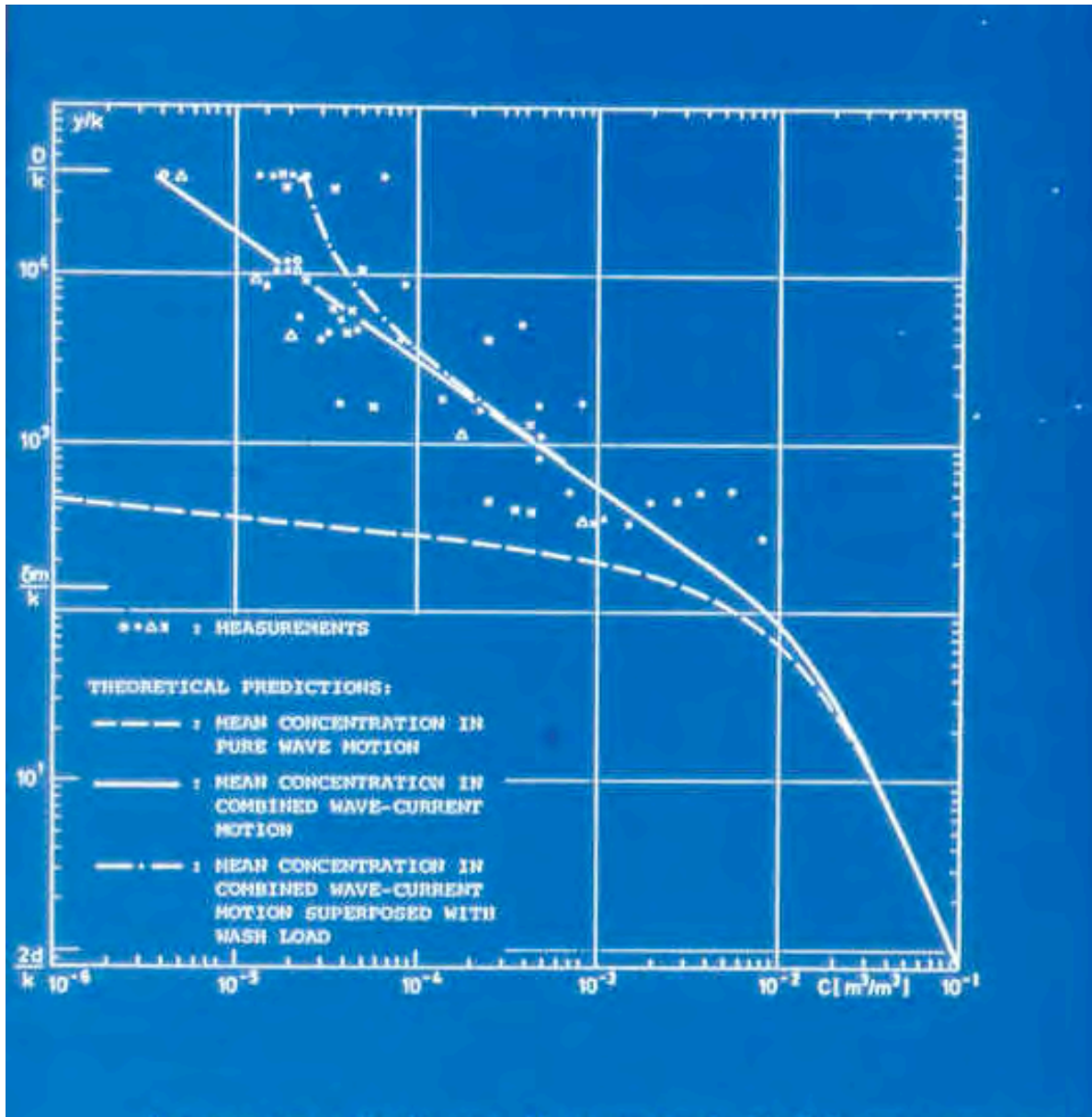


$$c_{bed} = c_b(\theta)$$

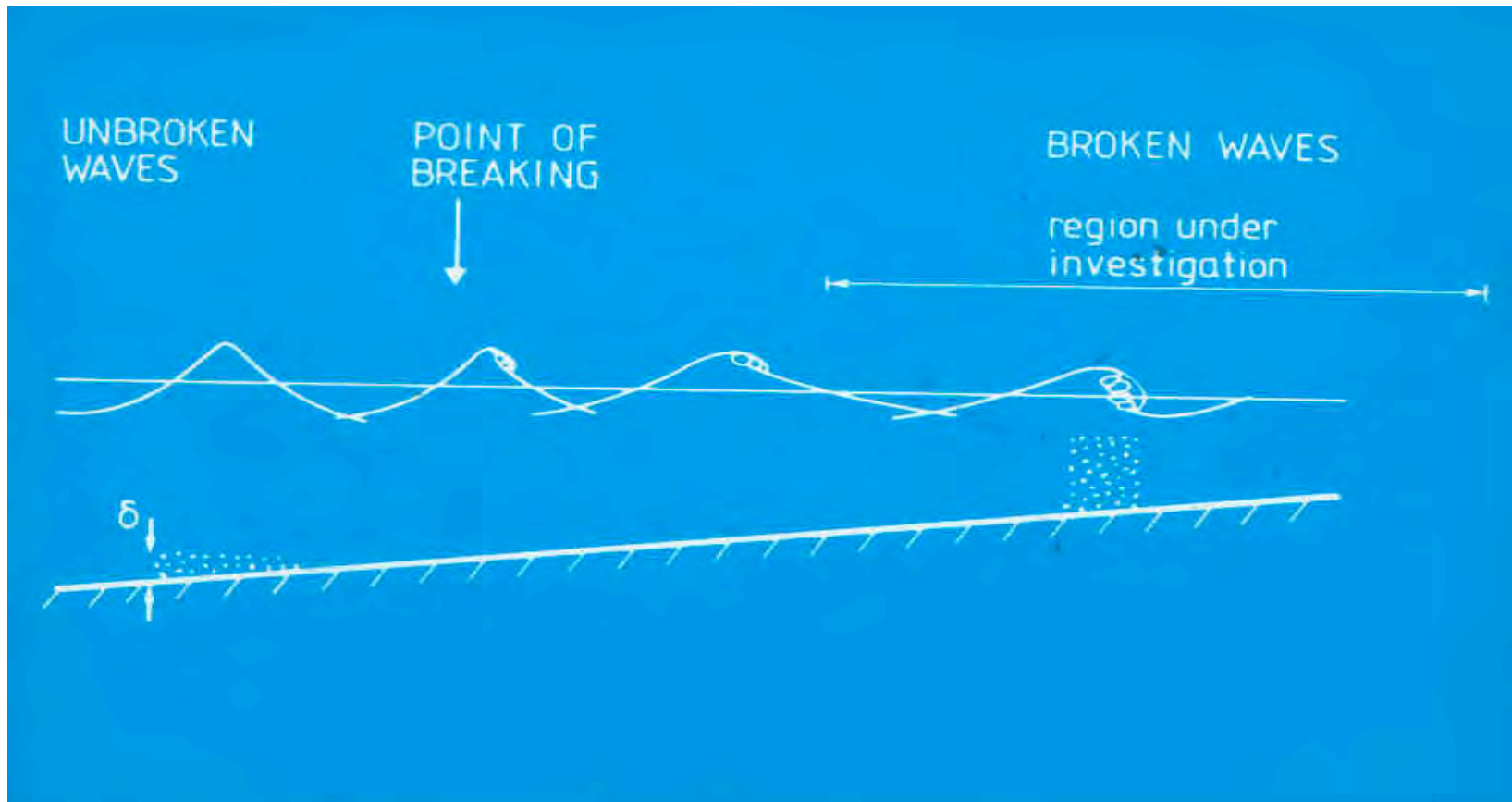
Distribution of suspended sediment: comparison with lab measurements



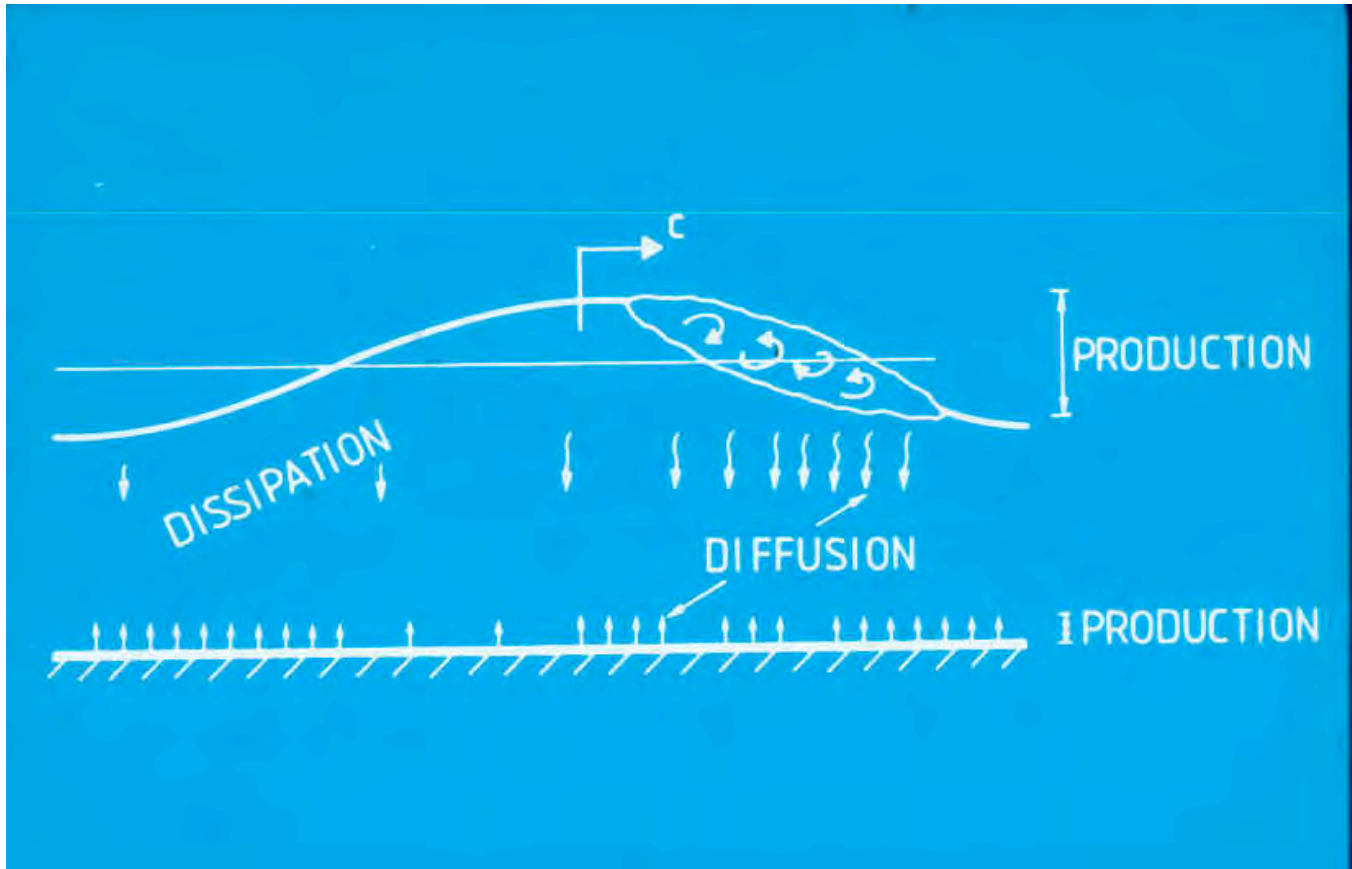
Distribution of suspended sediment: comparison with field measurements



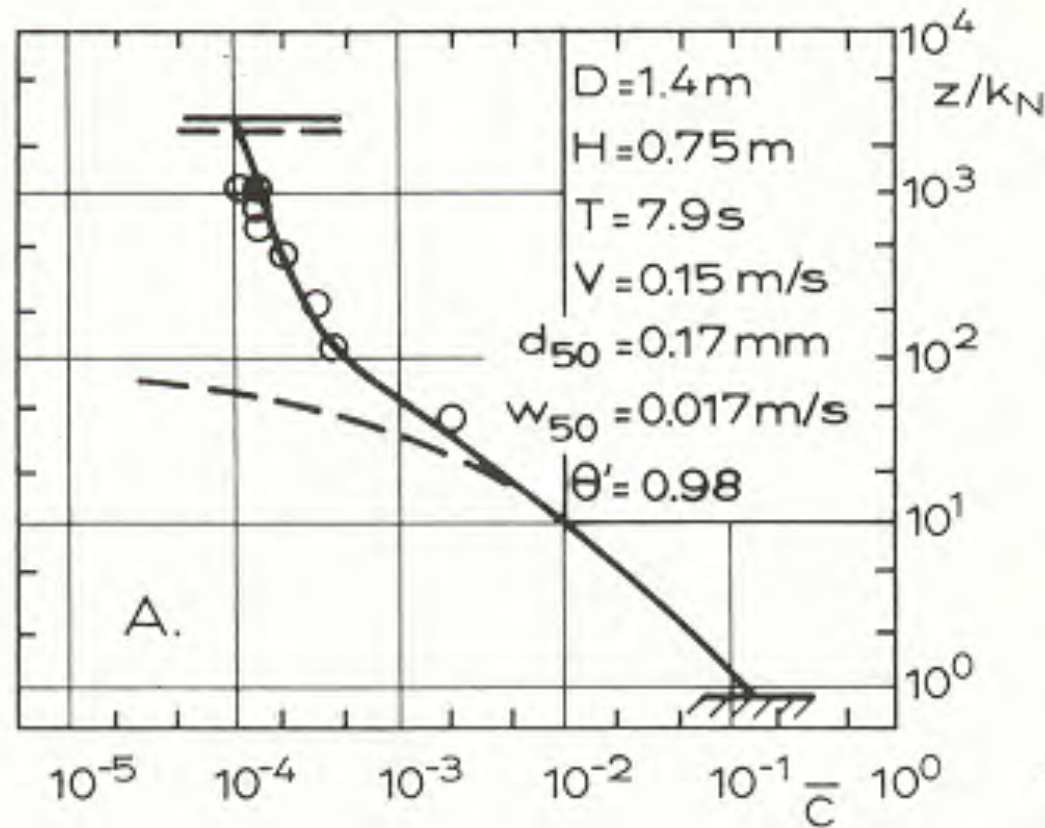
Sediment in broken waves







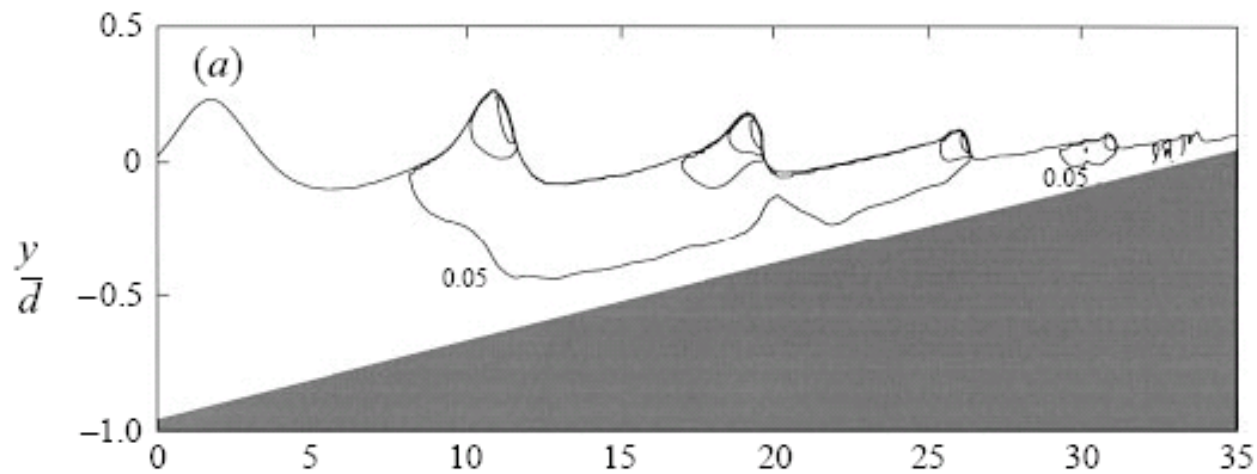
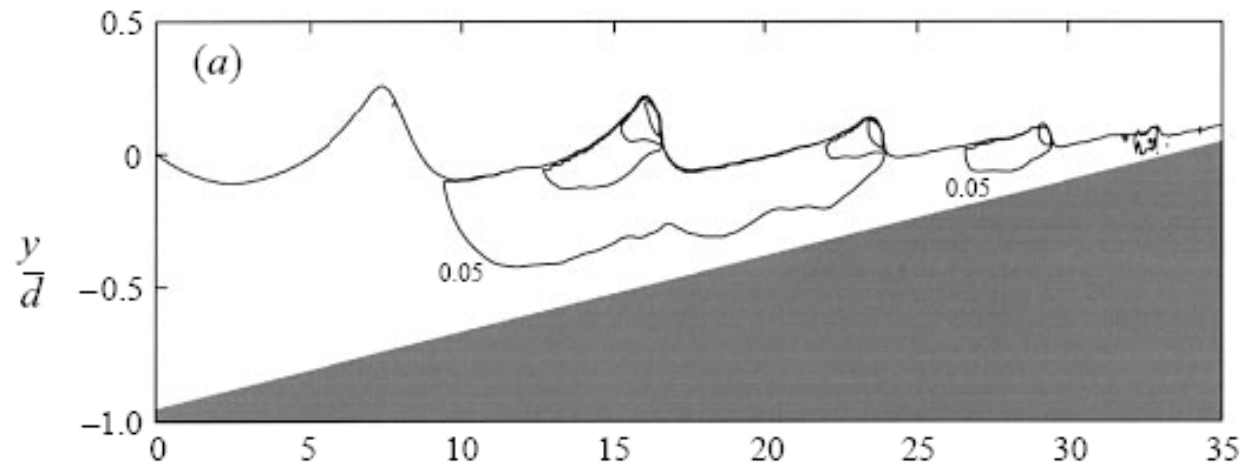
Distribution of sediment in a spilling breaker



Lin and Liu, 1998:

VOF (RIPPLE)+k- ϵ Normalized turbulence intensity

Breaking waves in the surf zone



On or off shore transport

Waves:

Asymmetry in nearbed velocities

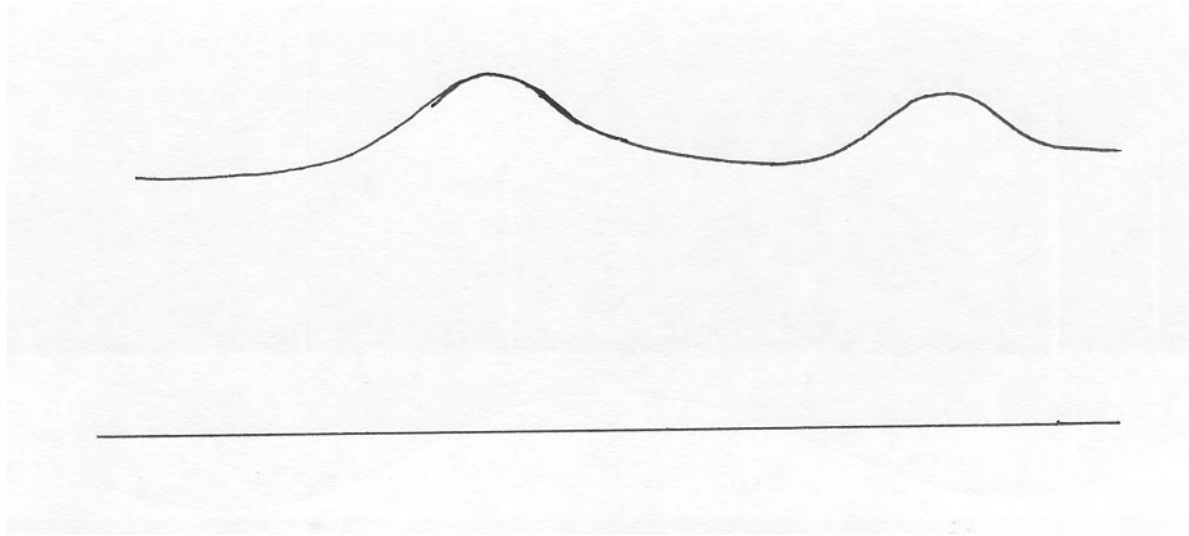
Drift (time averaged)

Streaming (time averaged)

Percolation

Wave breaking: Undertow (timeaveraged)

Wave asymmetry



- Larger flow velocities onshore than offshore
- Sed tr proportional to U^{*3}

Ribberink 2006: wave asymmetry

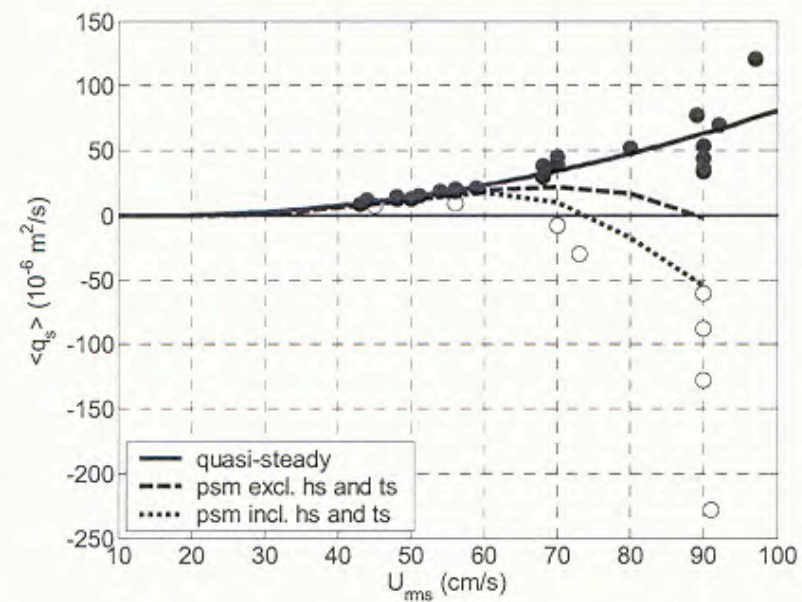
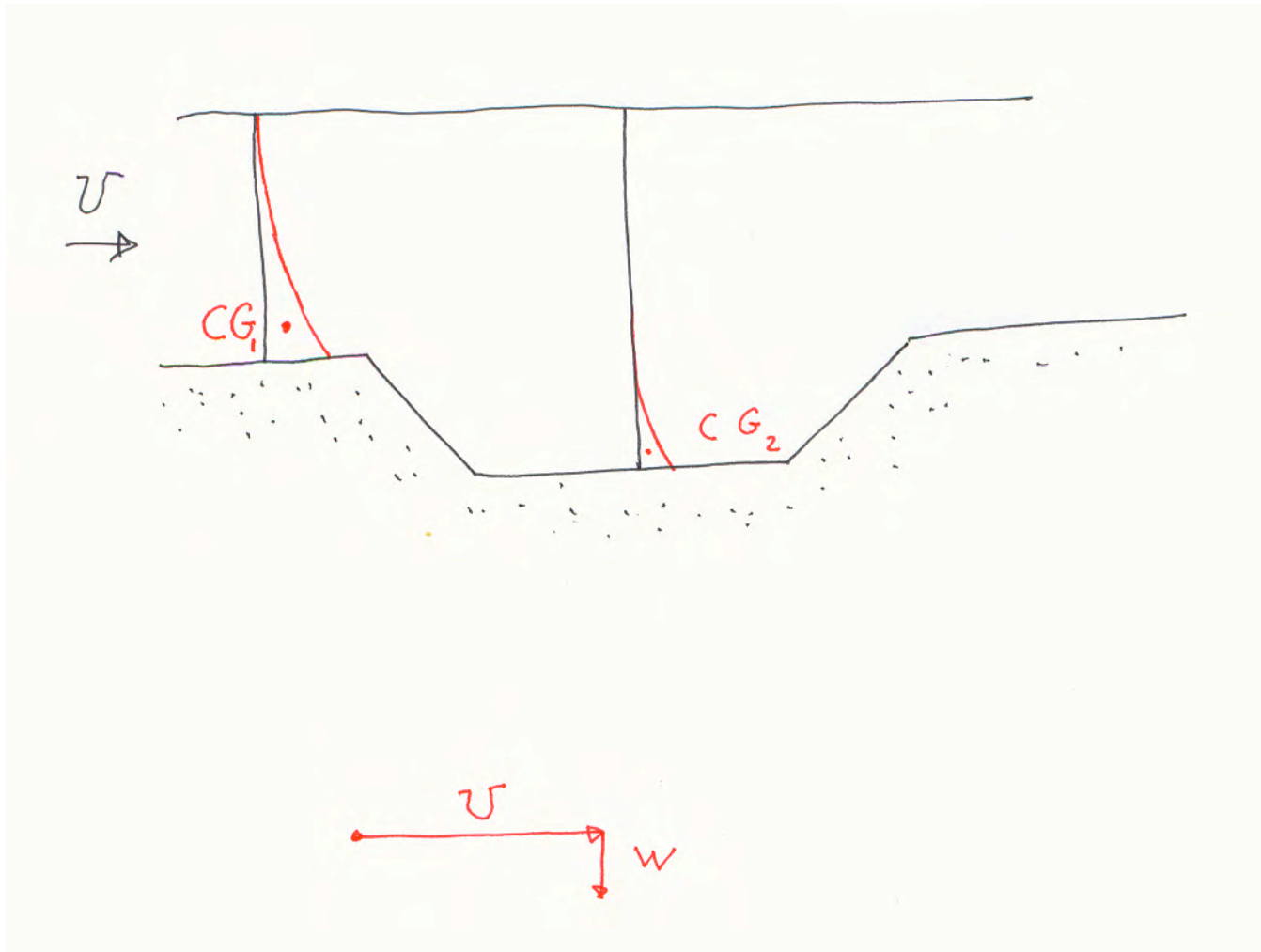
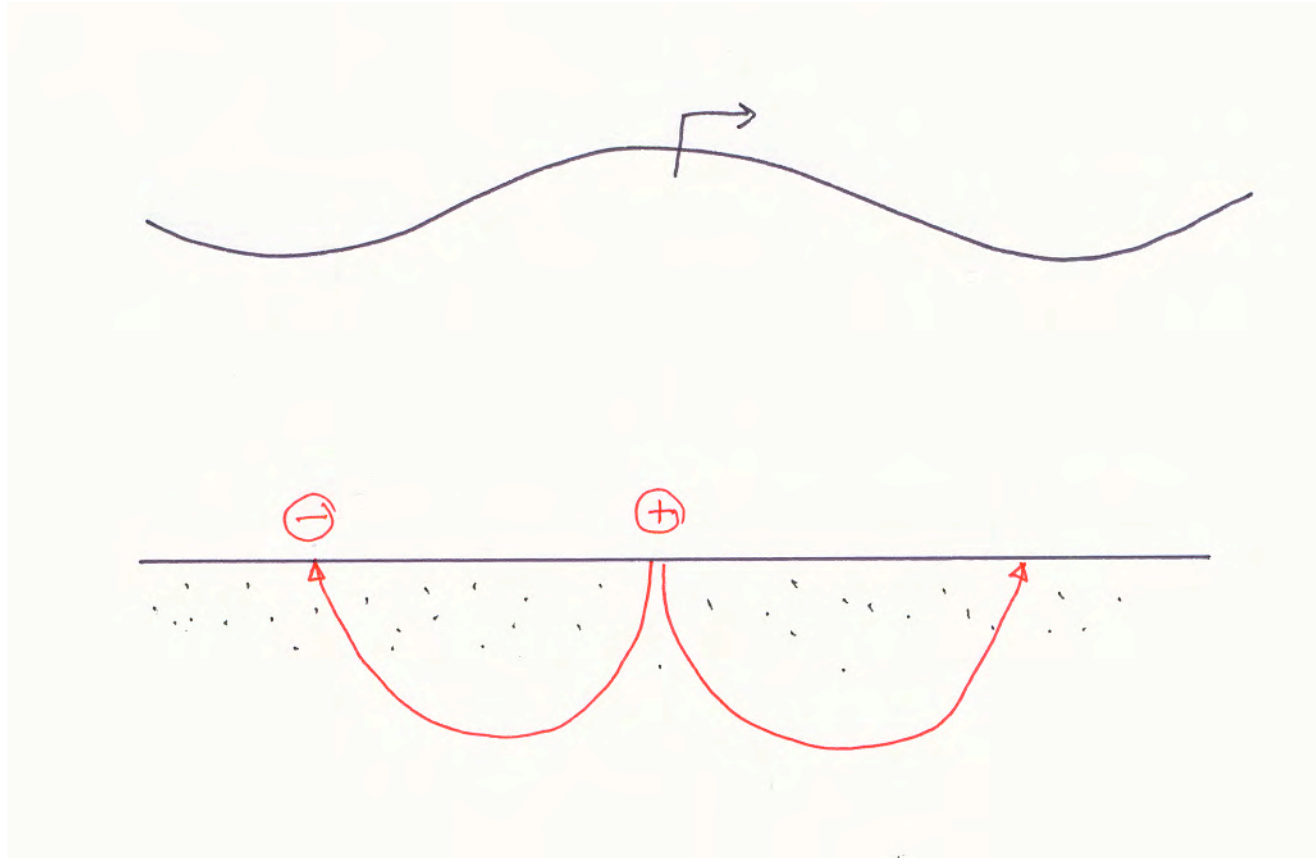


Fig. 7. Measured net transport rates (symbols) and predicted net transport rates with PSM (lines) for asymmetric waves as a function of U_{rms} (sheet flow regime). The solid line and black symbols refer to 3 medium sands (0.21, 0.32, 0.46 mm), the dashed lines and open symbols refer to 2 fine sands (0.13, 0.15 mm).

Adaptation length – or time



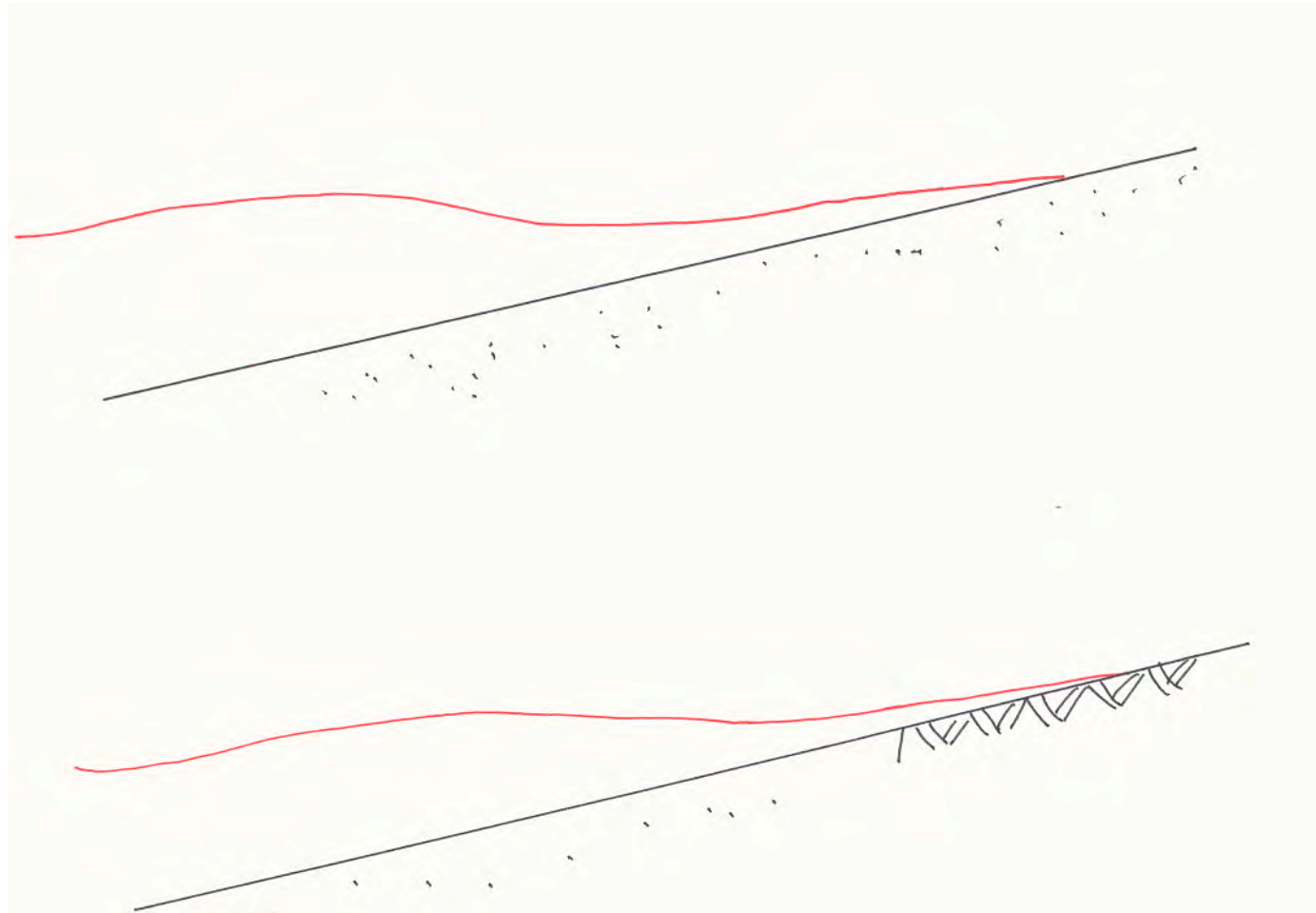
Percolation

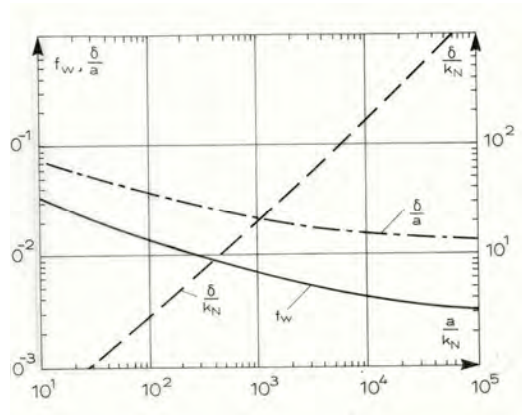


Web search

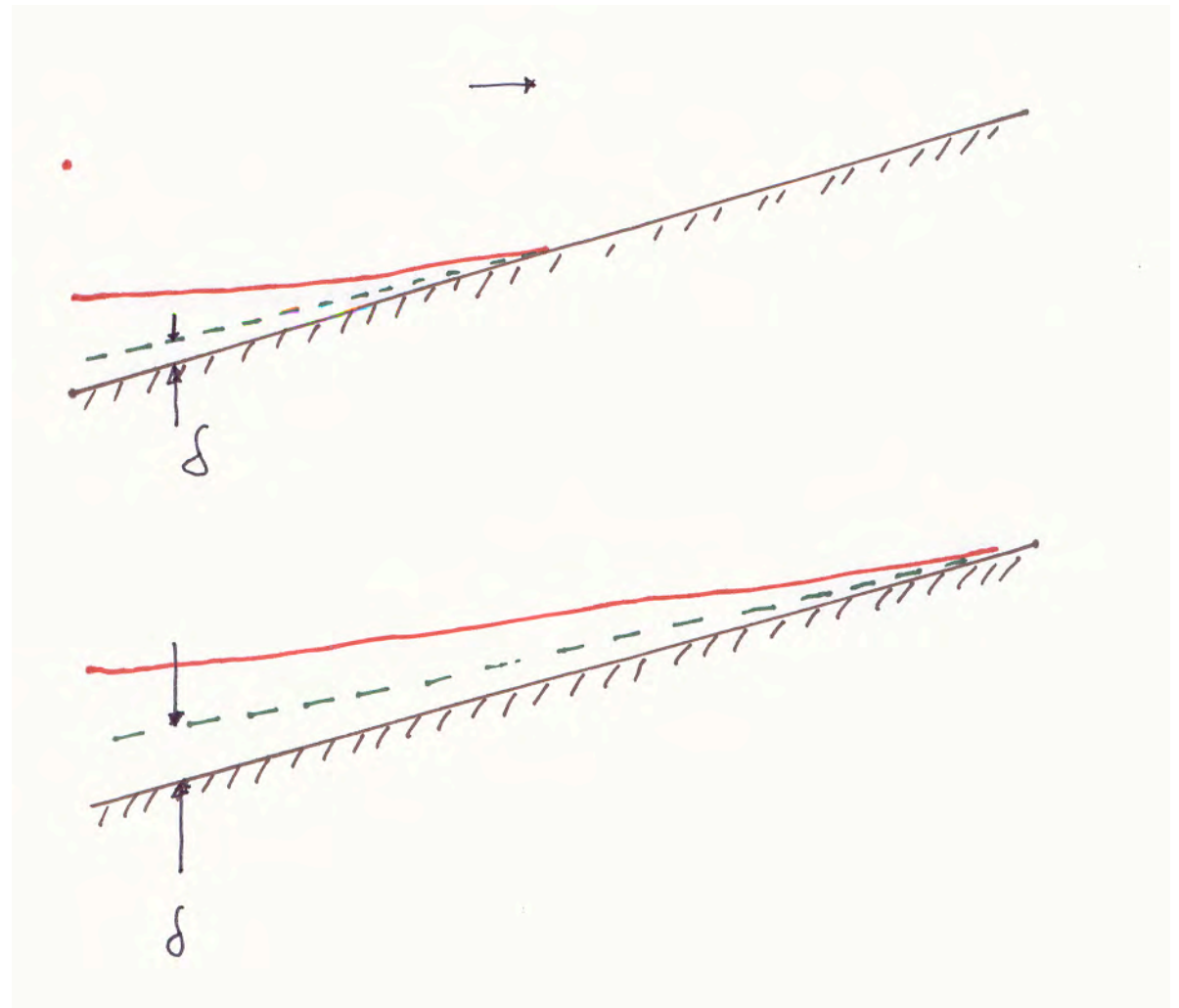
- Tsunami AND turbulence
- Boundary layer under a solitary wave

Net transport in a Tsunami (erosive or depositive) 1:the very much idealized case





Run up

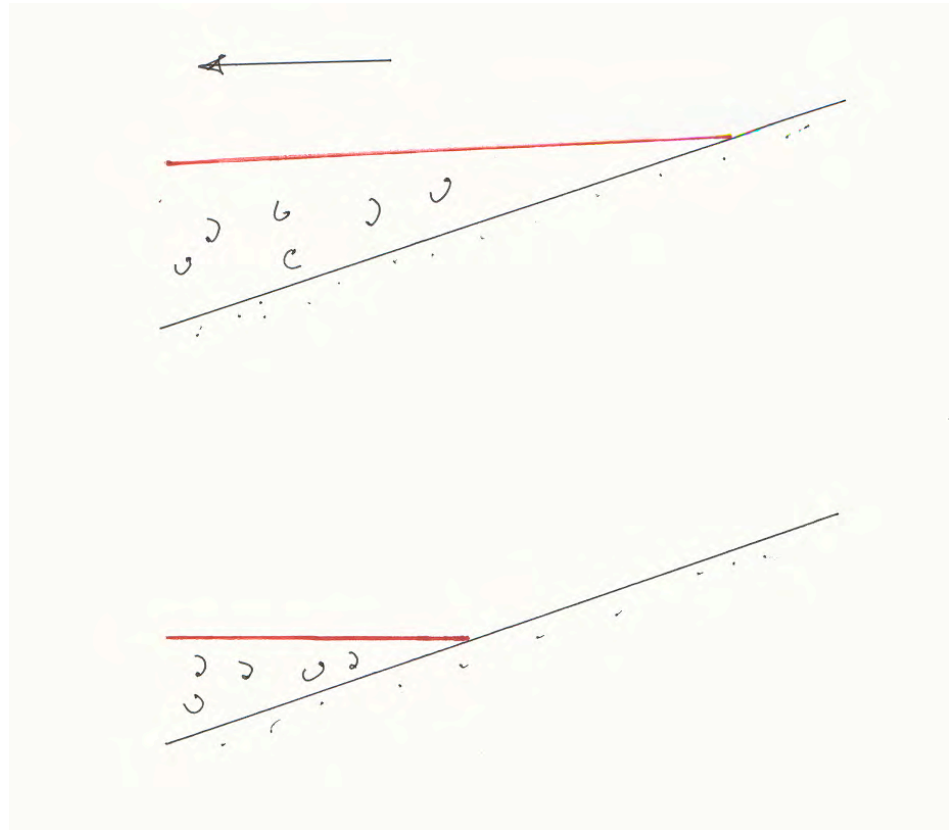


$U=5\text{m/s}$:

$\delta = 1\text{m}$ after
60 sec.

Draw down: boundary layer much thicker

Result: larger
friction on- than
off-shore (?)



Puelo and Holland, Coastal Eng 2001

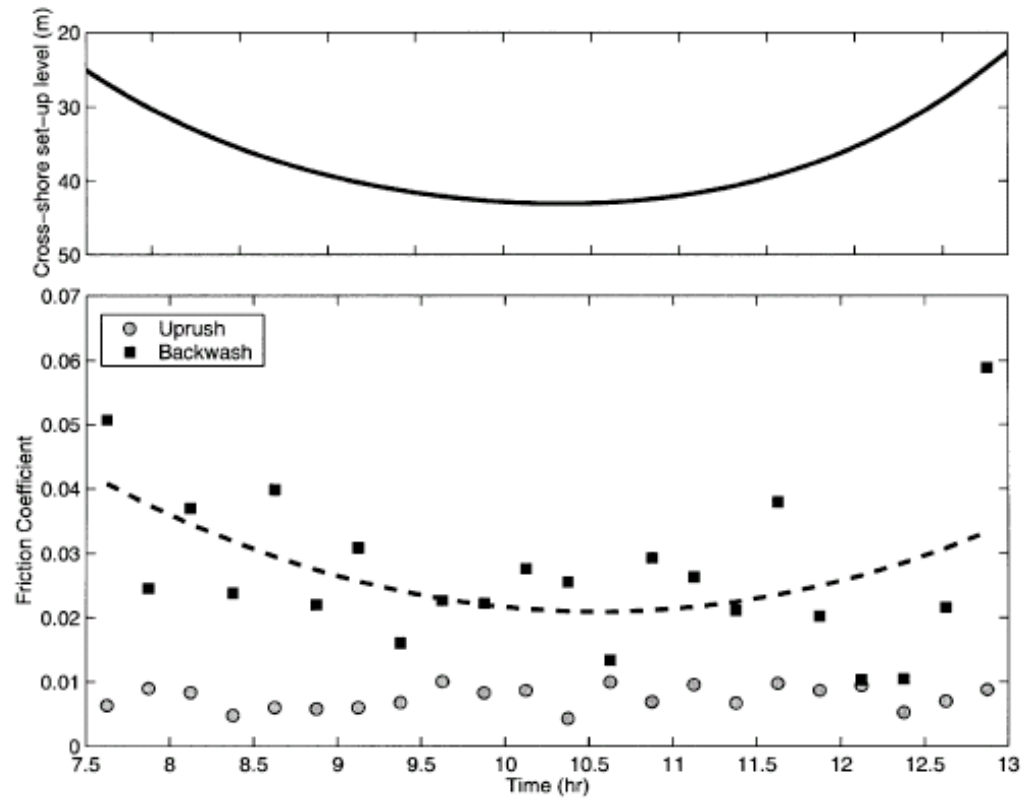
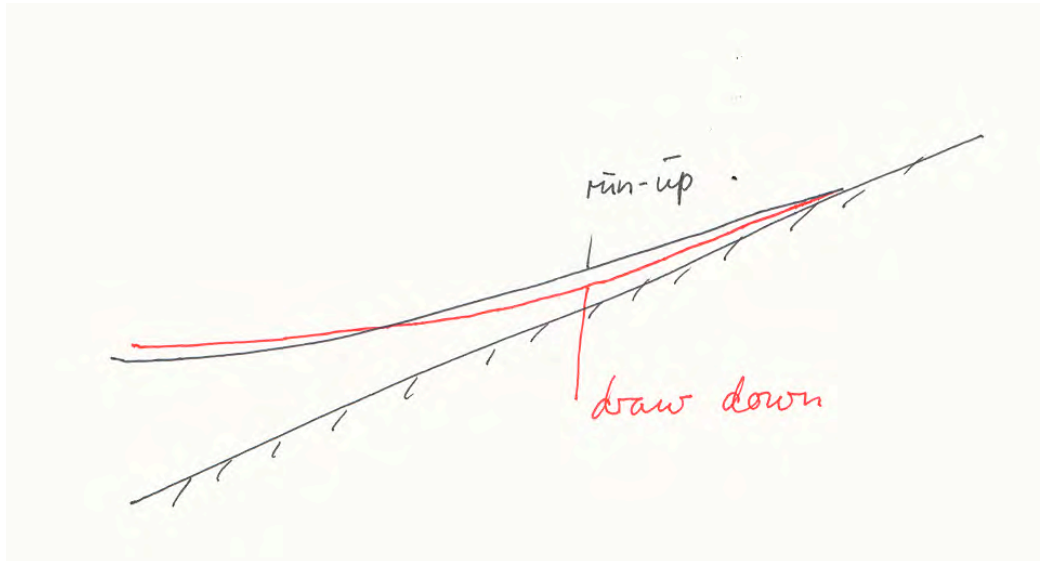


Fig. 6. Variation of f_u and f_b spanning the high tide cycle at Gleneden Beach, OR. Cross-shore set-up level as obtained from leading edge time series. Friction coefficients as estimated from comparisons between actual and ballistic swash trajectories. The dotted line is a second-order fit through the backwash data only.

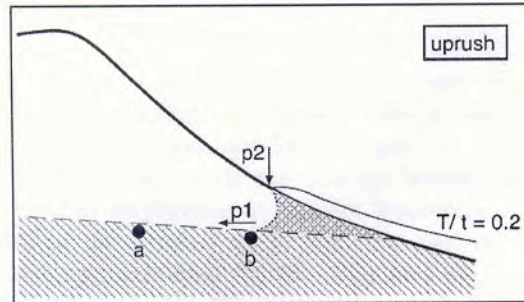
Larger flow velocities during draw down than in the Run-up.



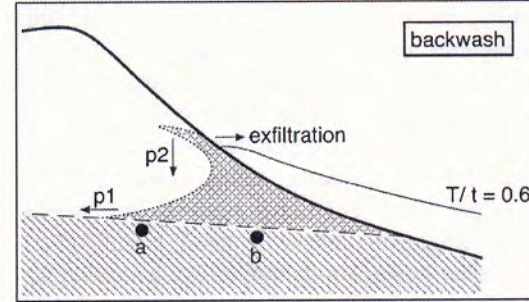
Flow in the sand

- Weak seepage
- Liquefaction
- Fluidization

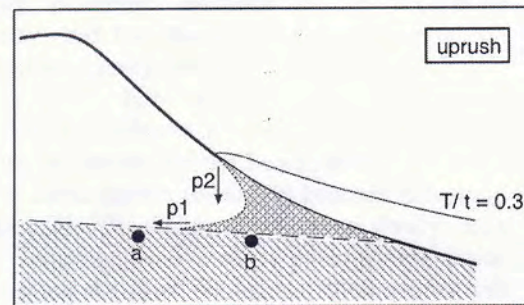
Austin et al 2006: Gravel beach



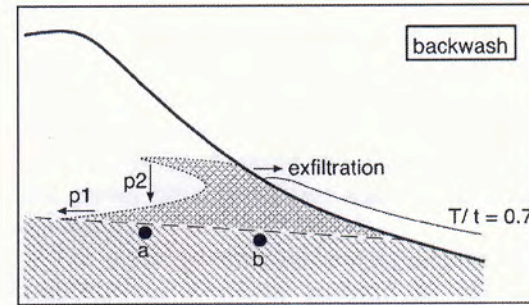
(a)



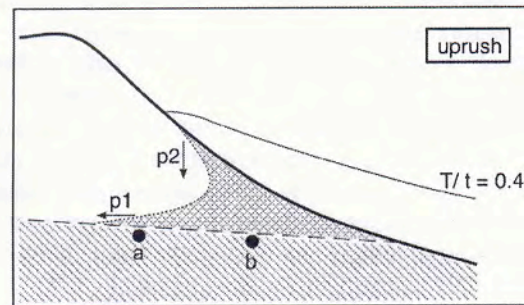
(d)



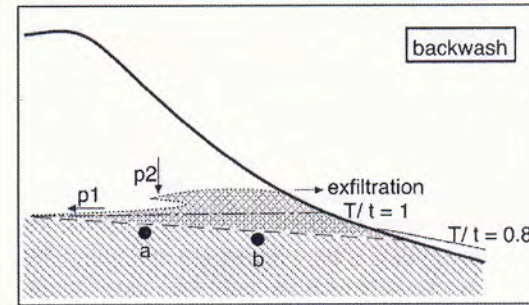
(b)



(e)

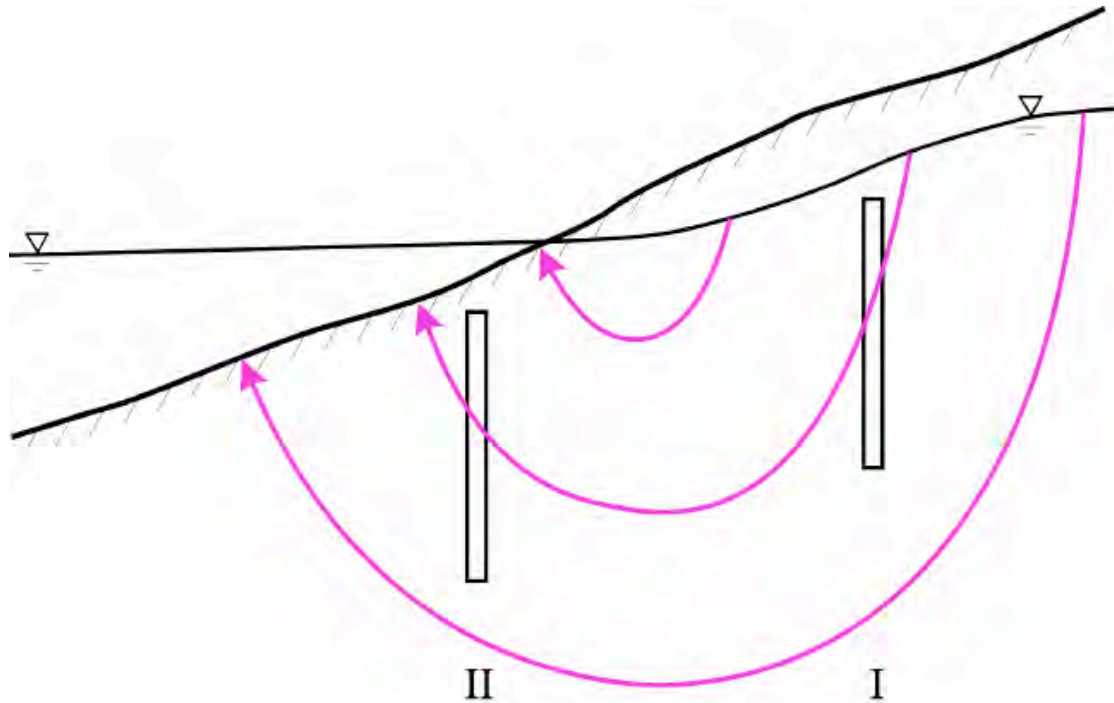


(c)

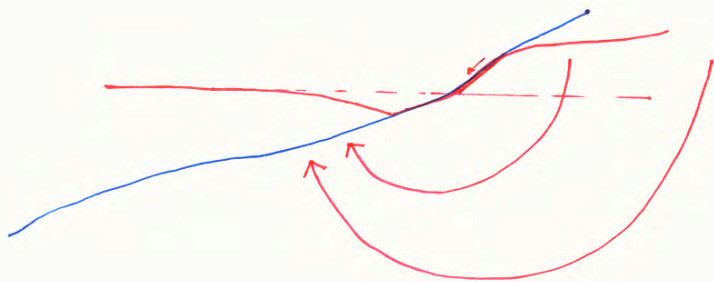
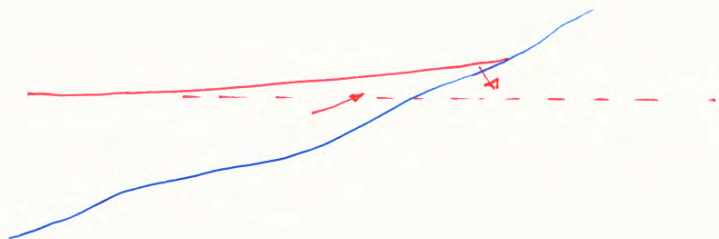


(f)

Seepage



Ground water flow pattern in the beach during falling sea level.



Fluidization

S.-Y. Tzang, S.-H. Ou / Coastal Engineering 53 (2006) 965–982

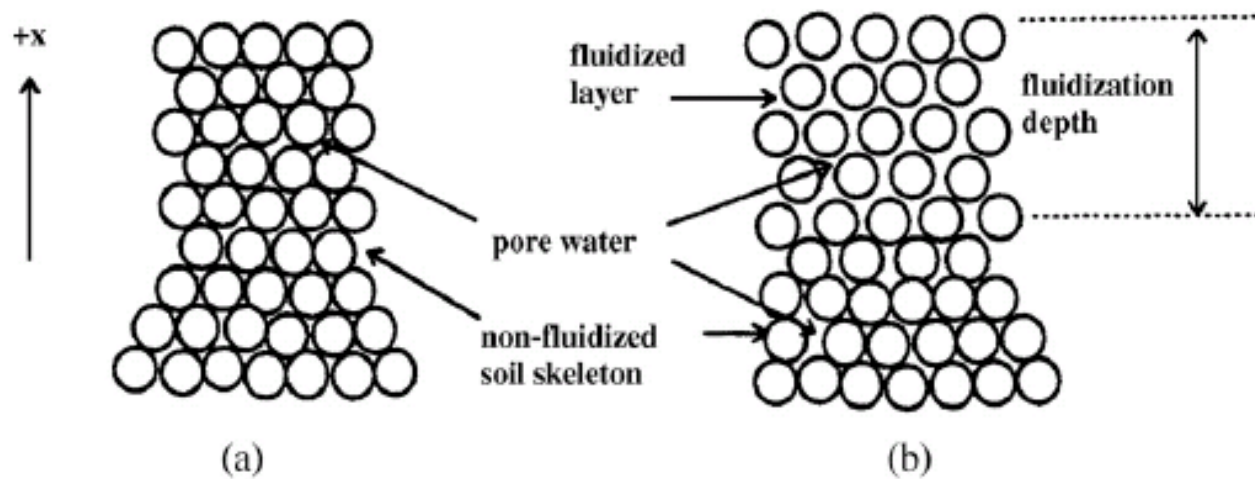


Fig. 1. Schematics of soil fluidization in a granular bed in stages of (a) unfluidized and (b) fluidized responses (Huang, 1996).

Seepage

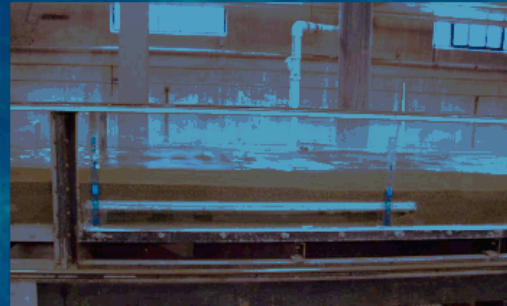
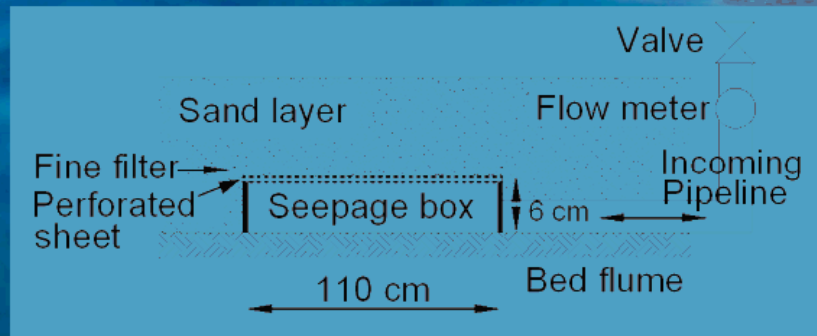
Simona Francalanci
University of Florence, Italy

Master Class

Lisboa 5 September 2006

Experimental set-up

The system was a sediment-recirculating, water-feed flume

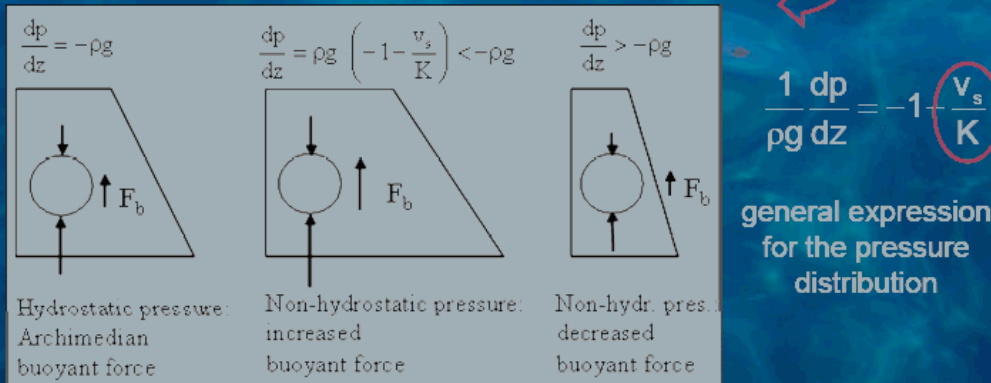


Theoretical background

A ground-water flow induces a non hydrostatic pressure distribution along the vertical

Darcy's law

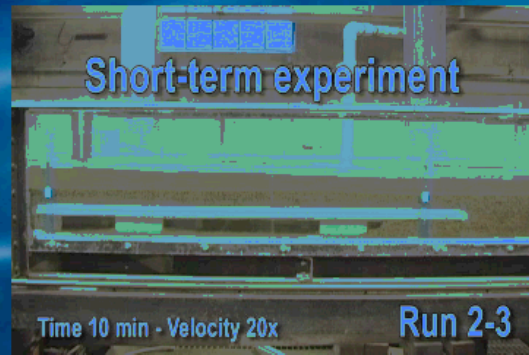
$$v_s = -K \frac{\partial h_p}{\partial z} \Rightarrow \frac{dh_p}{dz} = \frac{d}{dz} \left(\frac{p}{\rho g} + z \right) = -\frac{v_s}{K}$$



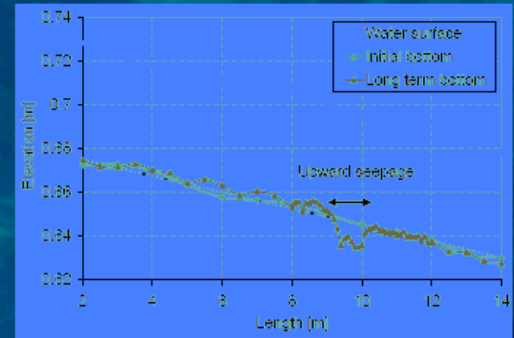
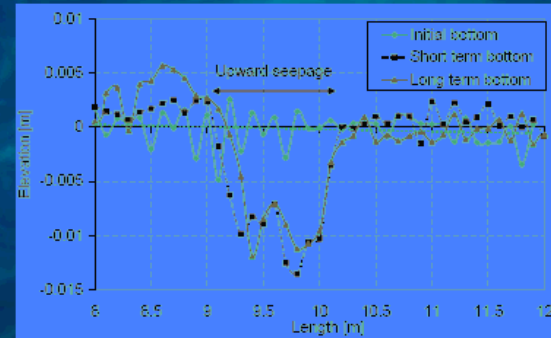
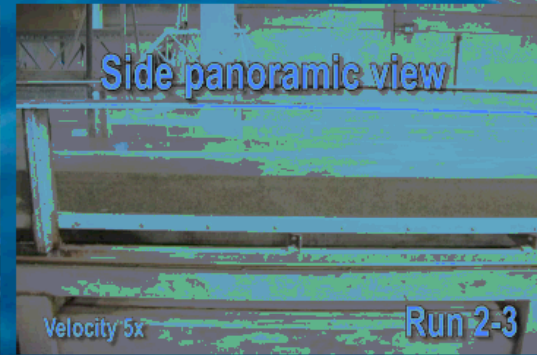
Vertical pressure gradient dp/dz near the bed and buoyant force F_b acting on a bed particle.

Effect of an upward seepage flow on bed dynamics

Short-term experiment



Side panoramic view



Results – the total shear stress

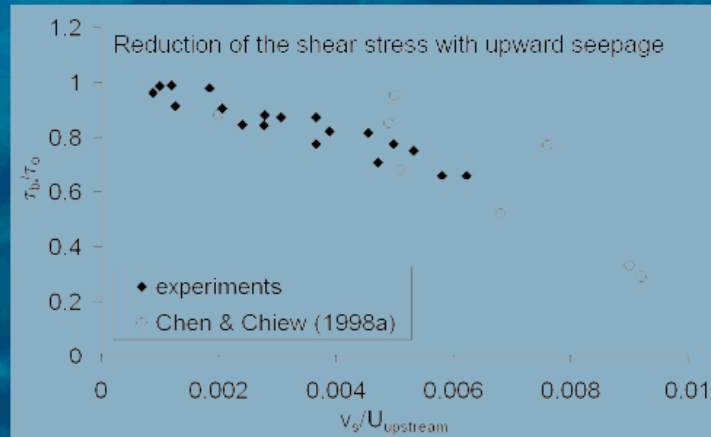
The evaluation of the shear stress at the bed is done through the momentum integral equations in the case of a boundary seepage, using the water surface slope, the bed slope, the seepage velocity and other flow parameters, depth-averaged velocity and water depth.

$$\tau_b = \rho u^2 = \rho g h \sin \phi_b - \rho g h \left(\frac{dh}{dx} \cos \phi_b - \frac{\beta U^2}{gh} \right) - 2\beta \rho U v_s \quad \text{Chen \& Chiew (1998a)}$$



Two combined effects on Shields parameter

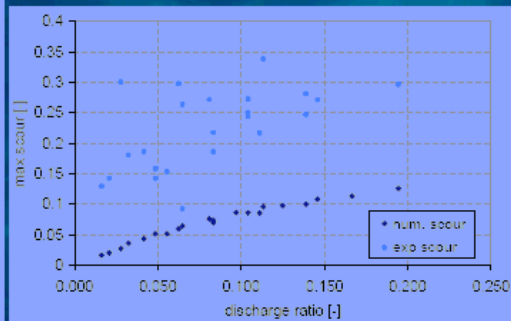
$$\tau^* = \frac{\tau_b}{\left(\rho_s - \rho \left(1 + \frac{v_s}{K} \right) \right) g D}$$



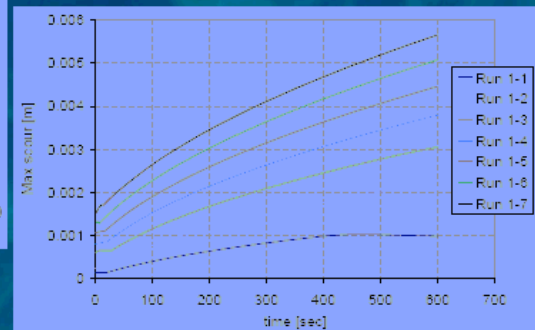
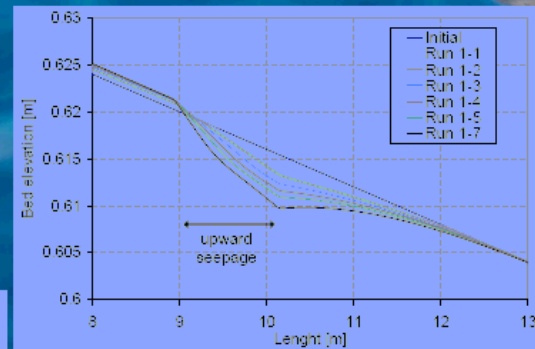
Theoretical and numerical model

Numerical results of short term experiments (10 min) with upward seepage flow, reduction of shear stress and no-correction in the Shields parameter

$$\tau^* = \frac{\tau_b}{(\rho_s - \rho)gD}$$



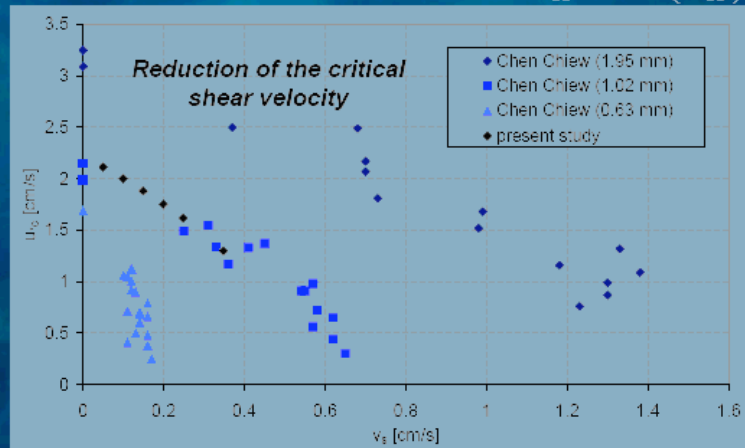
Under-estimation of local scour depth



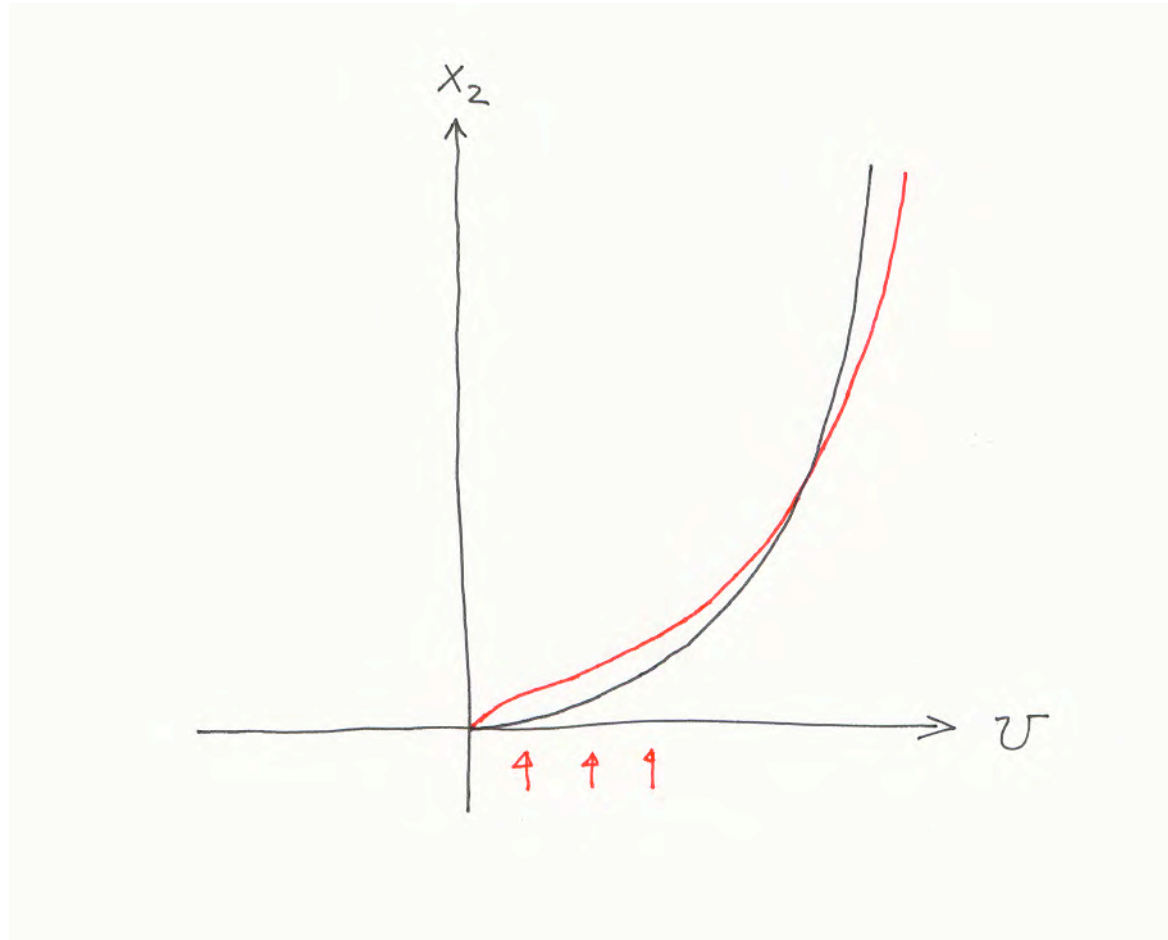
Results - On the incipient motion condition with upward seepage

The critical condition for the onset of motion is affected by the upward seepage: the critical shear stress required for a particle to move over the porous bed will decrease in the presence of an upward seepage (Cheng & Chiew, 1999).

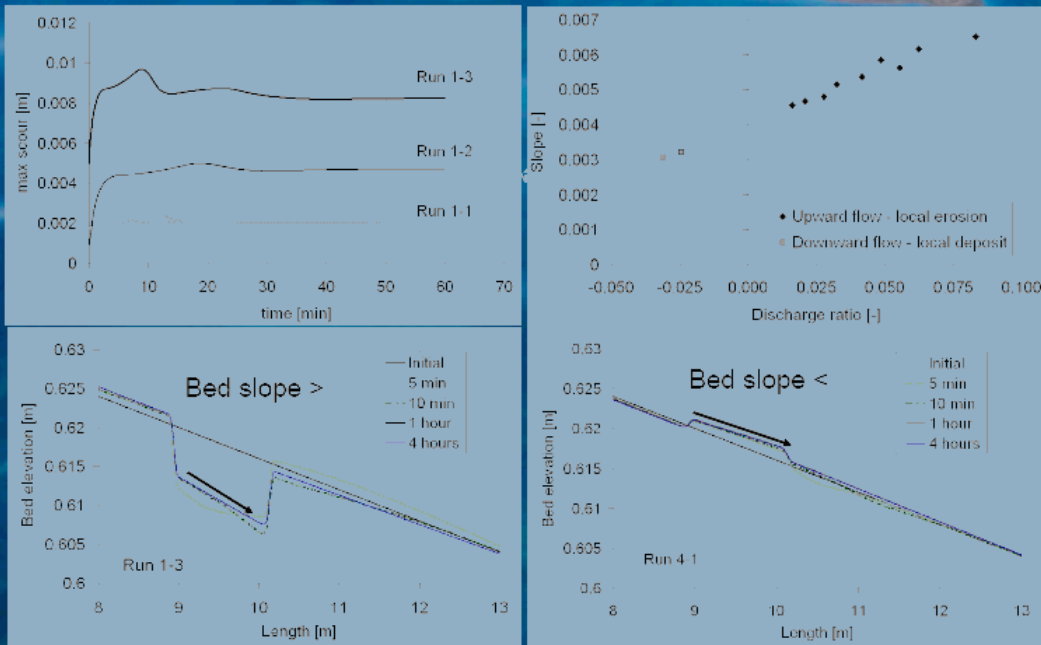
$$\left(\frac{u_{*c}}{u_{*oc}}\right)^2 = 1 - \left(\frac{v_s}{v_{sc}}\right)^m \quad \Rightarrow \quad \frac{\tau_{*c}}{\tau_{*oc}} = 1 - \left(\frac{v_s}{v_{sc}}\right)^m$$



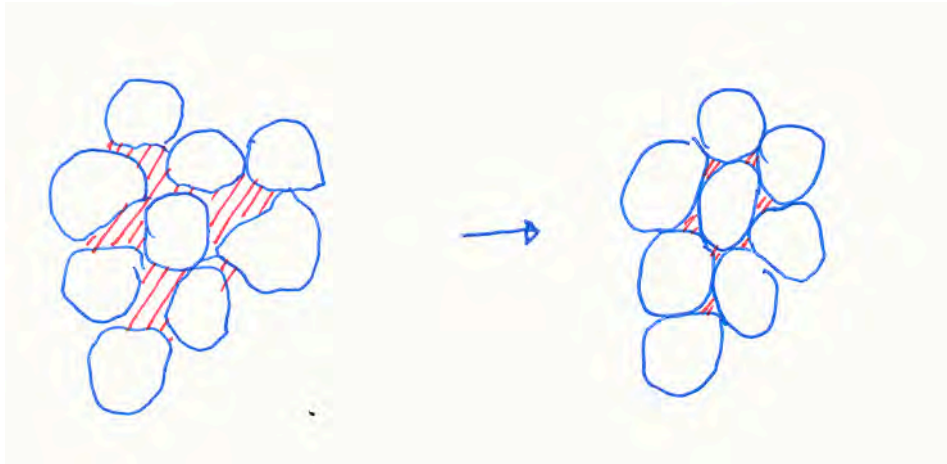
Seepage "destroy" the velocity profile



Theoretical and numerical model



Liquefaction: reshaping the grain skeleton



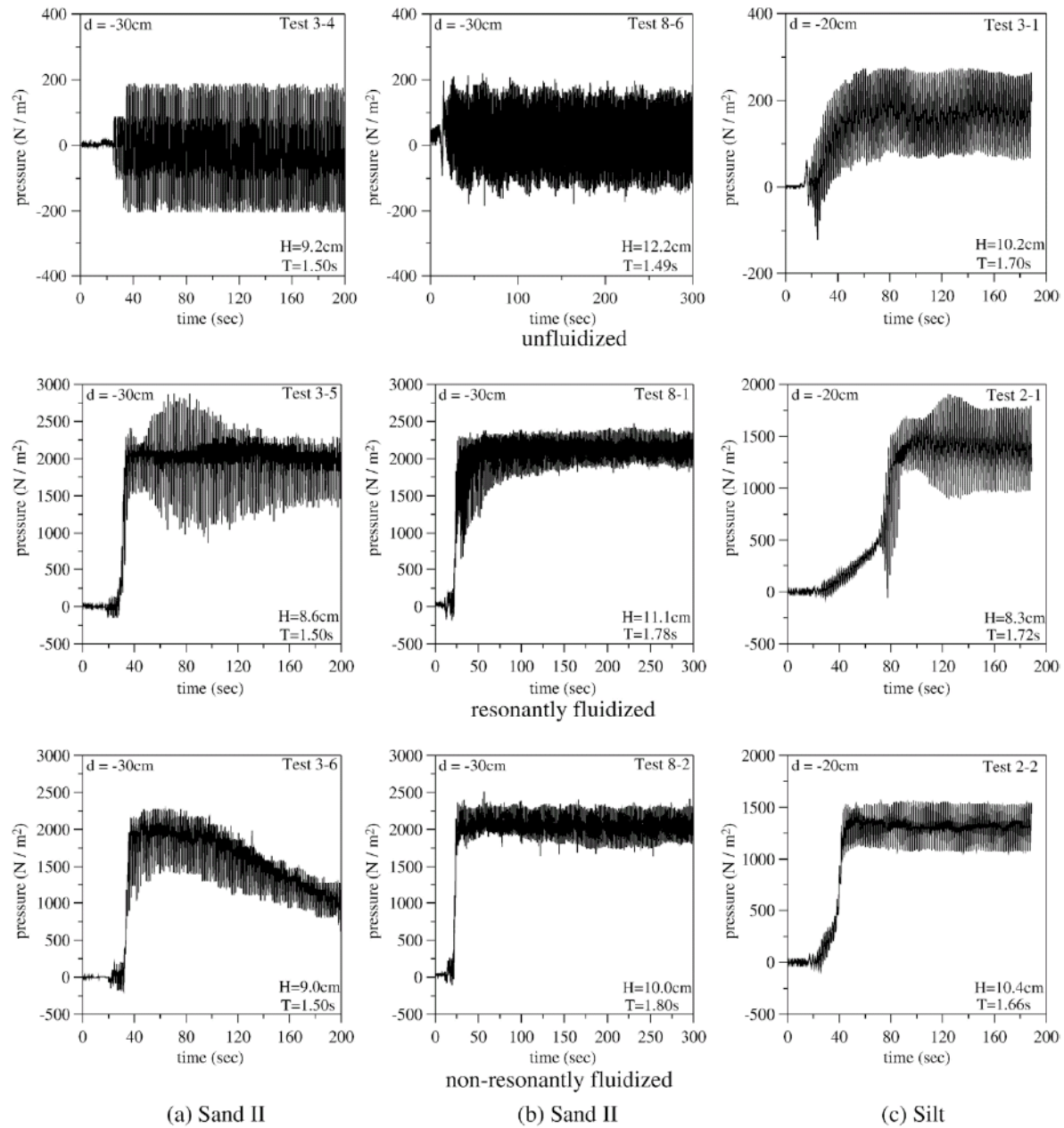
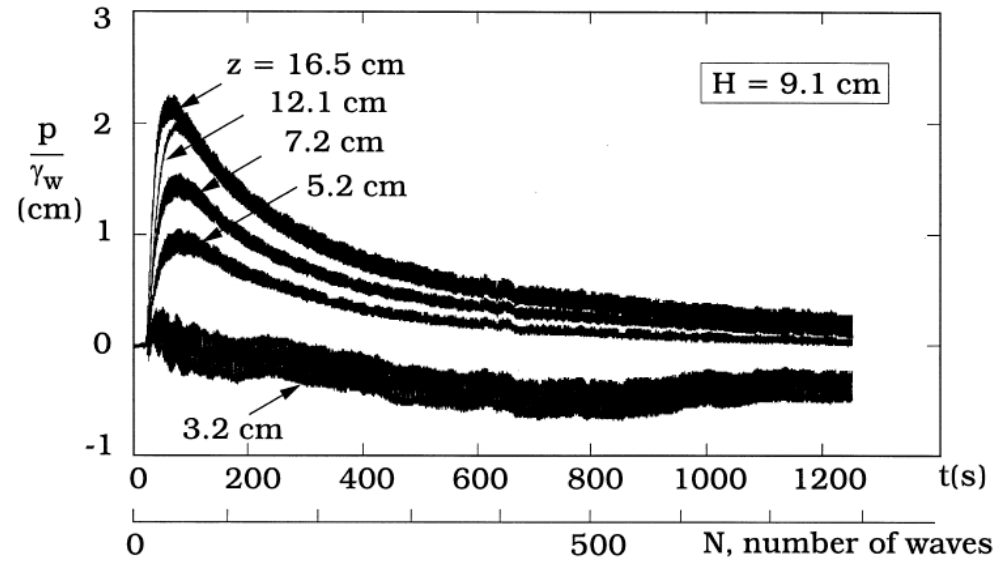
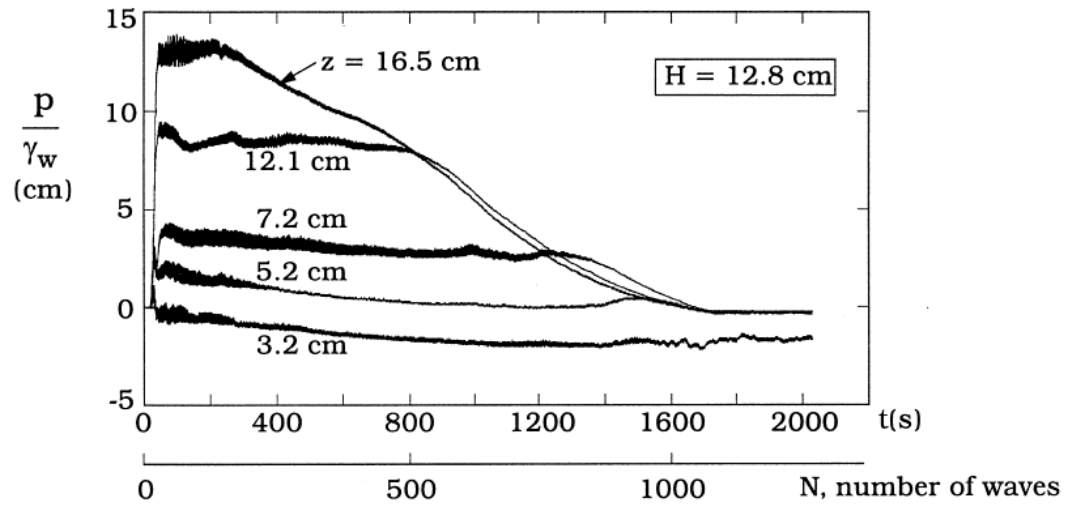


Fig. 6. Typical wave-induced unfluidized and fluidized pore pressure responses in Sand II ($d_{50} = 0.092\text{ mm}$) of (a) Test series 3, (b) Test series 8 and (c) in silt (Foda and Tzang, 1994).



a)



b)

Fig. 8. Behaviour of the accumulated pore pressure for large times. $h/L = 0.145$, $d/L = 0.059$, $H/d = 0.54$ for $H = 9.1$ cm, and 0.75 for $H = 12.8$ cm, and $c_v T/d^2 = 7.1 \times 10^{-4}$.

Momentary liquefaction

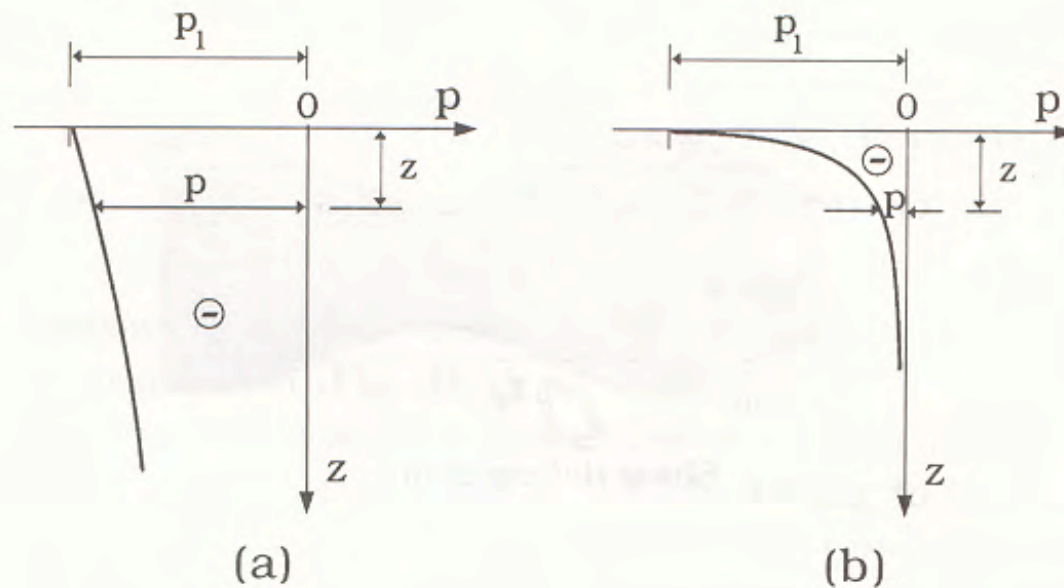
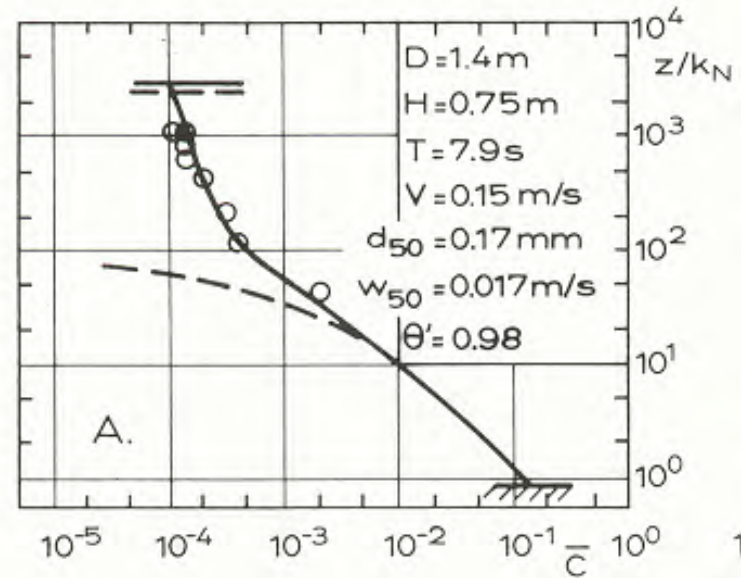
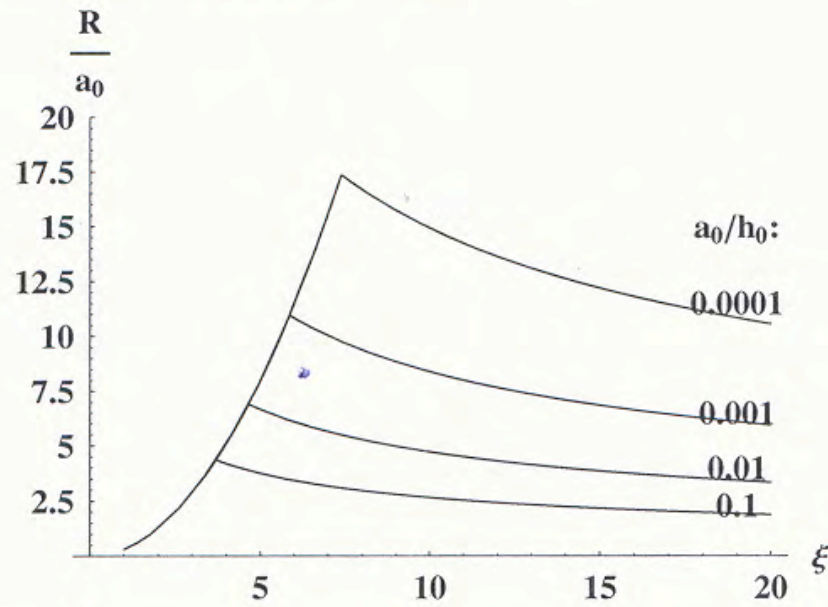


Figure 10.2: Typical distributions of pore pressure (in excess of hydrostatic pressure) during the passage of wave trough. (a) Saturated soil. (b) Unsaturated soil.

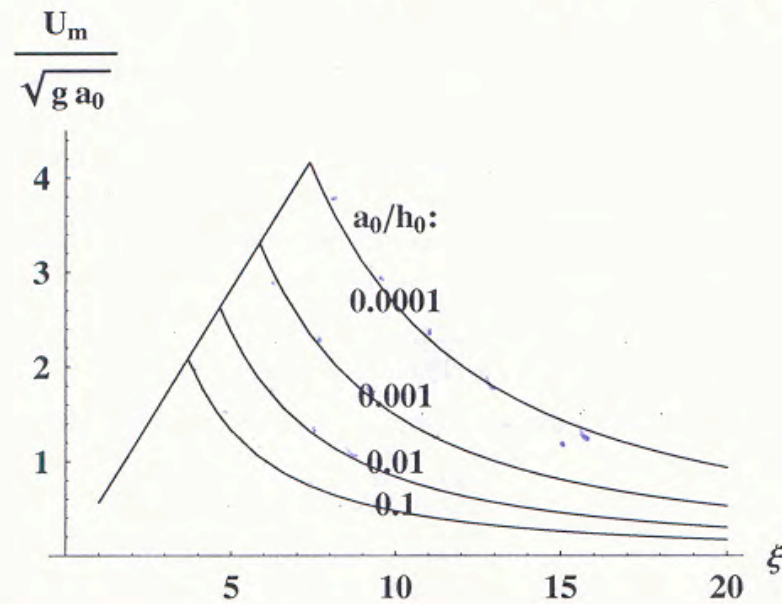
Is it a bore?? –or a fast rising tide- or a surge?? more sediment on-
 than $c \approx 1$



$$\xi = \frac{S}{\sqrt{H_0 / L_\infty}}$$



(a)



(b)

Fig. 1. Plot of the non-dimensional (a) run-up and (b) maximum horizontal velocity as a function of ξ for various a_0/h_0 .

Petti & Longo, Coastal Eng 2001

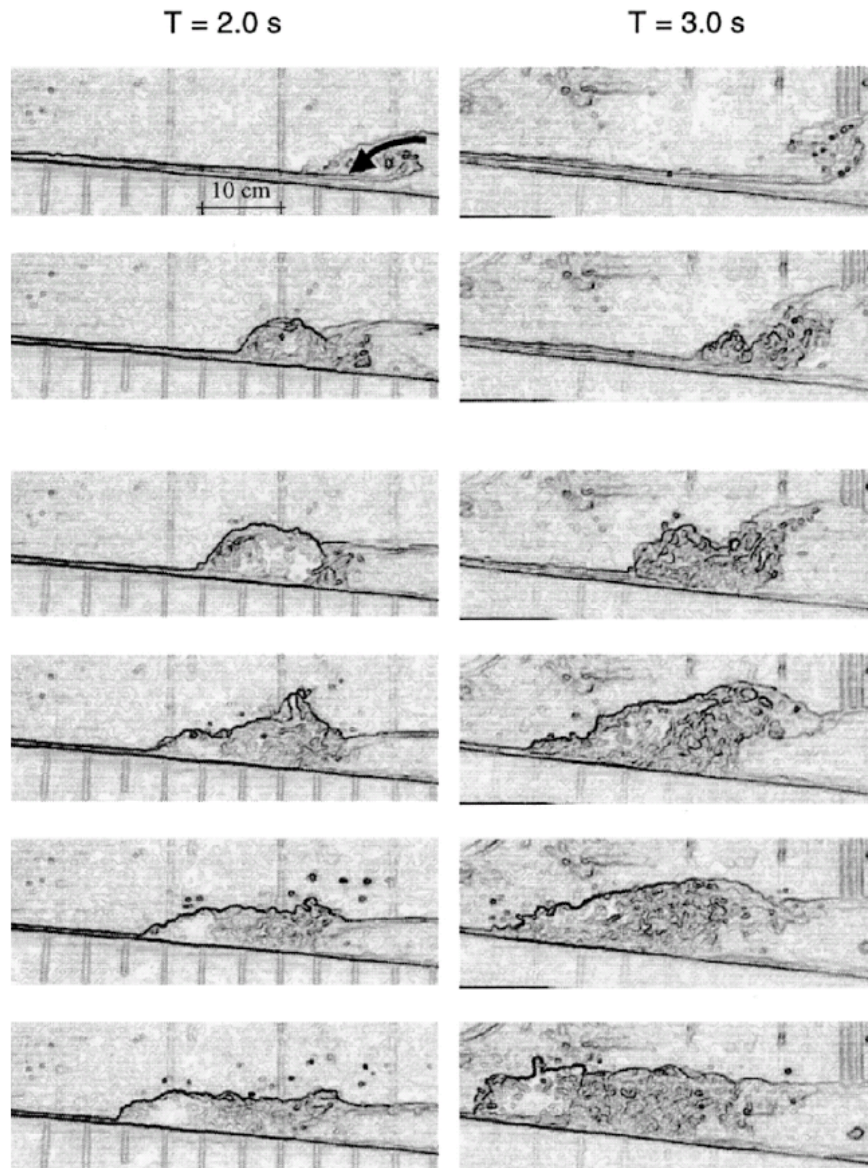
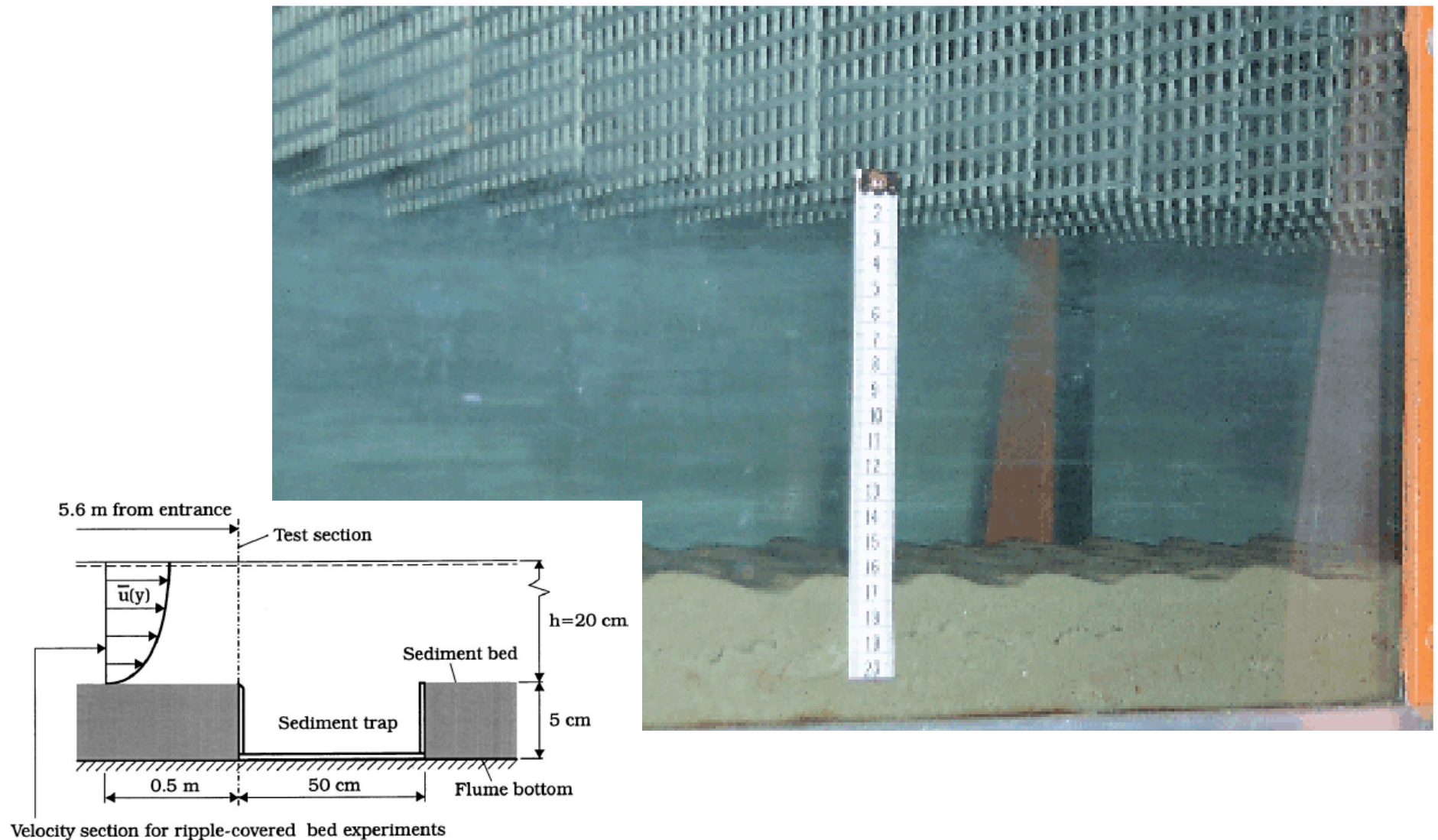
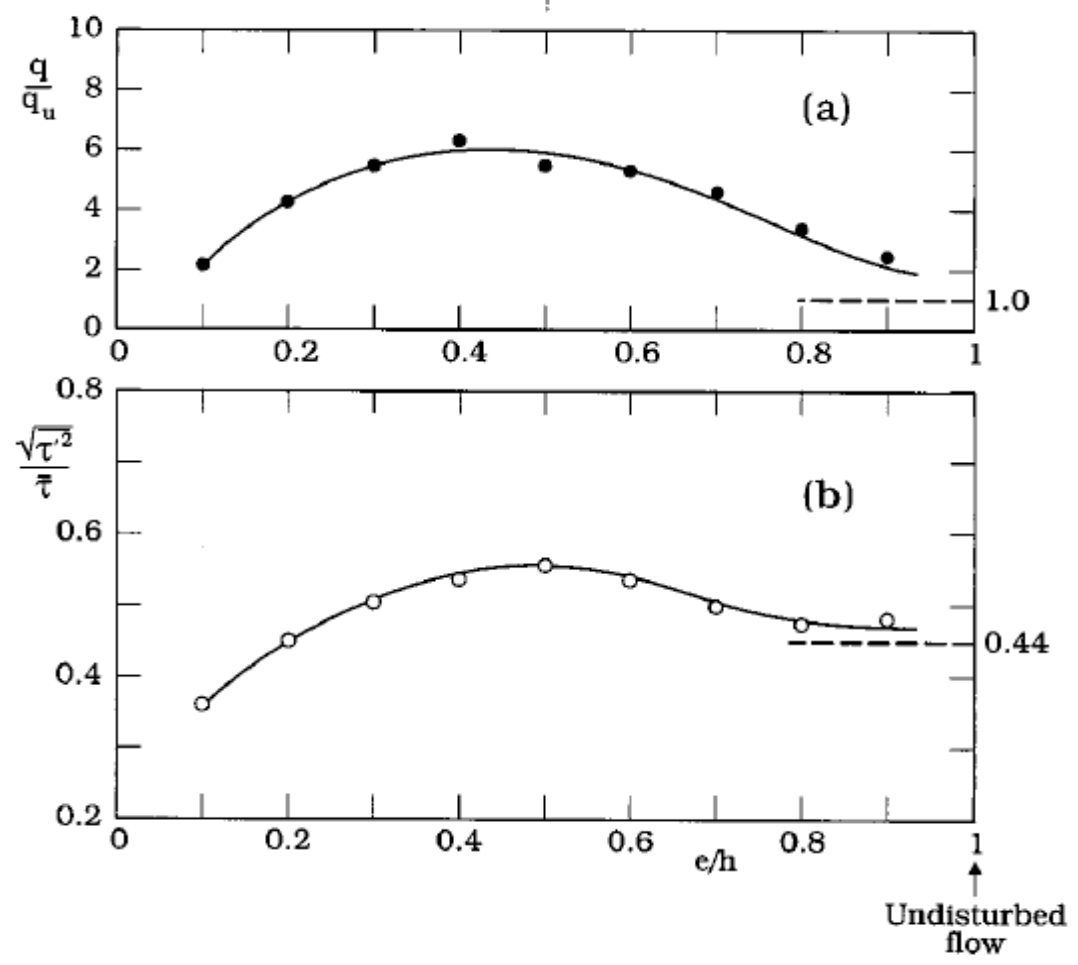
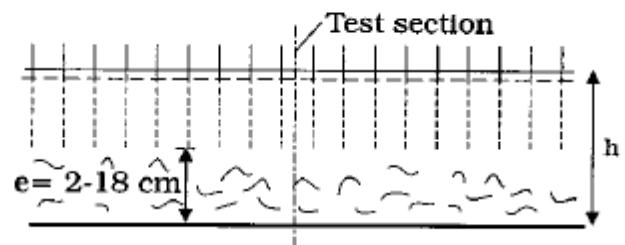
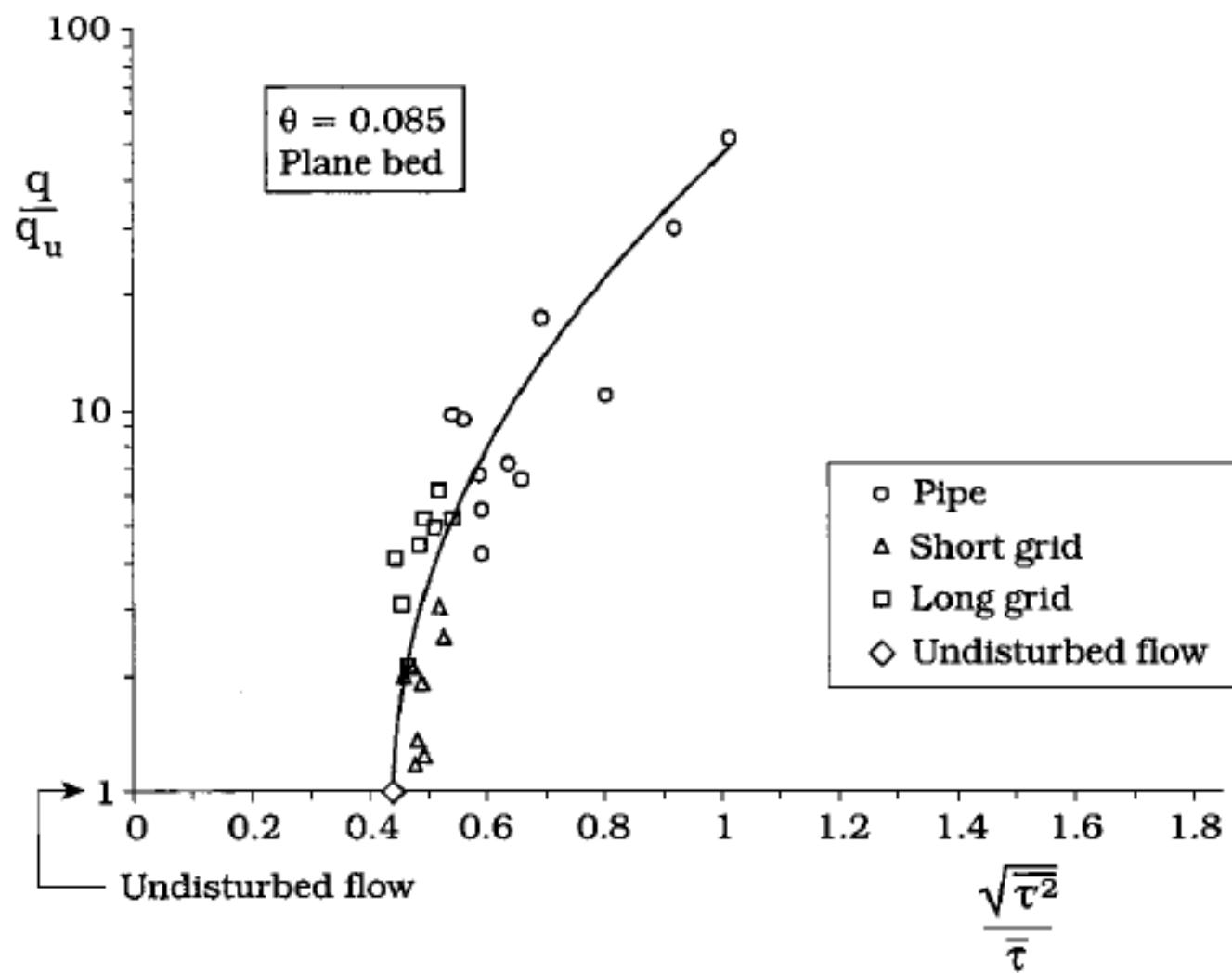


Fig. 10. Frame sequences at the breaking for tests $T = 2 \text{ s}$ and $T = 3 \text{ s}$ (time step $2/25 \text{ s}$).

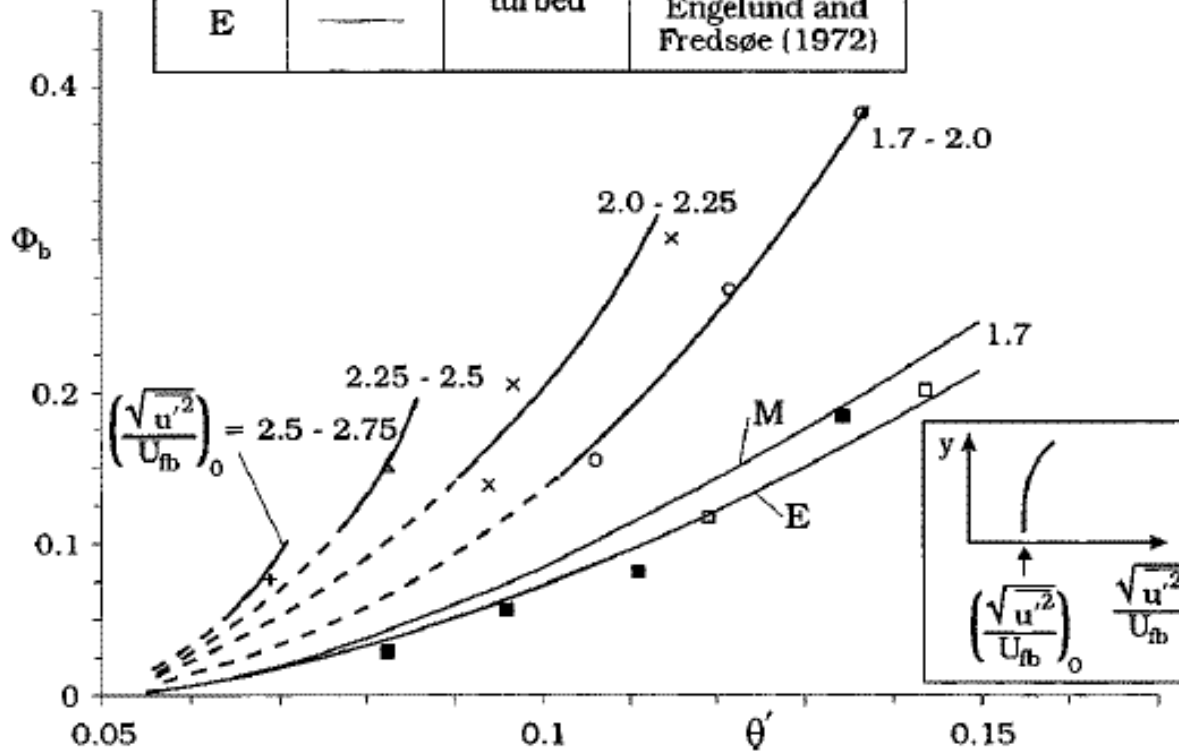
Effect of external generated turbulence on sediment-transport (Sumer et al. 2003)







Symbol	$\left(\frac{\sqrt{u'^2}}{U_{fb}}\right)_0$	Flow	Authors
■	1.7	Undis- turbed	Present
□	1.7	With turbulence generator; Long grid	
○	1.7 - 2.0		
×	2.0 - 2.25		
△	2.25 - 2.5		
+	2.5 - 2.75		
M	—	Undis- turbed	Meyer-Peter and Muller (1948)
E	—	Undis- turbed	Engelund and Fredsoe (1972)



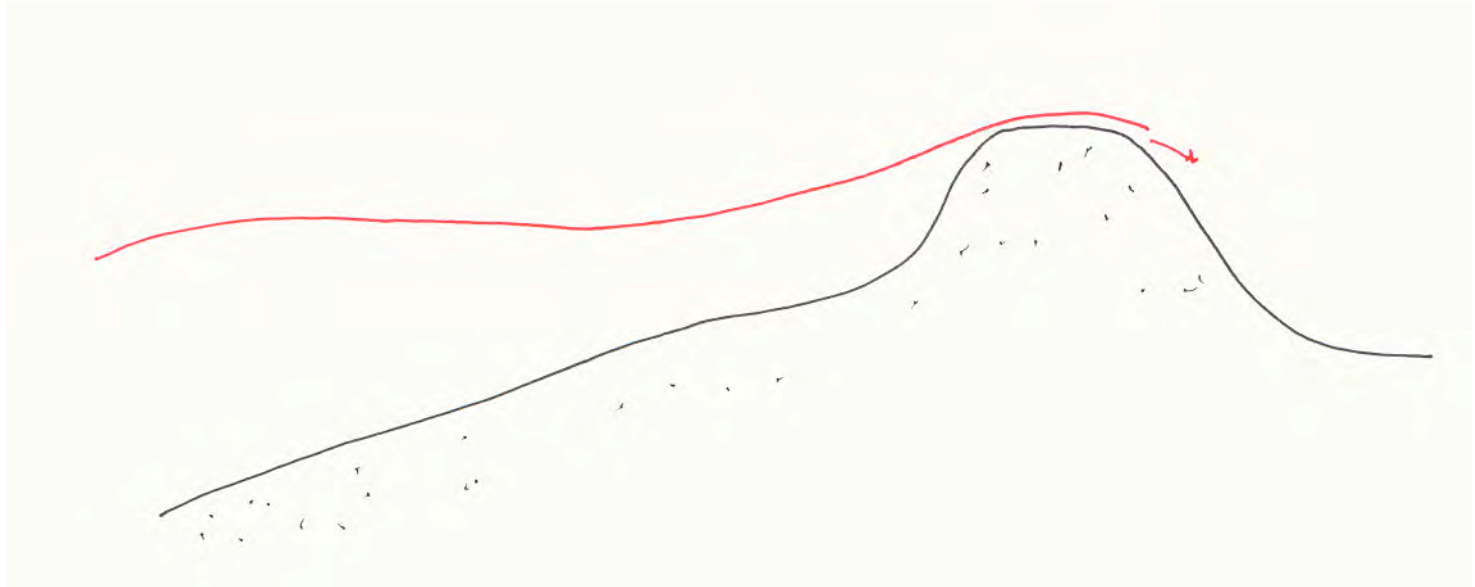
Scour

Part 1: SCOUR IN DUNES:

Important for a Tsunami: timescale

Dunes







b. Looking east, at breach cut through the beach berm.

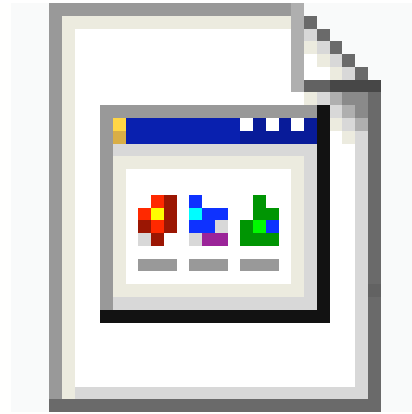
Figure 1. Mecox Pond, breached the morning of February 14, 1998, (photographs by N. Kraus, afternoon of February 14).

Breach 1d



BarrierBreach_1D.avi

Breach 2d



BarrierBreach_2D.avi

Need for research

- Wave boundary layers in runup and drawdown, and under breaking waves
 - Impact of sheet flow on near bed turbulence – and the bed condition for suspended sediment in the sheet flow regime
 - Transport of mixtures in the sheet flow

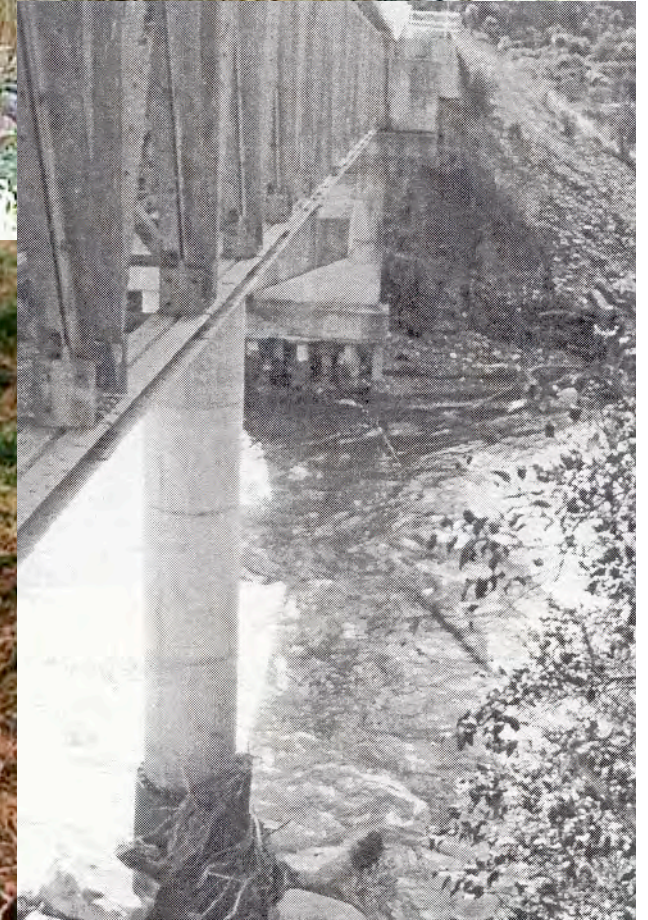
Part 2

- Scour around structures in a Tsunami-like environment

roads, bridges, buildings, etc.



- Culverts
- Bridge abutments





Types of scour (Melville and Coleman)

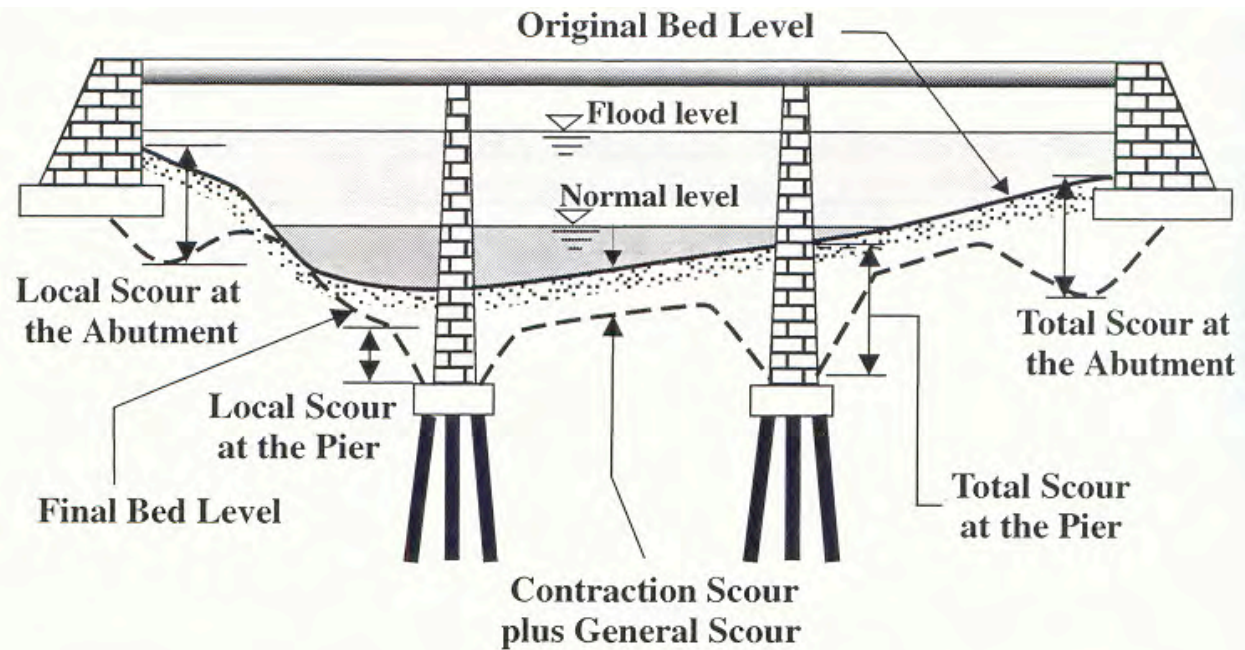


Figure 1.1. The types of scour that can occur at a bridge.

Degradation



Figure 4.8. Degradation exacerbated by sand extraction for Republic of China.

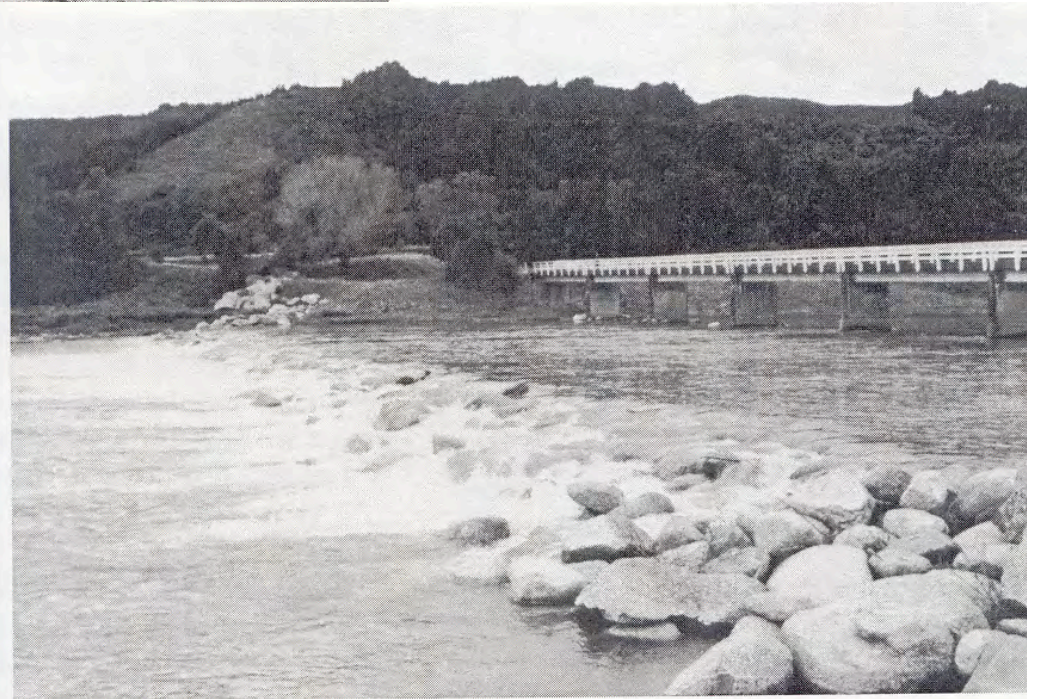


Figure 9.15. Example of the use of check dams to control degradation.

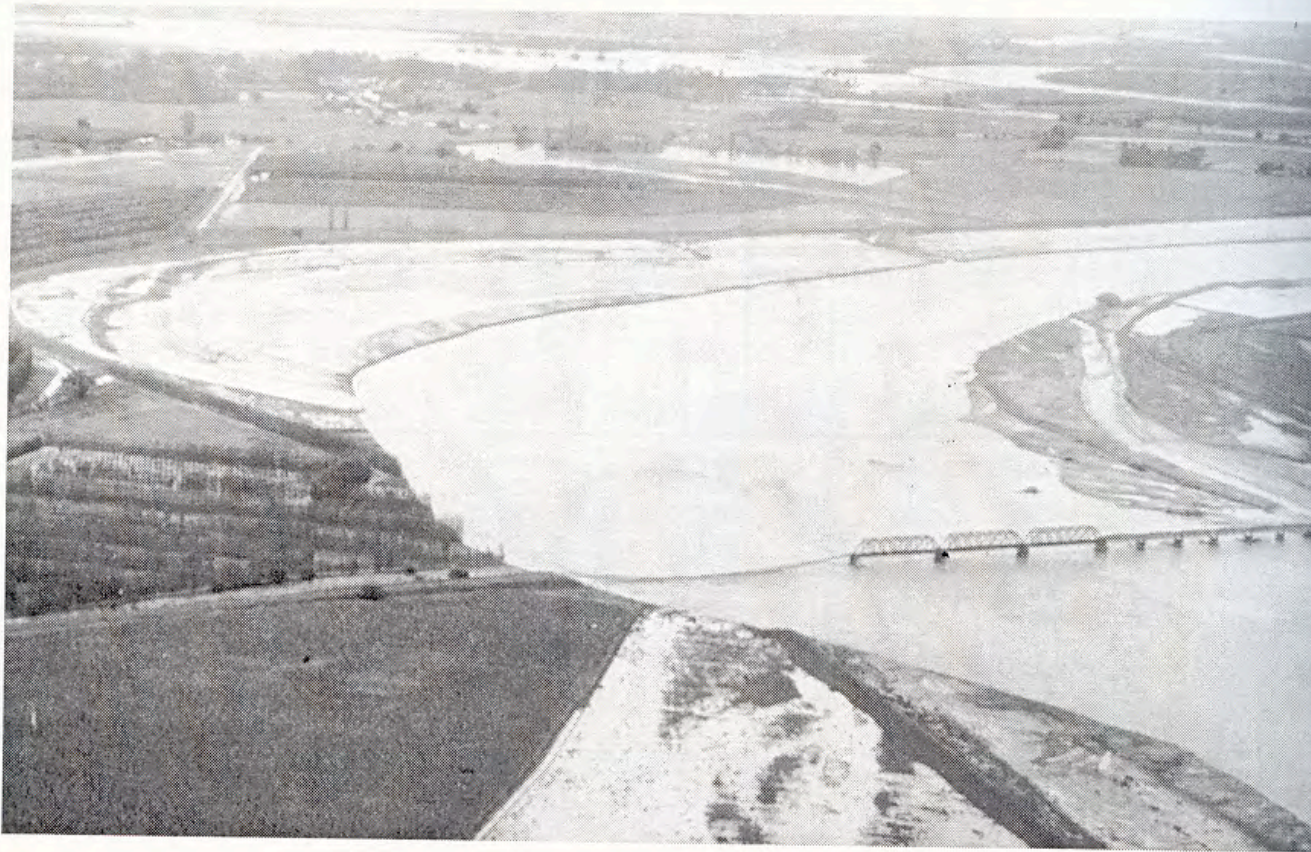


Figure 1.3. Failure of Waipaoa River Rail Bridge (situated near Gisborne, New Zealand) during Cyclone Bola, March 1988, due to channel shift at the bend (flow from the top to the bottom of the figure).

(Melville and Coleman)



Figure 1.5. Floating debris accumulation at a bridge pier, bridge on Tauwhareparae Road over Mangaheia River, New Zealand, Cyclone Bola, 1988.

The wood increases the effective width of the pier and decreases the effective clear span for the flow. In addition it spoils the smooth lines of the pier

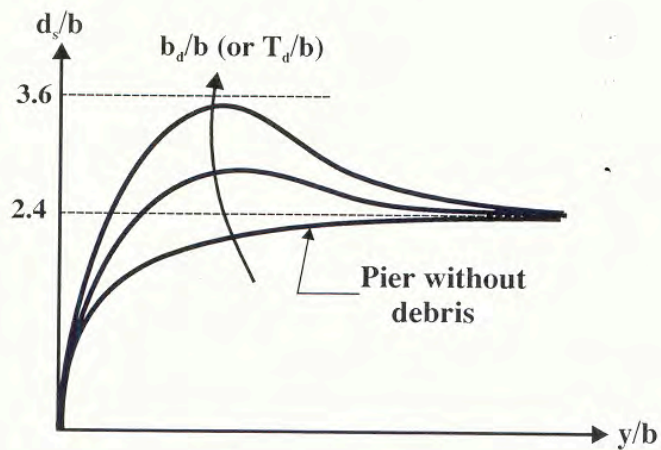
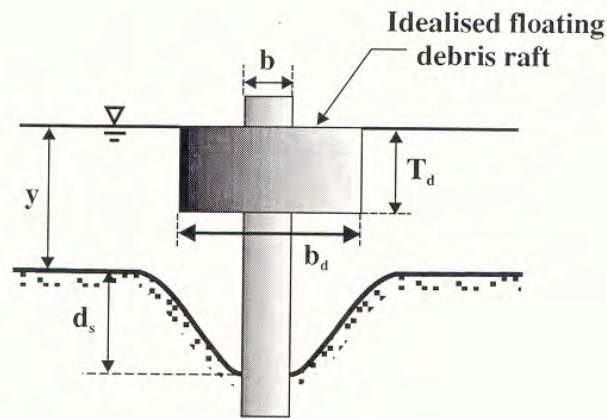
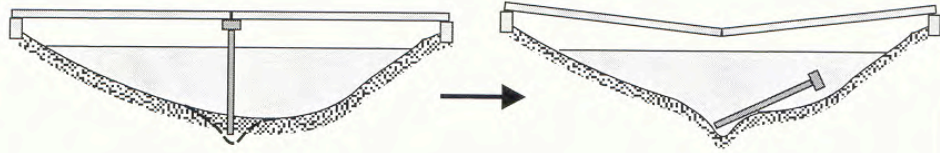
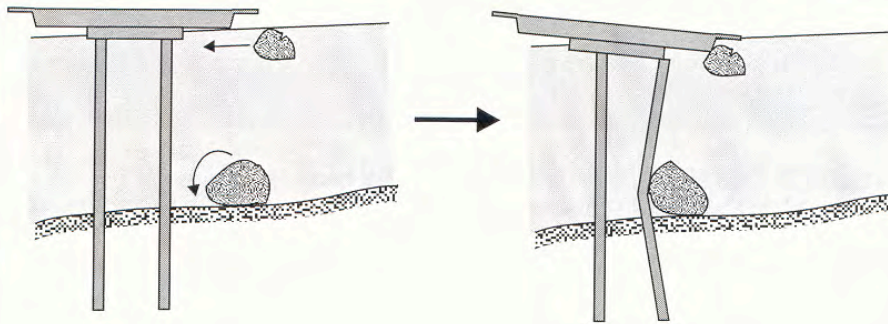


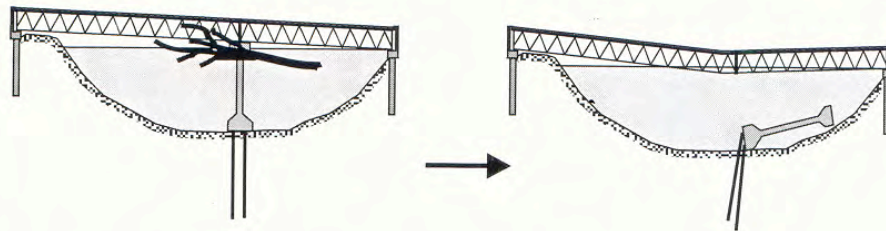
Figure 6.35. Local scour depth variation with quantity of floating debris.



(a) Pier undermining
(complete undermining or due to a loss of friction length)



(b) Boulder impact

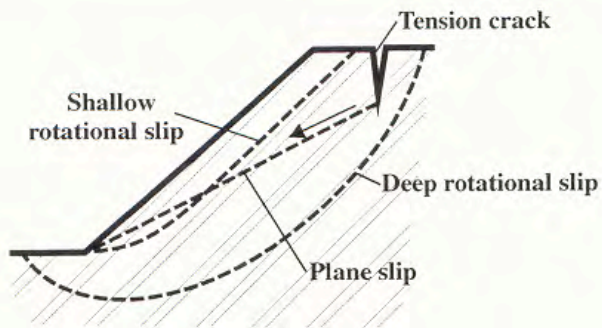


(c) Debris rafting/impact

Figure 1.10. Bridge failure mechanisms.



(a) Noncohesive - Flow Slides



(b) Cohesive



Melville and Coleman

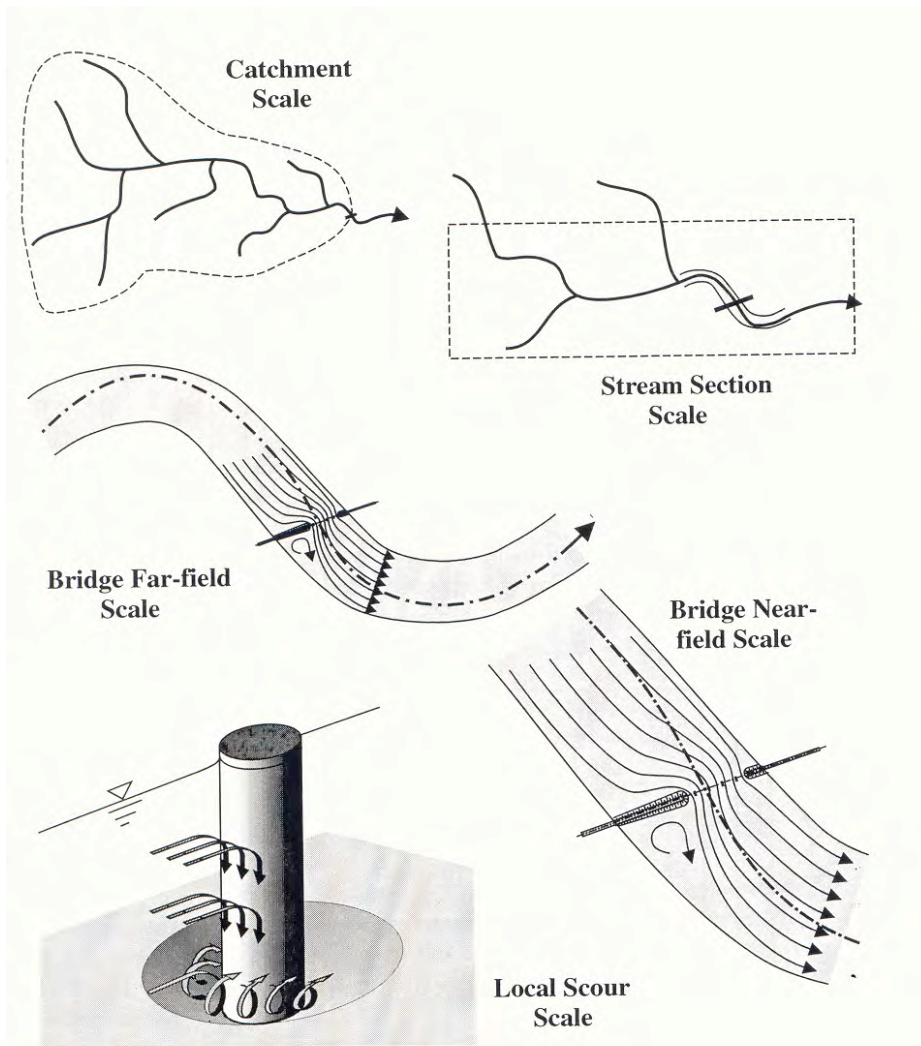
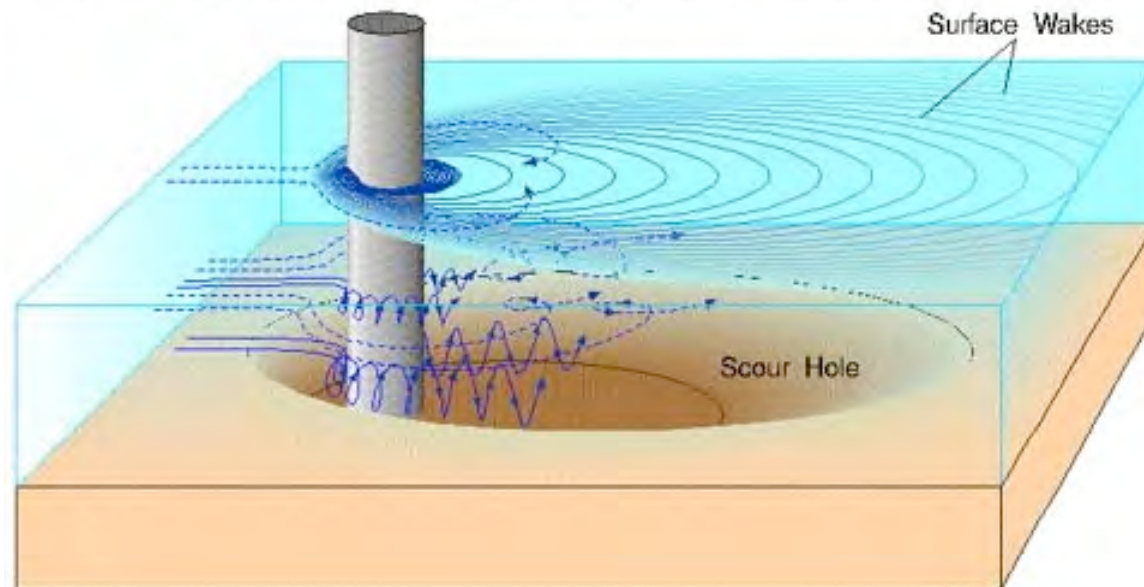


Figure 3.1. Spatial scales appropriate to the different types of scour.

Scour in a current: Bridge scour:

Horseshoe and Wake Vortices around a Cylindrical Element



$$d_s = K_{yb} K_I K_d K_s K_\theta K_G K_t$$

yb=depth-size

I=flow intensity

d=sediment size

s=shape

θ = pier alignment

G=channel geometry

T=time

Scour depth variation with velocity

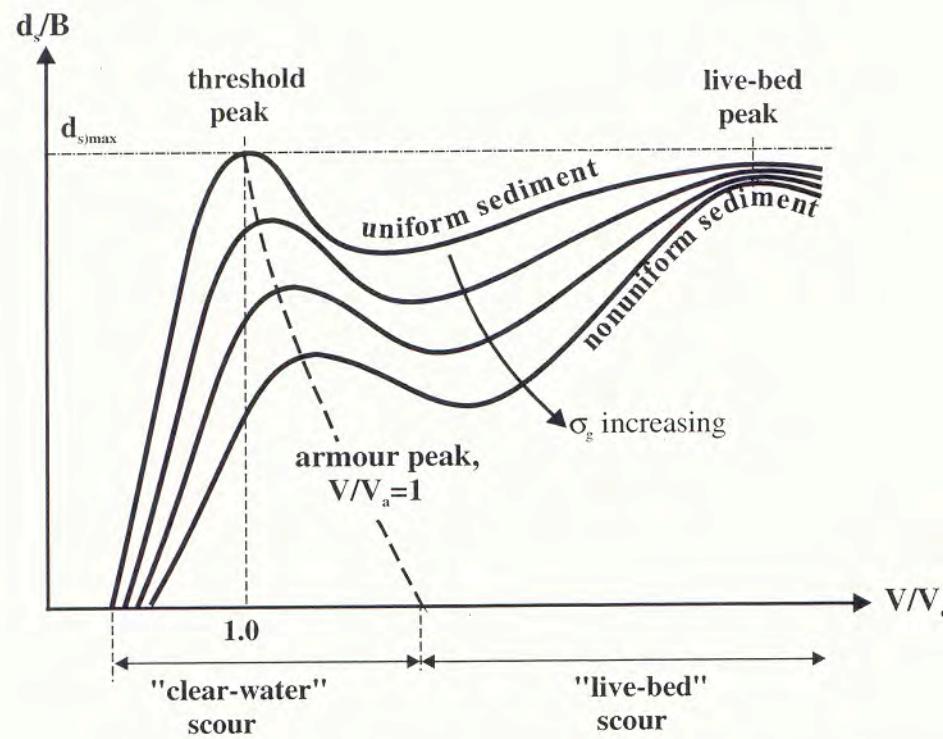


Figure 6.7. Local scour depth variation with flow intensity.

Sediment gradation

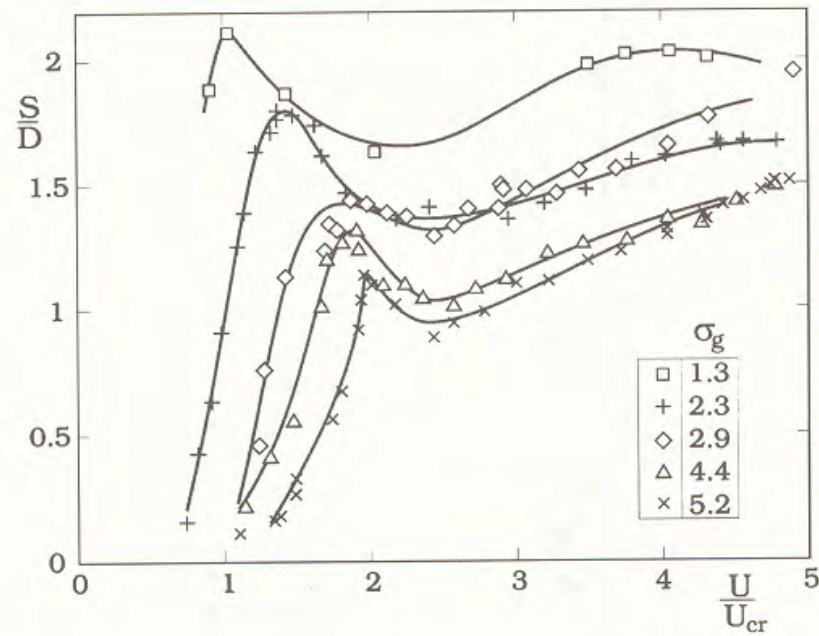
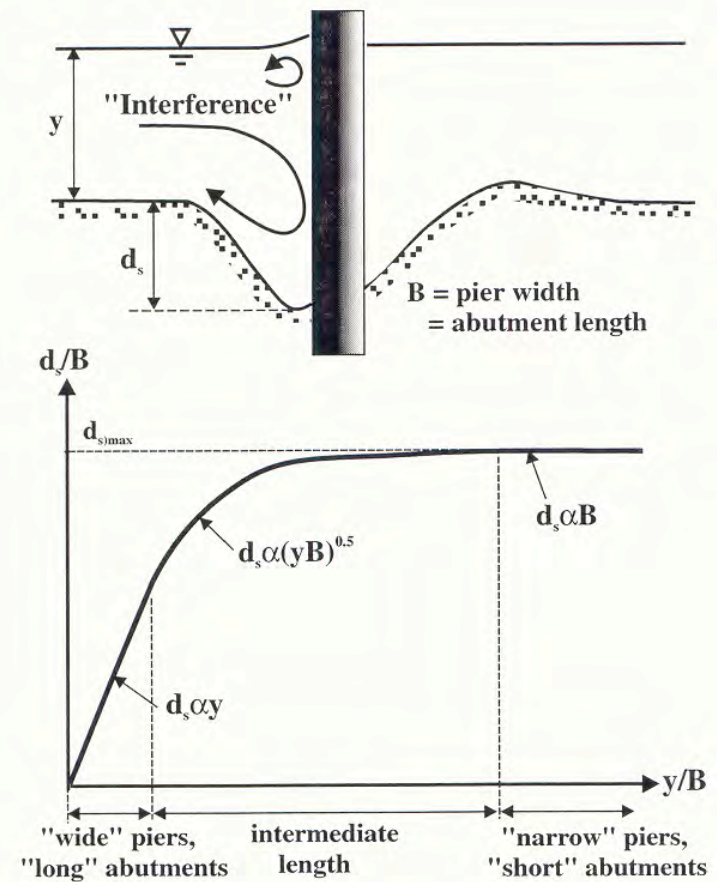
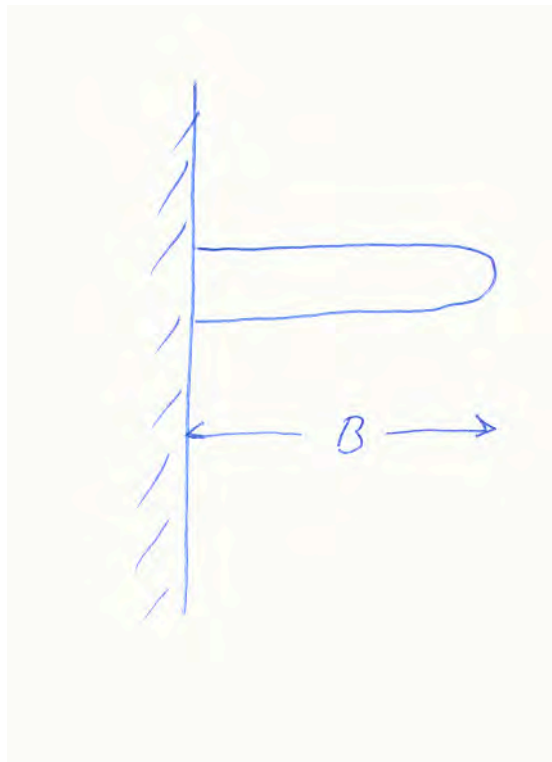


Figure 3.25: Effect of sediment gradation. Data by Baker (1986). $d_{50} = 0.6$ mm. From Melville and Surtherland (2000).

Foundation Type	Class	B/y	Local Scour Dependence
Pier	Narrow	$b/y < 0.7$	$d_s \propto b$
	Intermediate width	$0.7 < b/y < 5$	$d_s \propto (by)^{0.5}$
	Wide	$b/y > 5$	$d_s \propto y$
Abutment	Short	$L/y < 1$	$d_s \propto L$
	Intermediate length	$1 < L/y < 25$	$d_s \propto (Ly)^{0.5}$
	Long	$L/y > 25$	$d_s \propto y$

Variation with shallowness



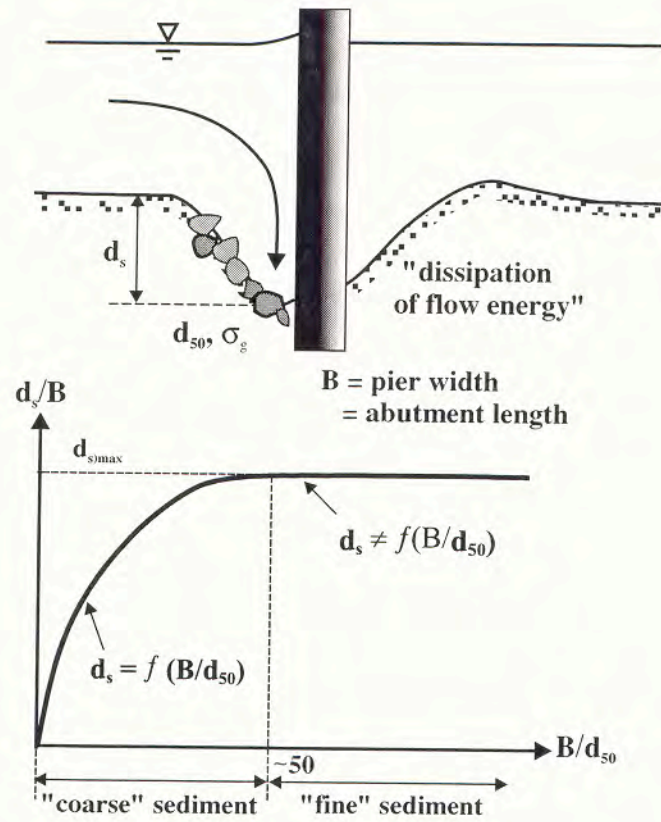


Figure 6.10. Local scour depth variation with sediment coarseness.

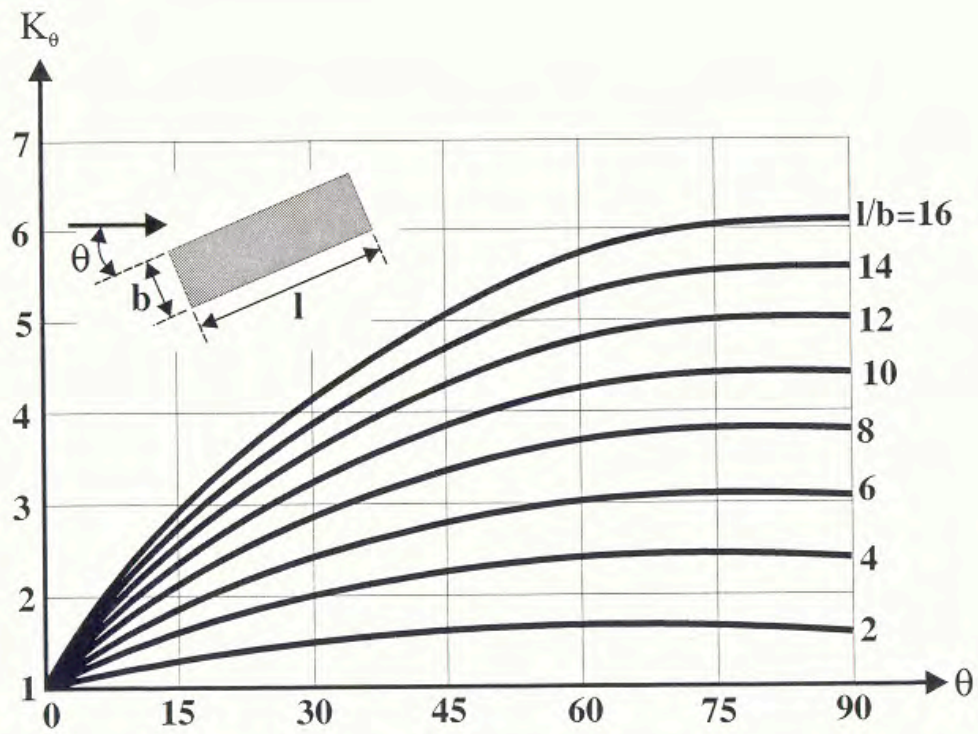


Figure 6.17. Local scour depth variation with pier alignment.

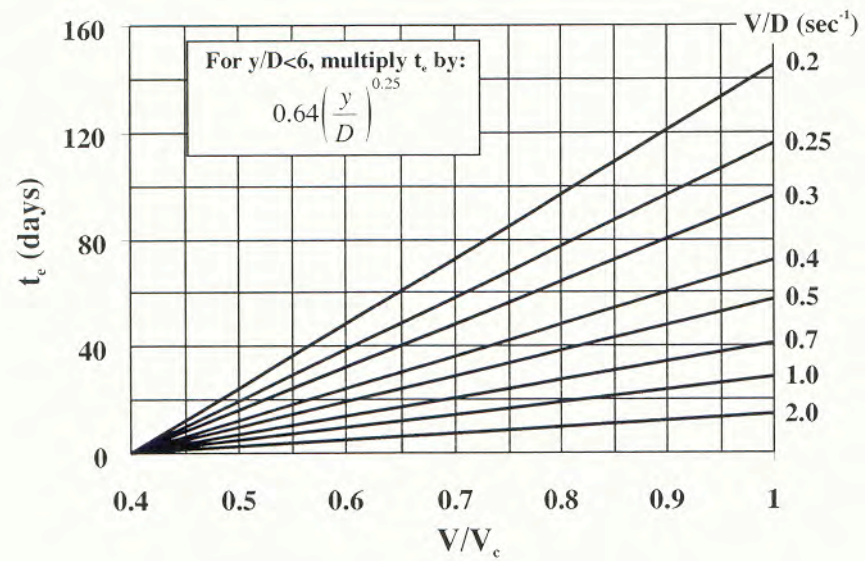


Figure 6.32. Plot of (6.14) for equilibrium time ($y/D > 6$).

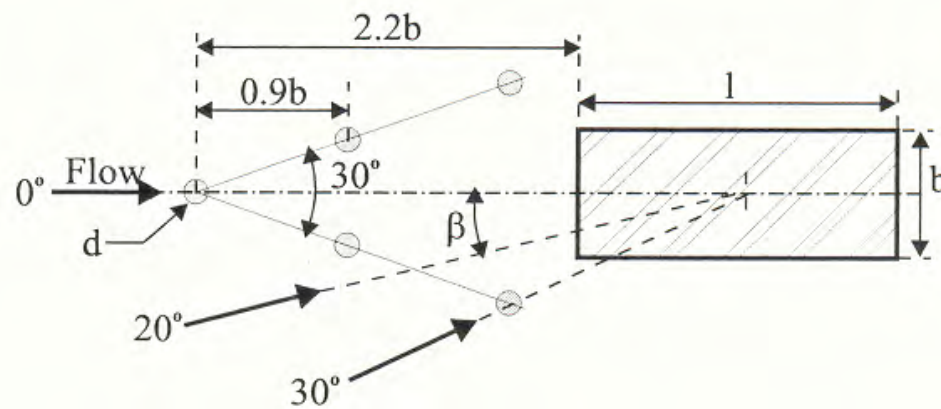
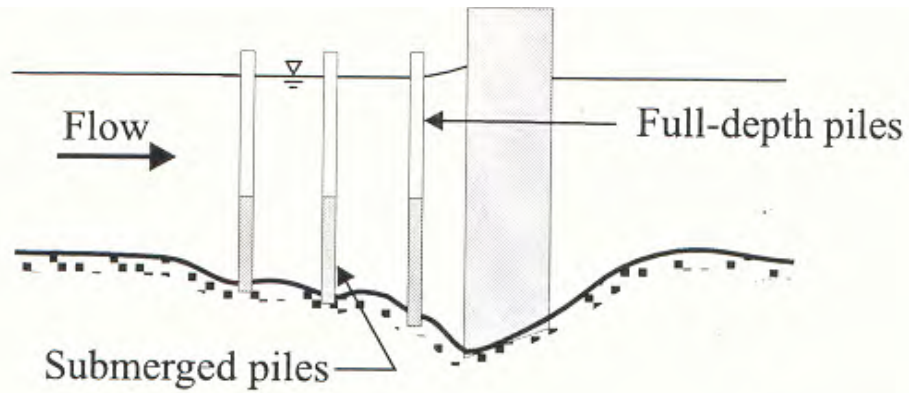
- Scour movie by Roulund

Stone-protection



- [foredrag\Copy of Riprap1.avi](#)

Sacrificial piles: deflects the high velocity flow



Vanes: inducing secondary currents which interfere with the horseshoe vortex

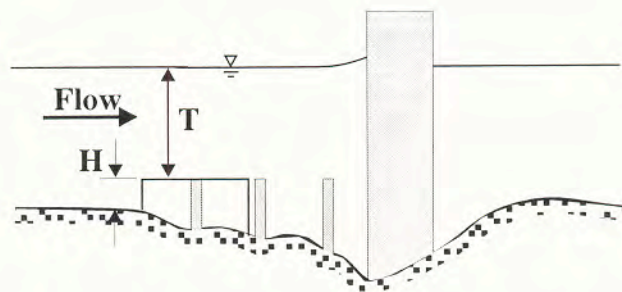
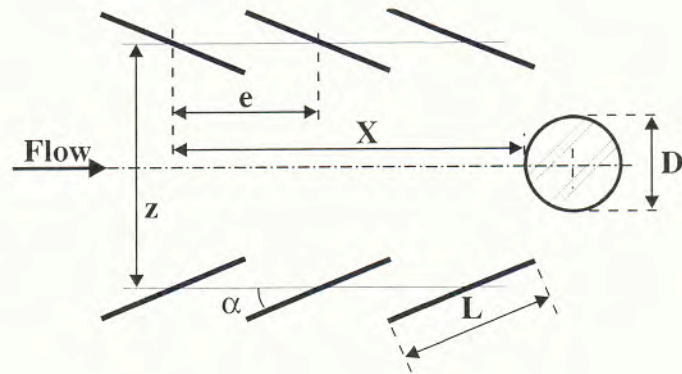
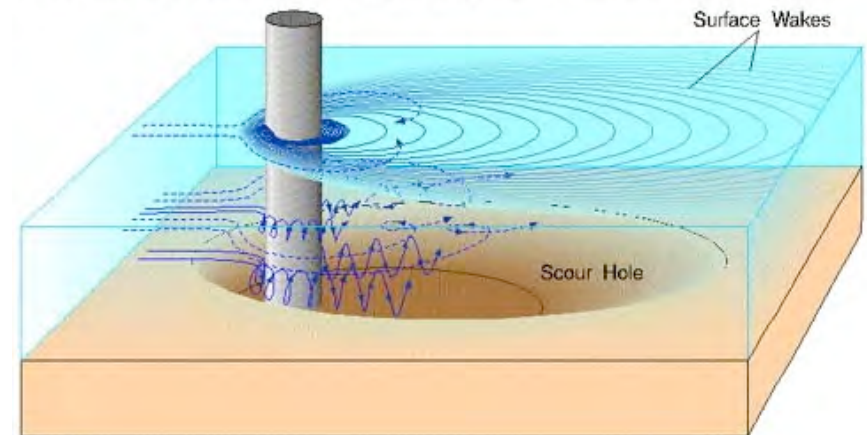
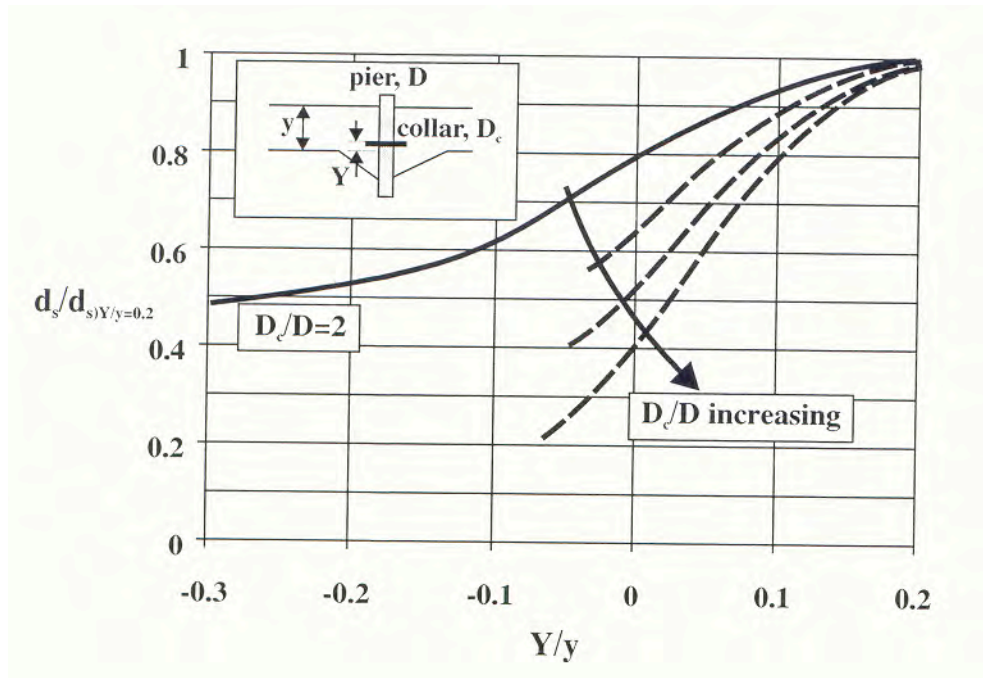


Figure 9.26. The use of Iowa vanes as a pier scour countermeasure.

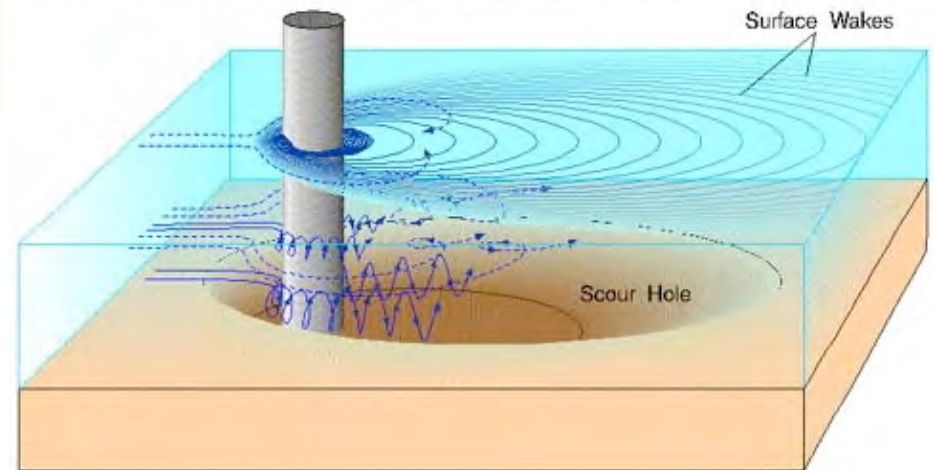
Horseshoe and Wake Vortices around a Cylindrical Element



Collar: Shields sediment bed from the downflow and the horseshoe vortex

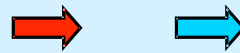


Horseshoe and Wake Vortices around a Cylindrical Element

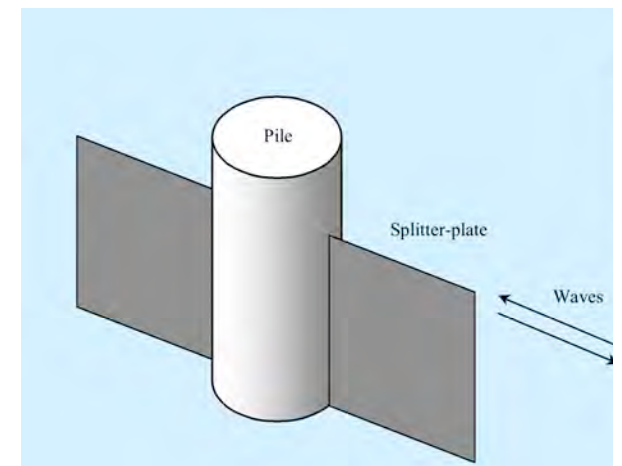


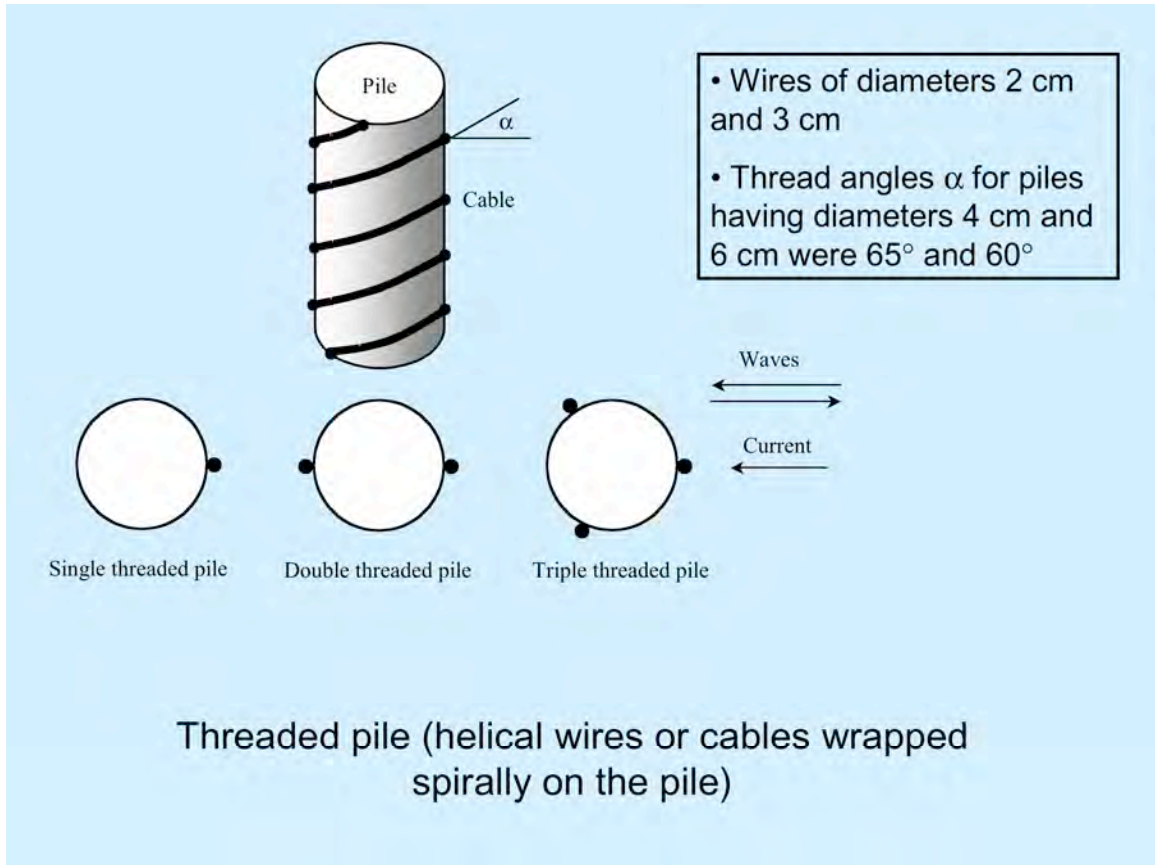


Unprotected pile, where vortex is well-defined before shedding



Pile with splitter-plate, where vortex grows initially and finally breaks down





Marine environment

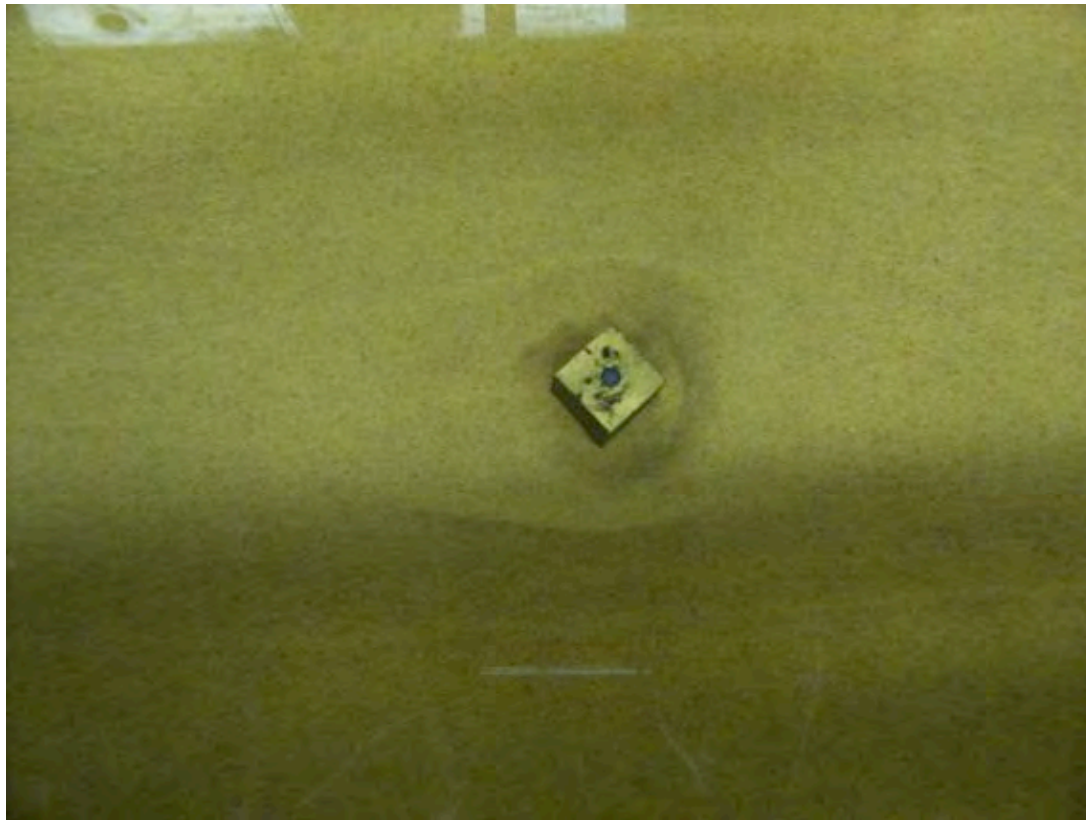


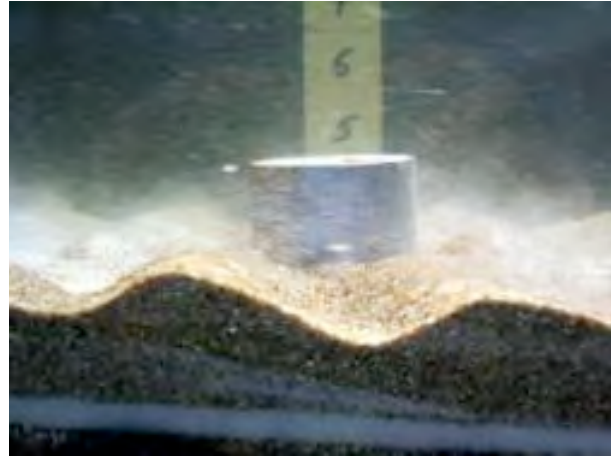




Scour around a cube under wave action

(Univ. Sydney)





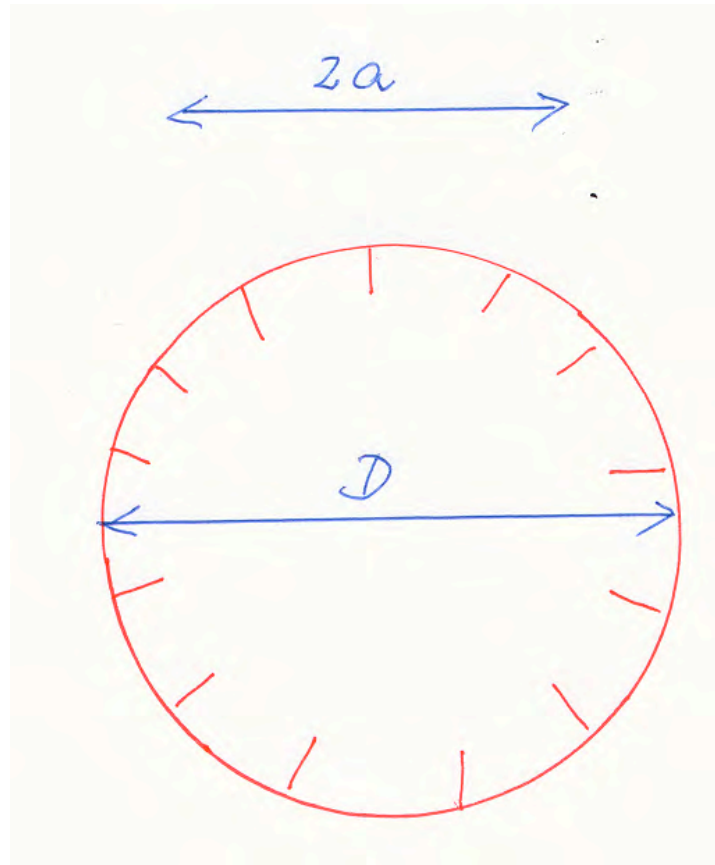
Difference in scour mechanism in between current and waves:

Flow attack from two directions

KC-dependence (maybe no vortex shedding)

Wave scour depends on KC

$$KC = \frac{2\pi a}{D}$$



Tsunami scour

Does the flow last long enough time
so the scour will develop fully? :

Time-scale!

Additional problems:

- liquefaction: reshaping the grain-skeleton
- Momentary fluidization: the effective stresses between the grains disappear due to groundwater flow.

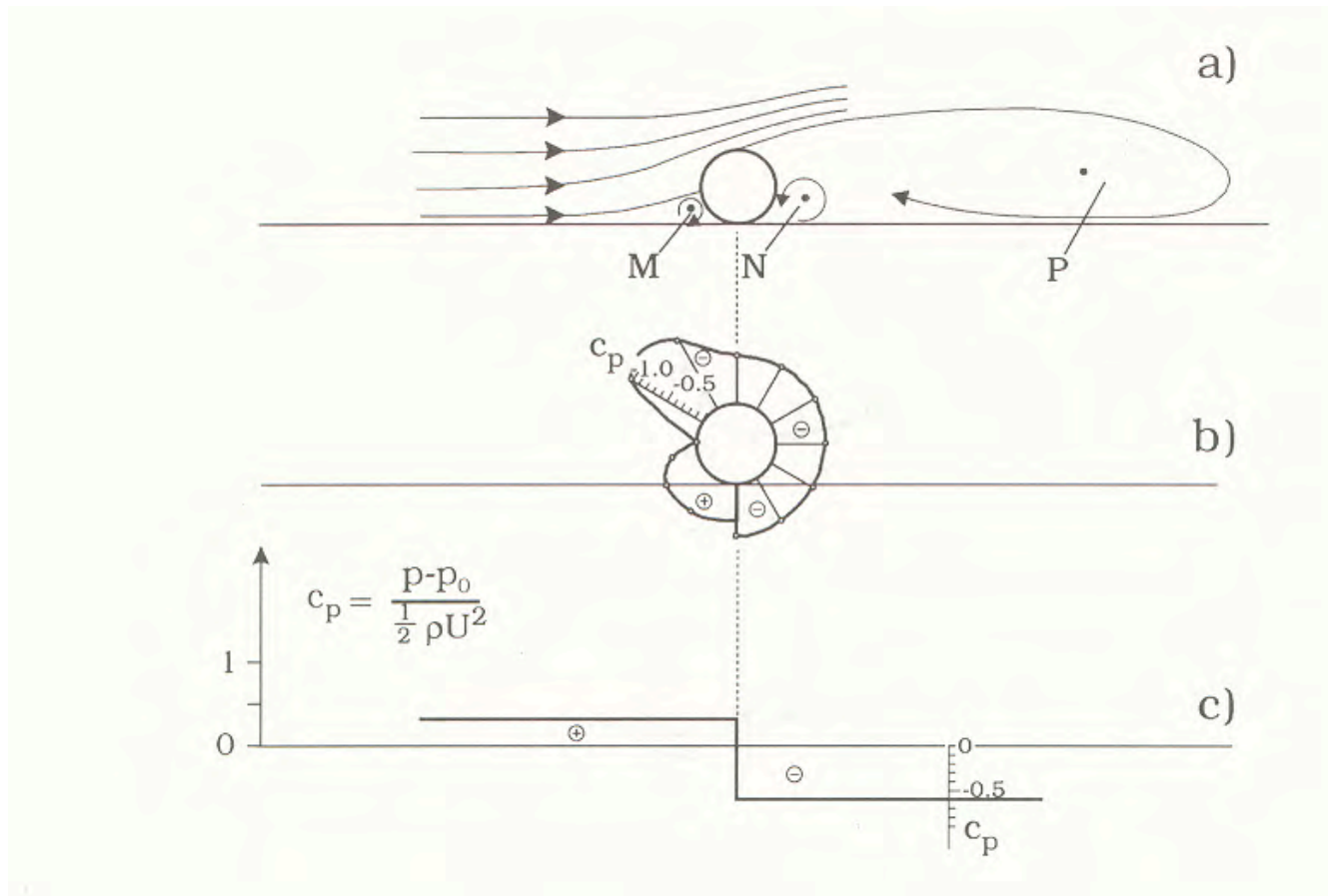
Two very idealized cases:

- The vertical cylinder (pile)
- The horizontal cylinder (pipeline, sewage pipe etc).

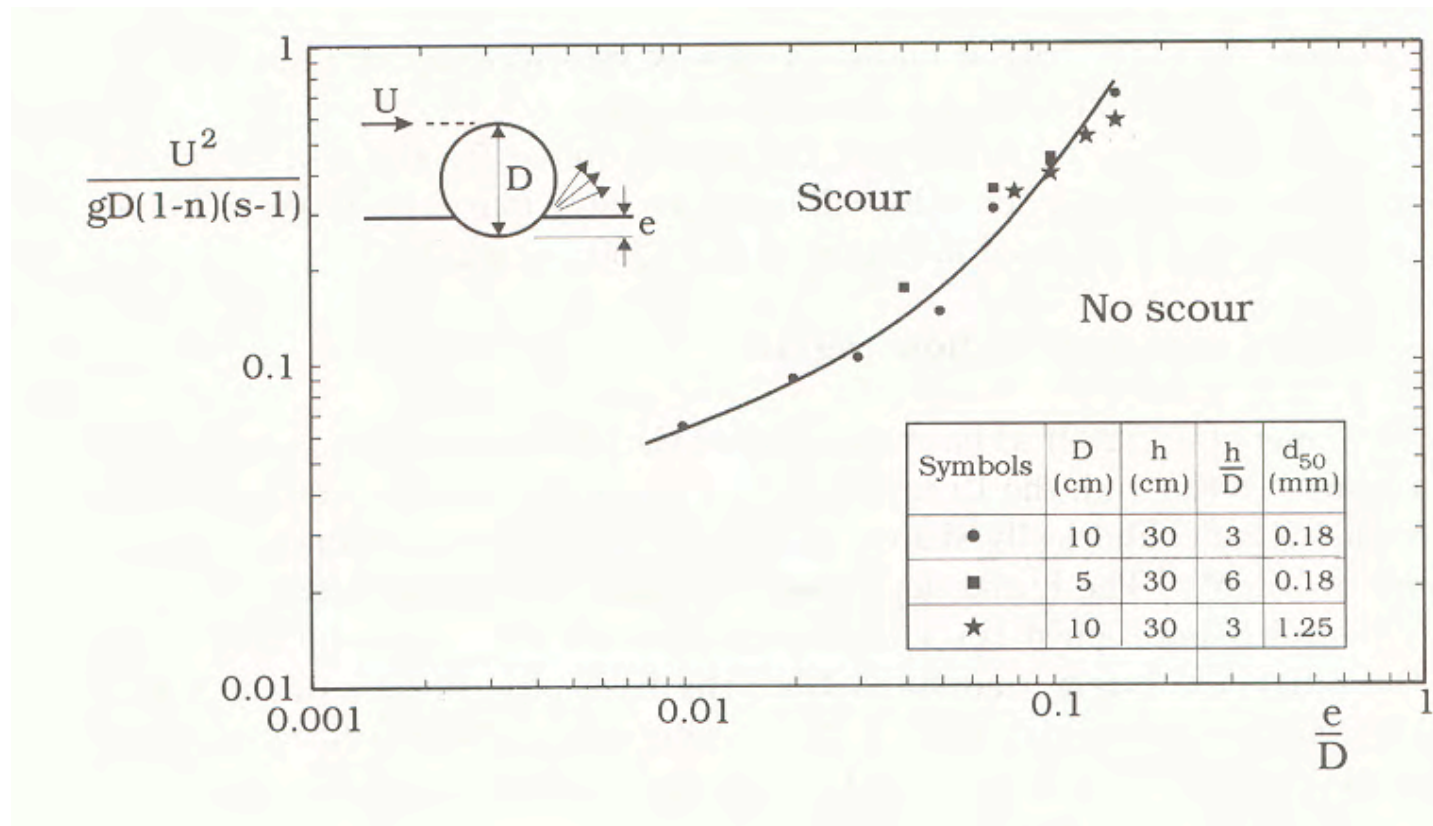


Pipeline, placed on the ground

Pressure variation in a current



- Onset of scour: Seepage flow



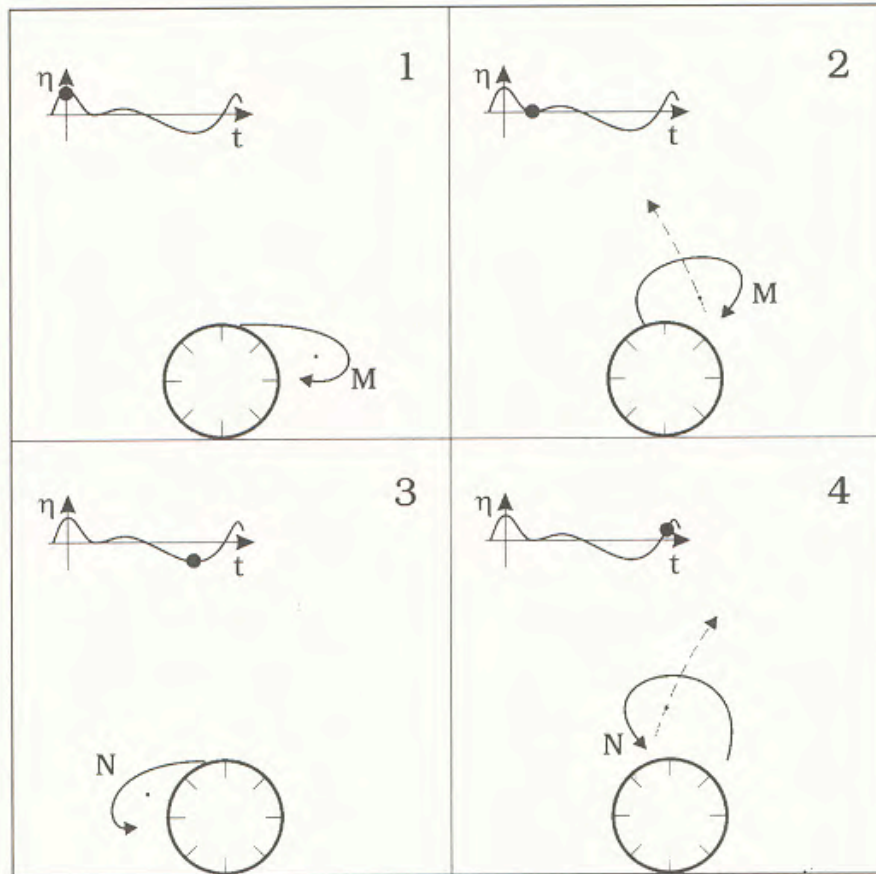
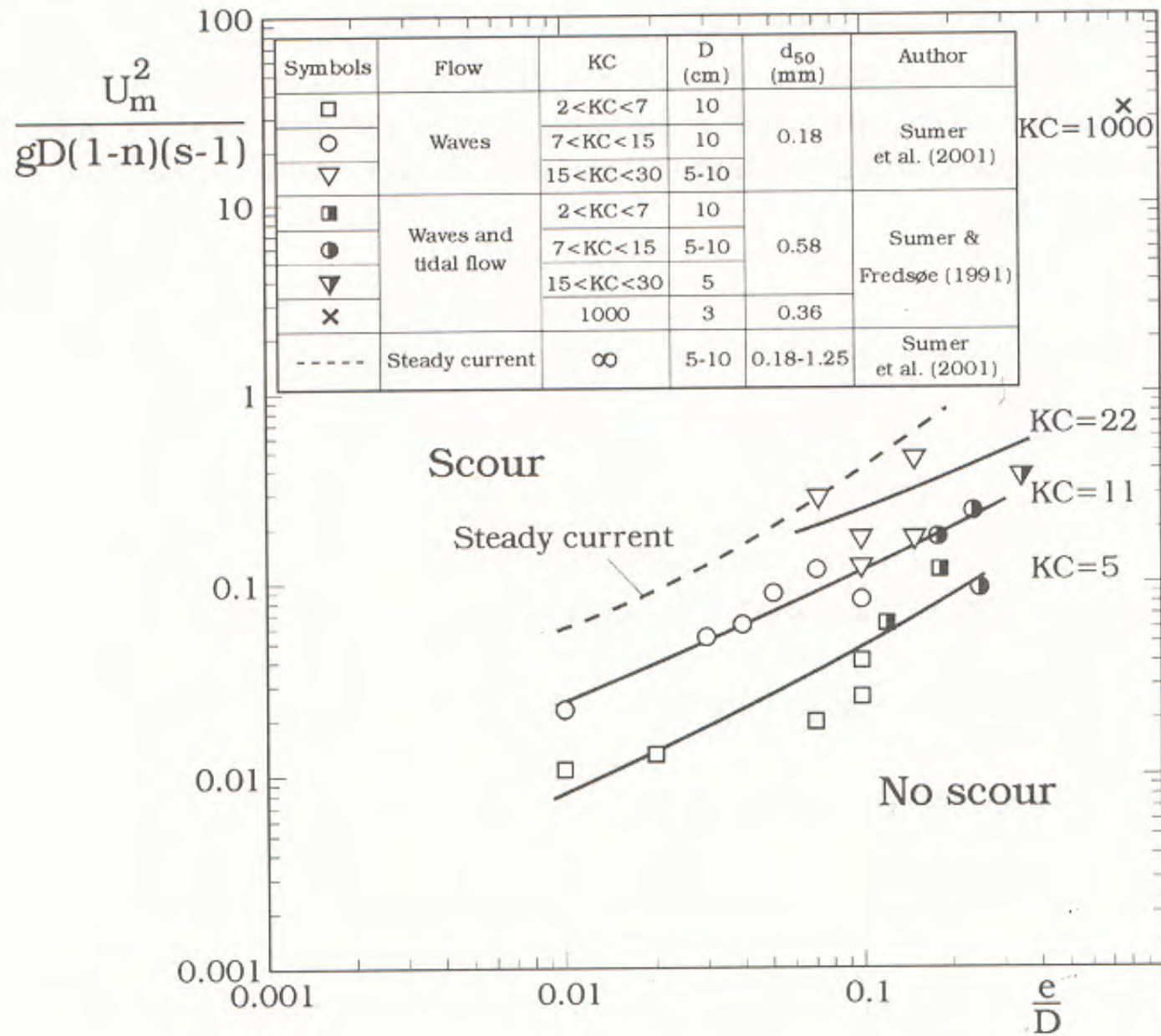
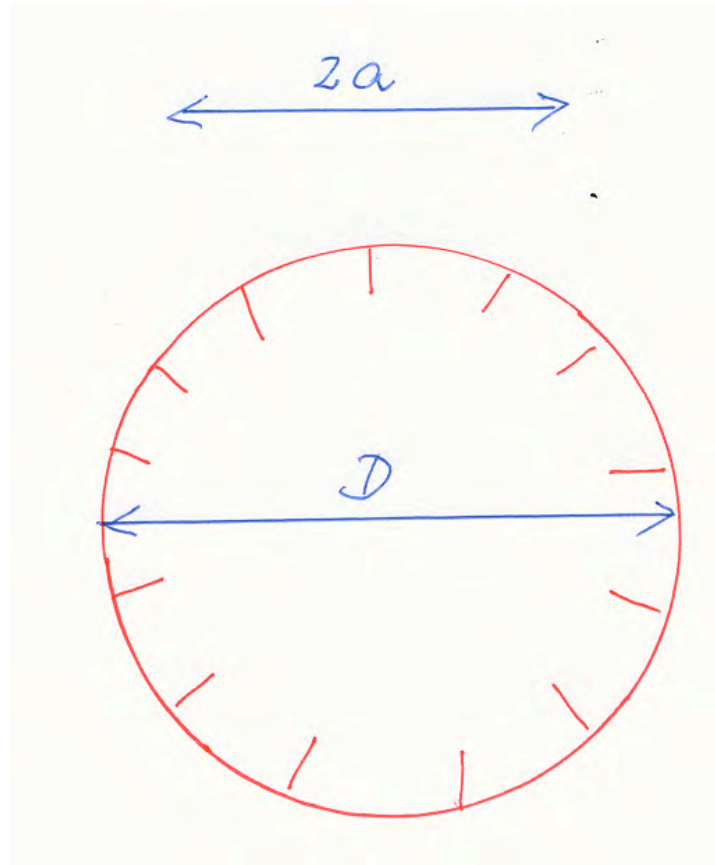


Figure 2.6: Sequence of flow pictures over one wave cycle. Sumer et al. (2001 a).



Onset of Wave scour depends on KC

$$KC = \frac{2\pi a}{D}$$



Tunnel erosion (piping)

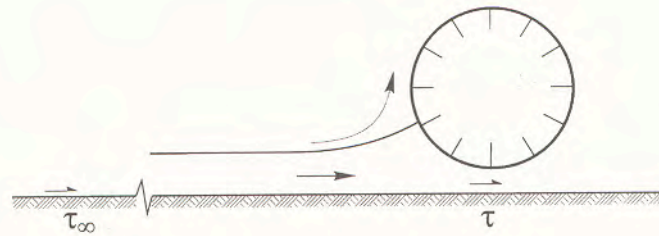


Figure 2.10: Definition sketch of approach flow.

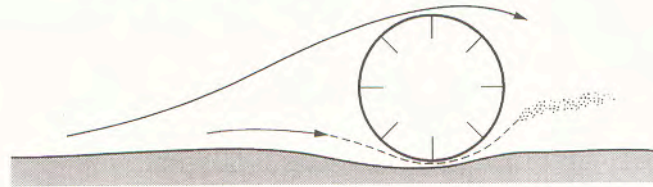


Figure 2.11: Tunnel erosion below a pipeline.

Scour development, current

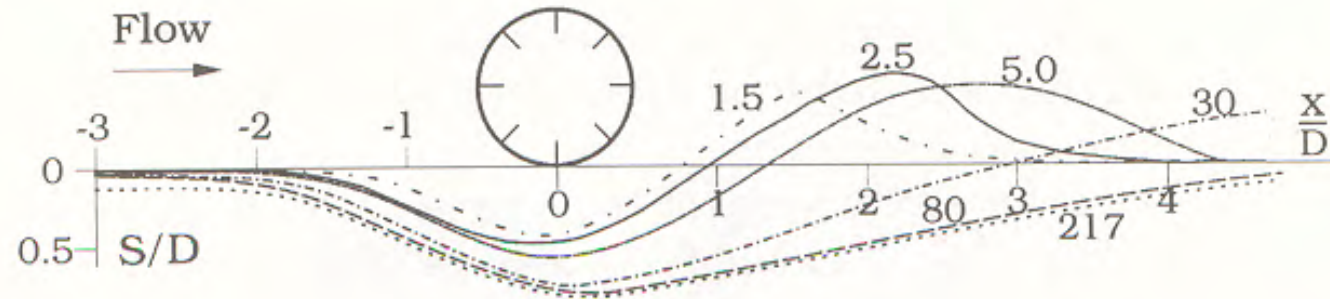
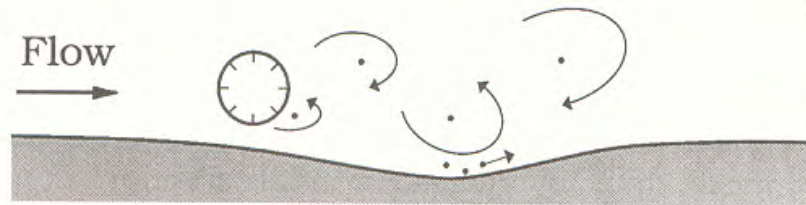


Figure 2.13: Scour development. Times in minutes. $\theta = 0.098$. Current. Mao (1986).



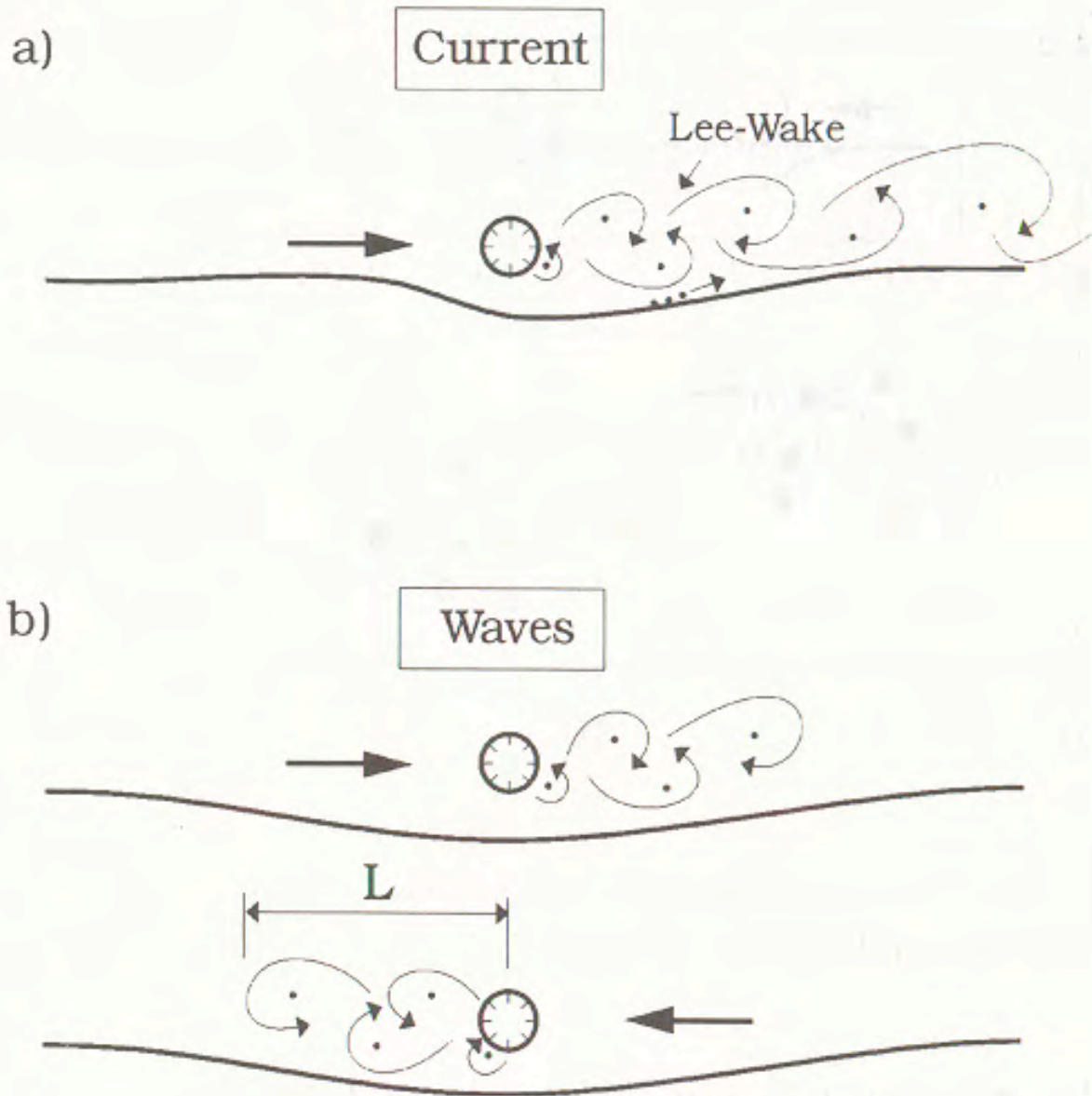
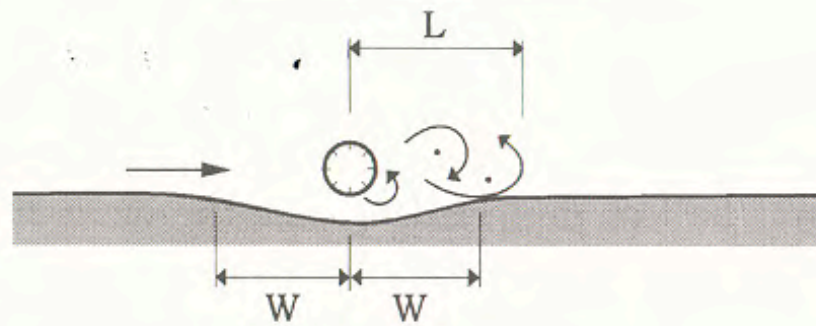
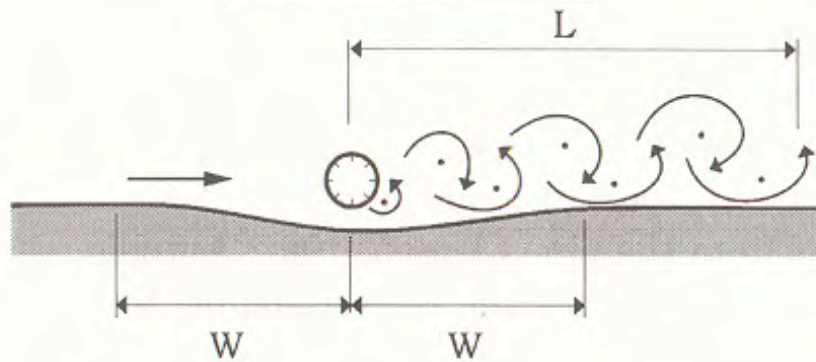


Figure 2.21: Lee-wake effect.

Small KC number

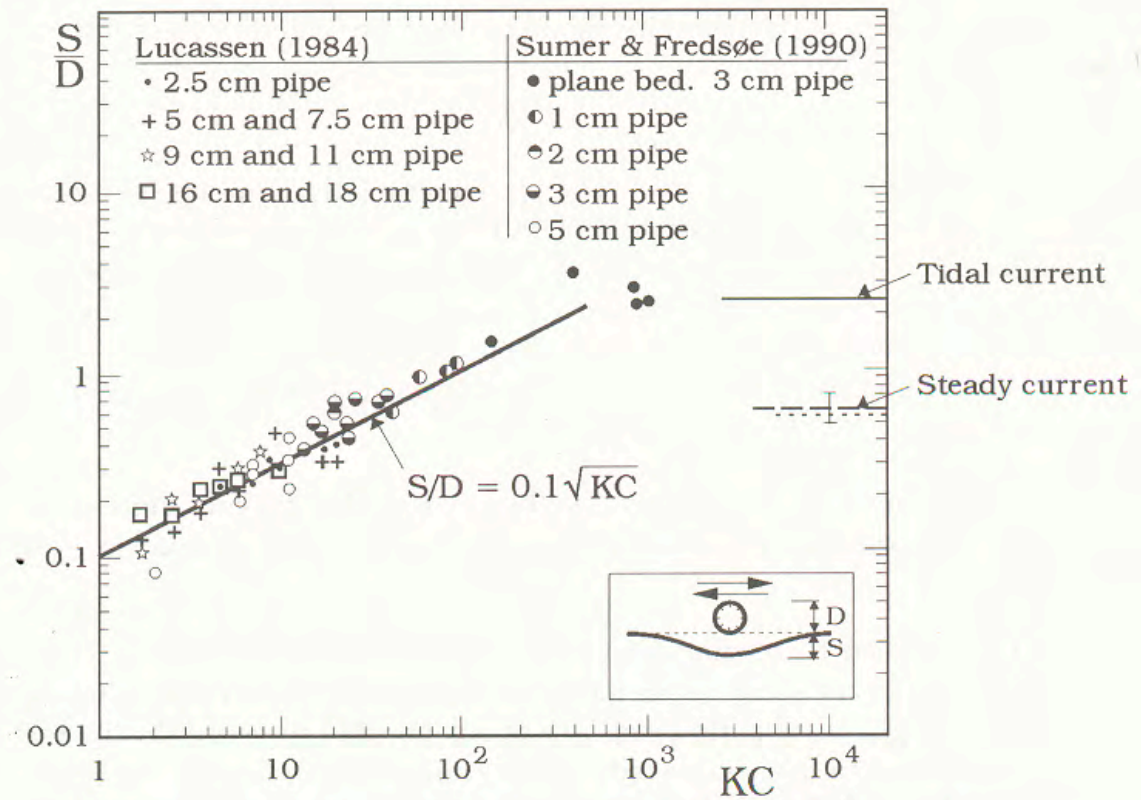


Large KC number



Final scour depth

Tsunami??



$$T^* = \theta^{-5/3} / 50$$

$$T^* = \frac{\sqrt{g(s-1)d^3}}{D^3} T$$

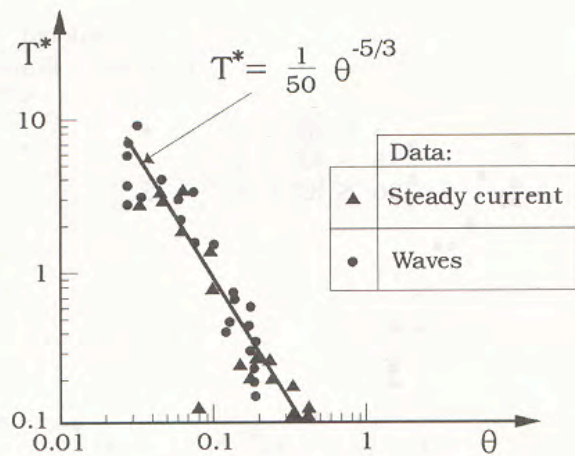
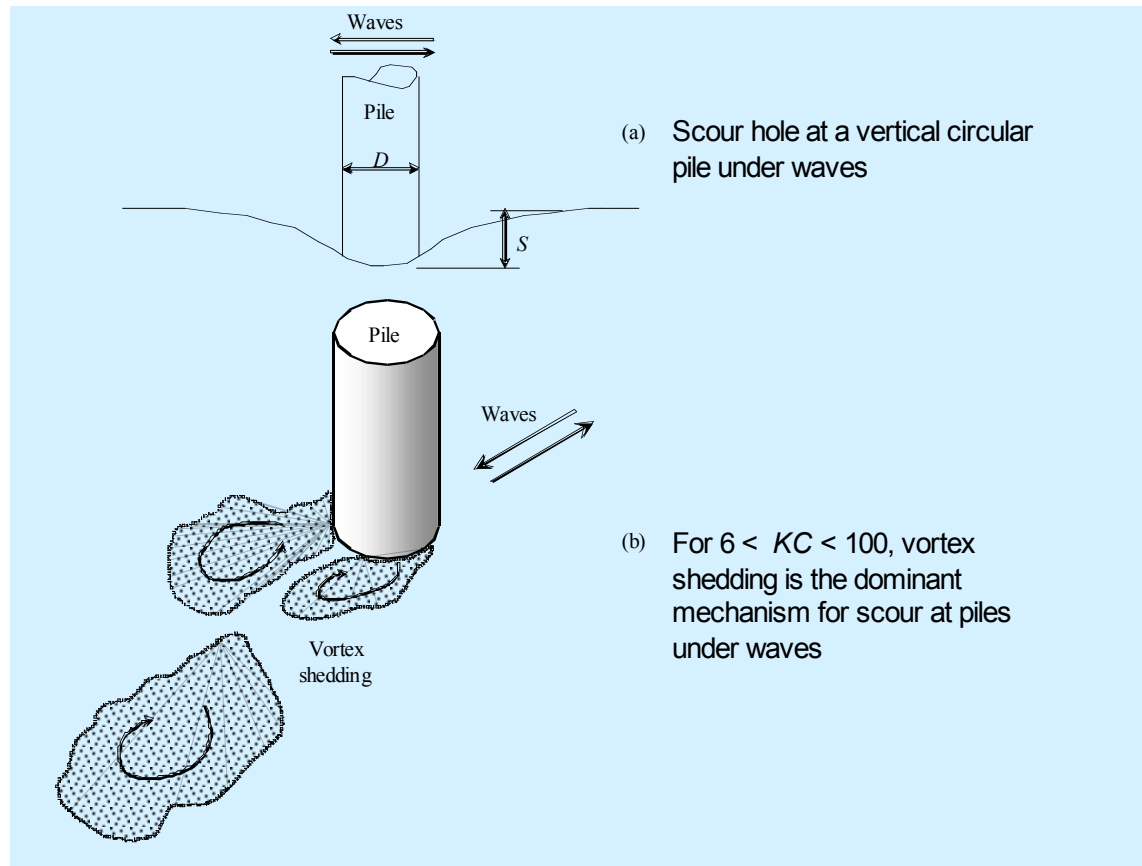


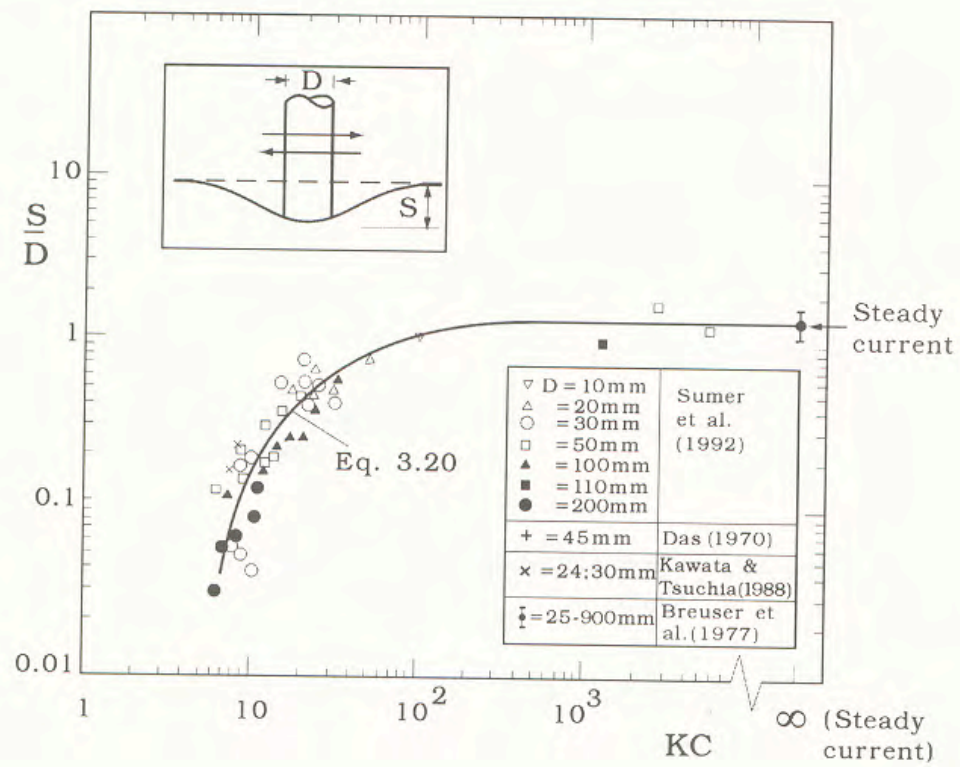
Figure 2.43: Time scale. All data (current/wave). Live bed ($\theta > \theta_{cr}$). Fredsøe et al. (1992).

Example: Diameter=30 cm
grain size=.5 mm
Waterdepth=5 m

- Flow velocity=.6 m/s T=1.4 hour
- Waves: waveperiod=10 sec H=2m
depth=10m: T=5min
- Flow velocity=6m/s T= 3 sec.

Vertical structure: the single pile





Shape-effect

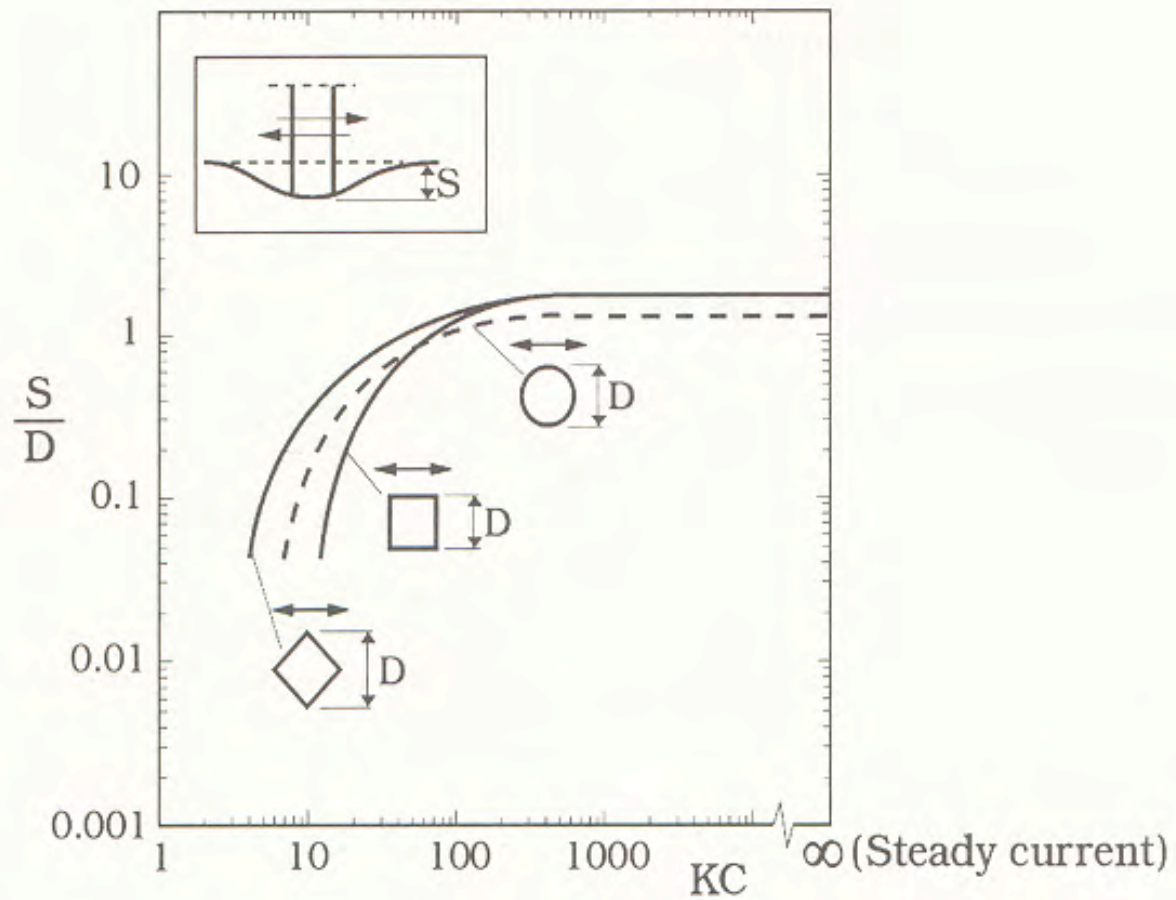
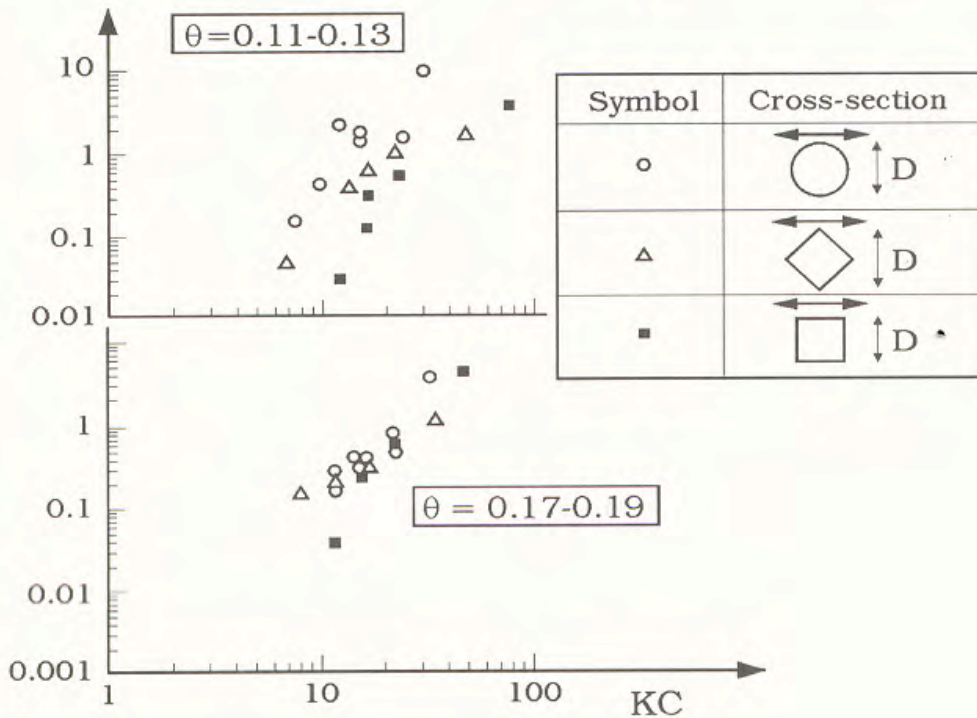
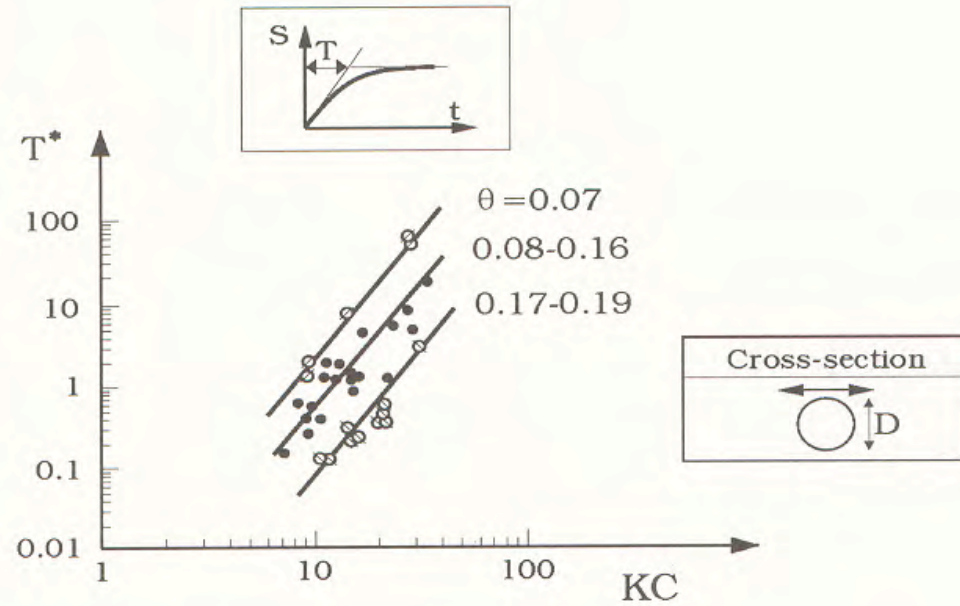


Figure 3.37: Equilibrium scour depth. Effect of cross-sectional shape. Live bed ($\theta > \theta_{cr}$). Sumer et al. (1993).



Current

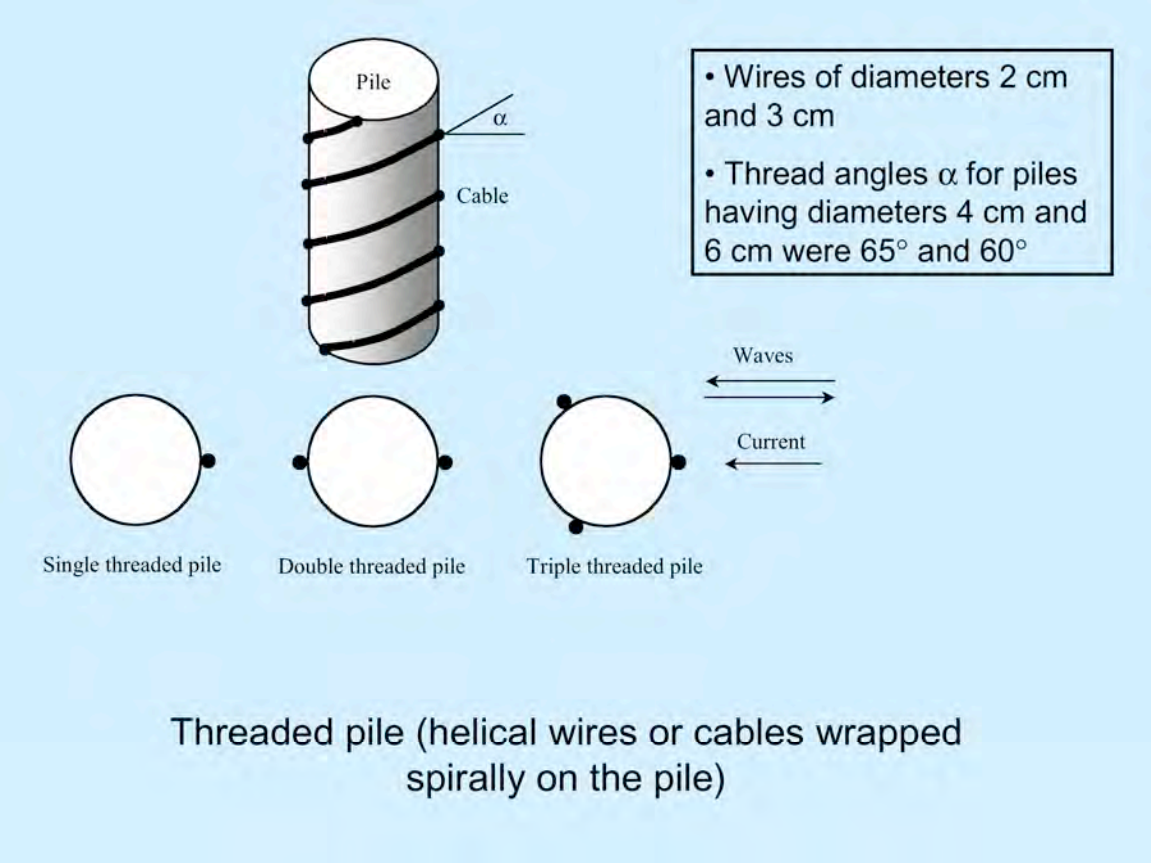
$$T^* = \theta^{-2.2} h / D / 2000$$

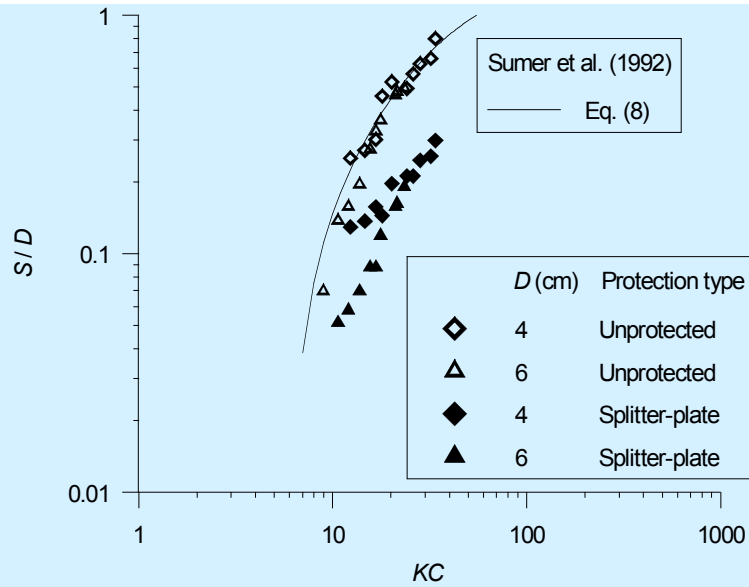
$$T^* = \frac{\sqrt{g(s-1)d^3}}{D^2} T$$

Waves

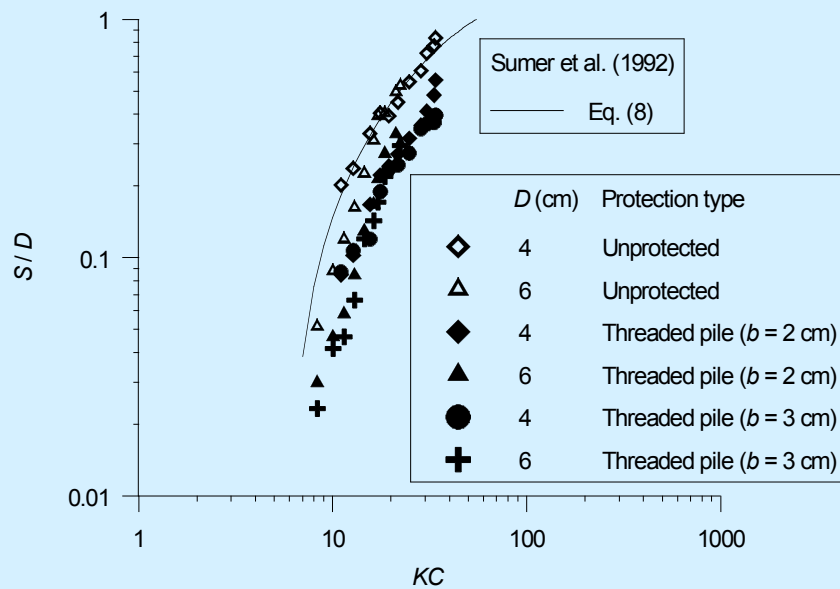
$$T^* = 10^{-6} \left(\frac{KC}{\theta} \right)^3$$

- $D=3\text{m}$ $d=.5\text{ mm}$ $V=.6\text{ m/s}$ $h=5\text{ m}$: $T=50$
hours
- V instead 6 m/s : $T=8\text{ sec}$,





- Experimental results of unprotected piles correspond closely with the curve proposed by Sumer et al. (1992)
- Reduction of scour depth for protected piles is prominent



Variation of nondimensional scour depth S/D with KC number for unprotected and protected piles under waves

Fluidization

S.-Y. Tzang, S.-H. Ou / Coastal Engineering 53 (2006) 965–982

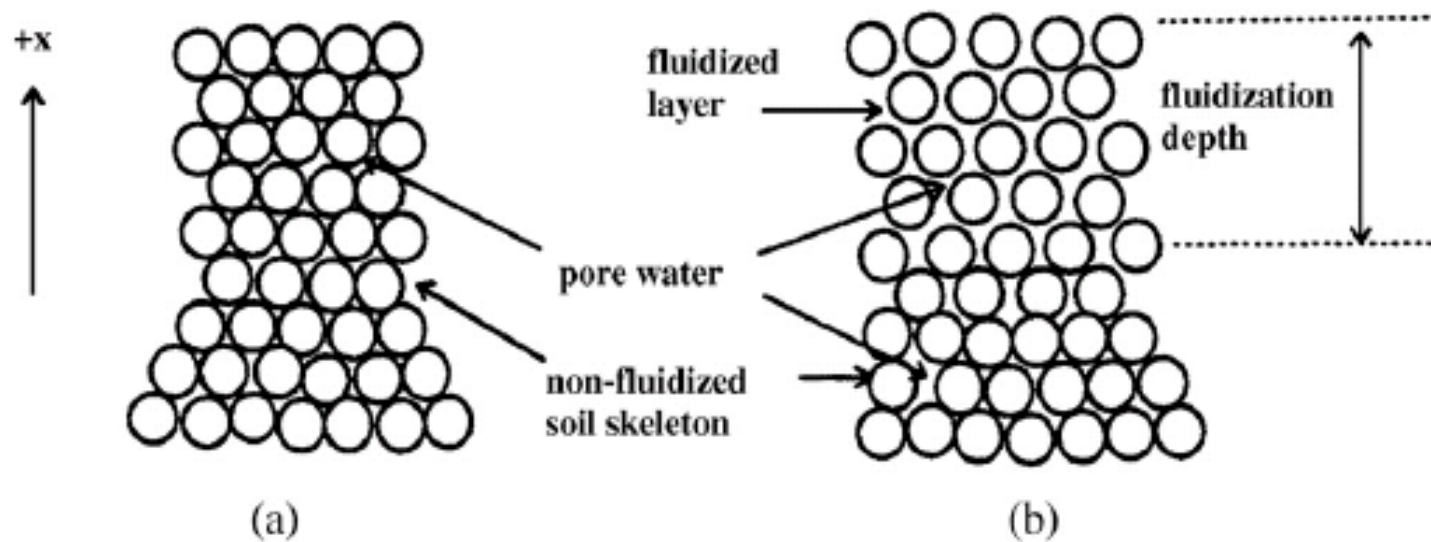
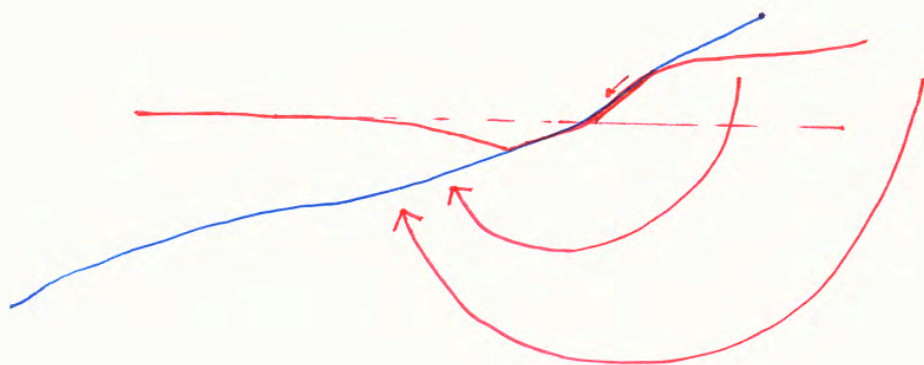
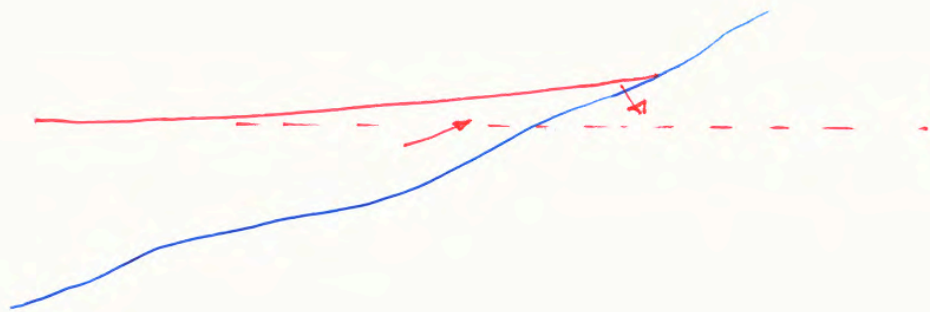


Fig. 1. Schematics of soil fluidization in a granular bed in stages of (a) unfluidized and (b) fluidized responses (Huang, 1996).



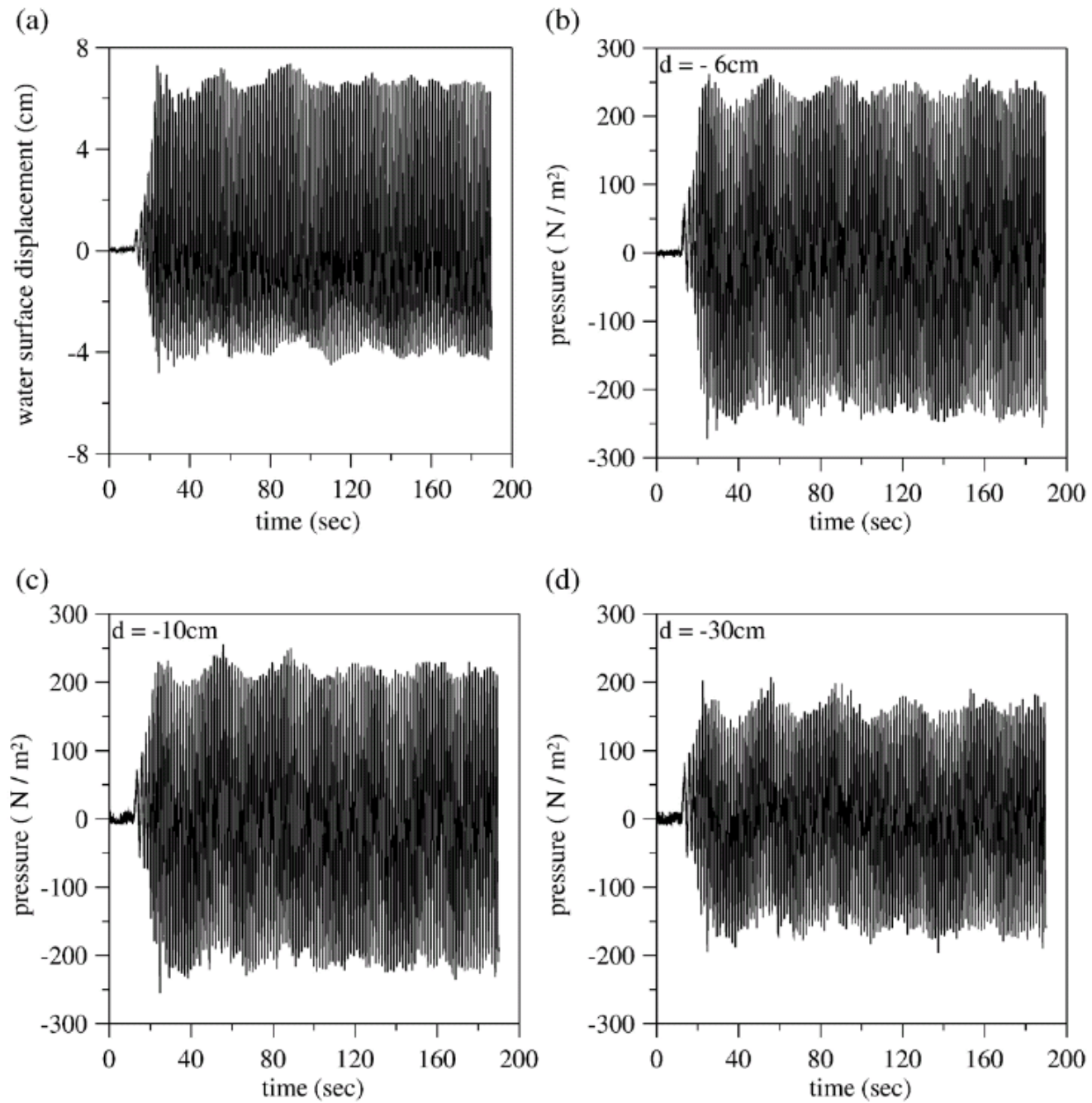


Fig. 5. Typical (a) wave records and wave-induced unfluidized pore pressure responses in Sand I ($d_{50}=0.134$ mm) at depths of $d=$ (b) -6 cm, (c) -10 cm and (d) -30 cm (Test 1-2: $H=10.3$ cm, $T=1.49$ s).

Sand

gravel

176

S. Tonkin, H. Yeh, F. Kato and S. Sato

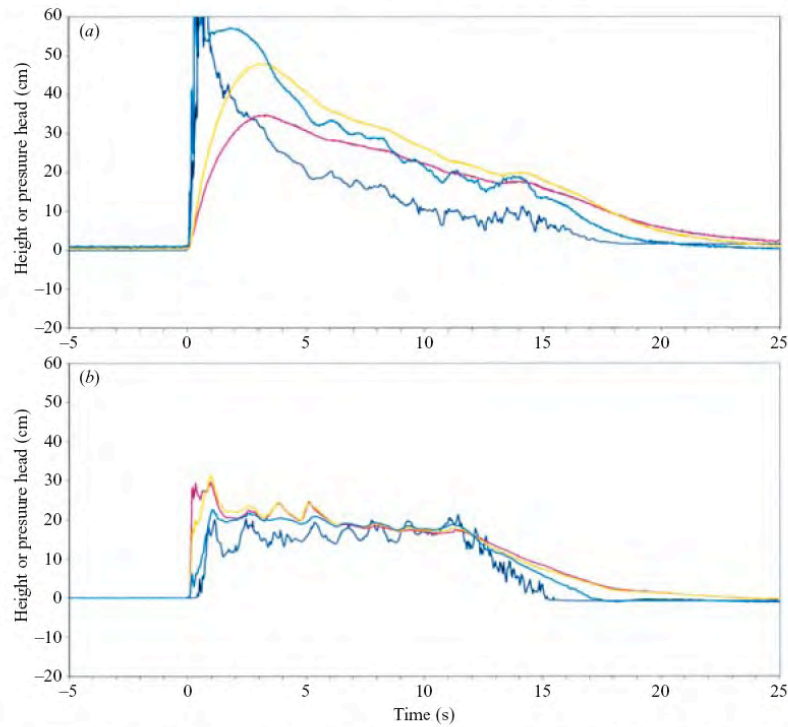


FIGURE 9. Wave height (blue line), and pore pressure heads at 10 cm (cyan), 20 cm (yellow) and 30 cm (pink) depth, measured for Case I: (a) at the front of the cylinder, (b) at the back of the cylinder.

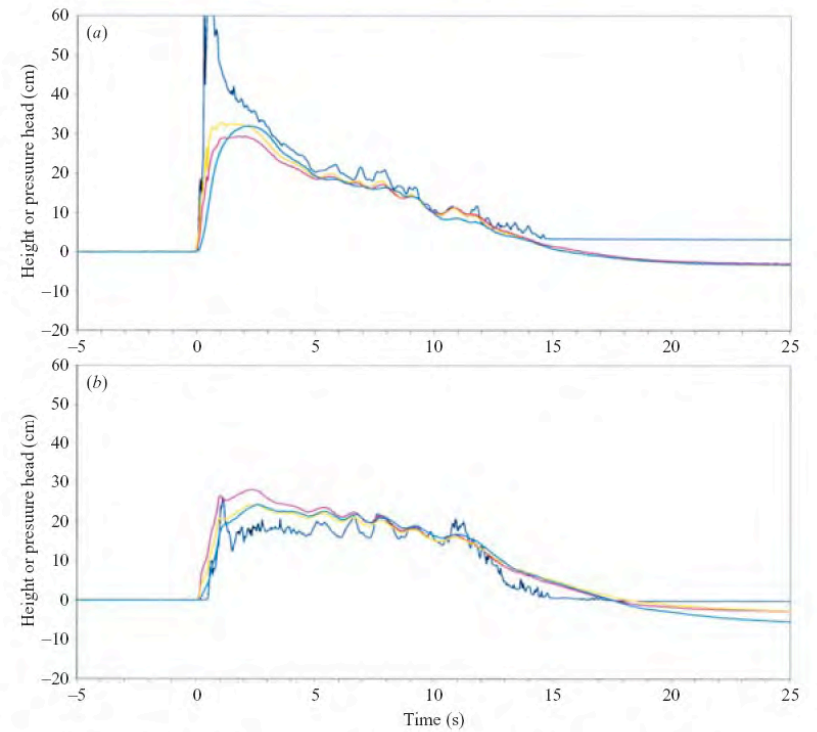


FIGURE 12. Wave height (blue line), and pore pressure heads at 10 cm (cyan), 20 cm (yellow) and 30 cm (pink) depth, measured for Case II: (a) at the front of the cylinder, (b) at the back of the cylinder.

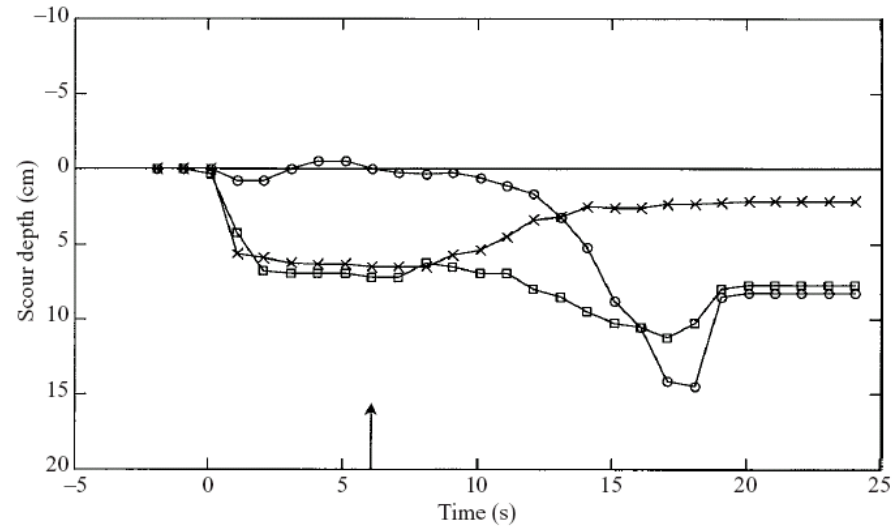


FIGURE 7. Scour depth as a function of time for Case I. Crosses, at the front of the cylinder; squares, at the side; circles, at the back. The arrow indicates the time of flow reversal, 6 s after wave impact.

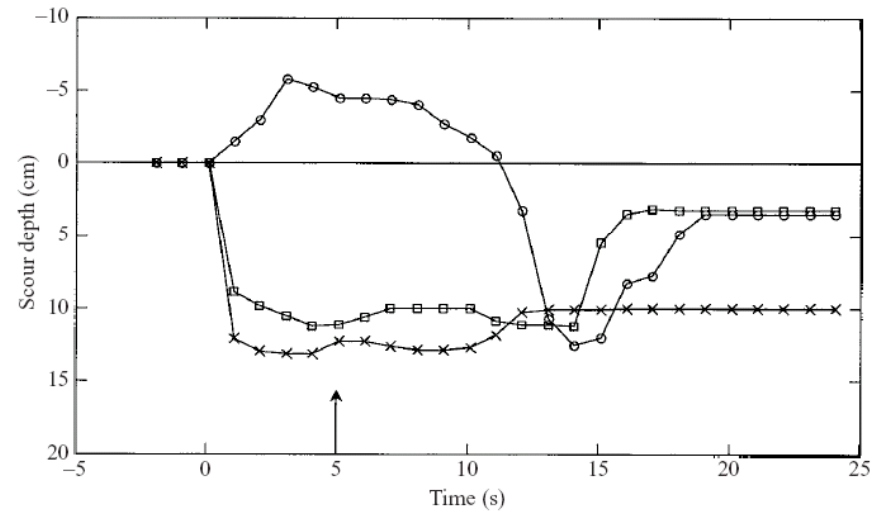


FIGURE 11. Scour depth as a function of time for Case II. Crosses, at the front of the cylinder; squares, at the side; circles, at the back. The arrow indicates the time of flow reversal, 5 s after wave impact.

Need for research

- Is scour different in the sheet flow regime
- Scour in super-critical regime
- Timescale for scour at large Shields parameters
- Scour around structures with large horizontal dimensions compared to waterdepth